In vitro nephrogenesis from human pluripotent stem cells

D i s s e r t a t i o n

zur Erlangung des akademischen Grades

d o c t o r r e r u m n a t u r a l i u m

(Dr. rer. nat.)

im Fach Biologie

eingereicht an der Lebenswissenschaftlichen Fakultät

der Humboldt-Universität zu Berlin

von

Hariharan, Krithika

Präsidentin der Humboldt-Universität zu Berlin

Prof. Dr. Sabine Kunst

Dekan der Lebenswissenschaftlichen Fakultät

Prof. Dr. Bernhard Grimm

Gutachter/innen: 1. Prof. Dr. Hans-Dieter Volk

2. Prof. Dr. Roland Lauster

3. Prof. Dr. Andreas Kurtz

Tag der mündlichen Prüfung: 15.02.2017

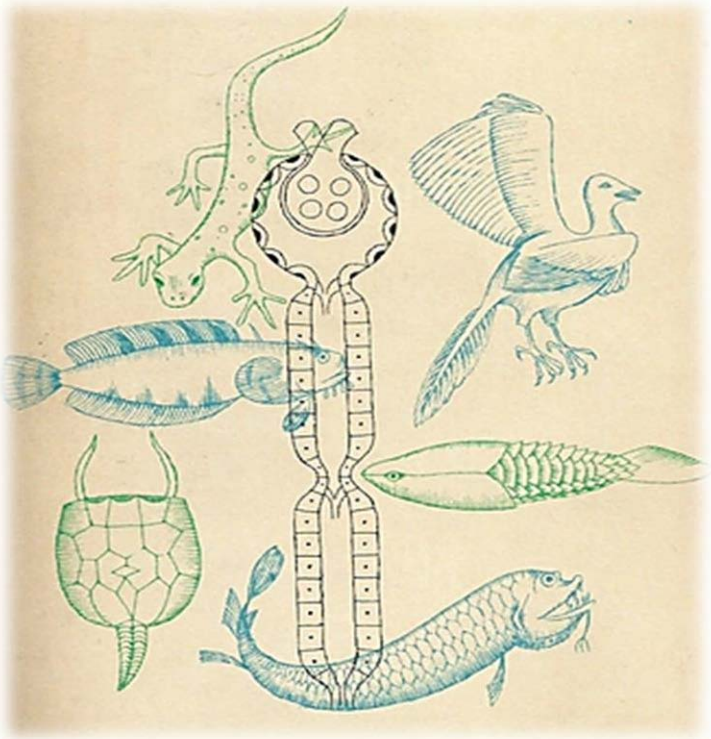

There are those who say that the human kidney was created to keep the blood pure, or more precisely, to keep our internal environment in an ideal balanced state. This I must deny. I grant that the human kidney is a marvelous organ, but I cannot grant that it was purposefully designed to excrete urine or to regulate the composition of the blood or to sub-serve the physiological welfare of Homo sapiens in any sense. Rather I contend that the human kidney manufactures the kind of urine that it does, and it maintains the blood in the composition which that fluid has, because this kidney has a certain functional architecture; and it owes that architecture not to design or foresight or to any plan, but to the fact that the earth is an unstable sphere with a fragile crust, to the geologic revolutions that for six hundred million years have raised and lowered continents and seas, to the predacious enemies, and heat and cold, and storms and droughts; to the unending succession of vicissitudes that have driven the mutant vertebrates from sea into fresh water, into desiccated swamps, out upon the dry land, from one habitation to another, perpetually in search of the free and independent life, perpetually failing, for one reason or another, to find it.

...let our kidneys fail for even a short time to fulfill their task, and our mental integrity, our personality, is destroyed.

— Homer William Smith
Figure and quote from the book,
From Fish to Philosopher (1953), 210-1

SUMMARY

Kidneys are the central organ for homeostasis for our body systems and composed of around a million functional units, the nephrons. Chronically damaged nephrons deteriorate progressively towards end stage renal disease (ESRD), owing to the limited regenerative capacity of adult mammalian kidneys. The generation of renal cells from human pluripotent stem cells (hPSCs) is a promising strategy to develop regenerative therapies for ESRD. In this study, we established a protocol to differentiate hPSCs to renal progenitors (RP), capable of producing nephronal cell types and structures *in vitro* and *ex vivo*. An effective combination of factors obtained after intensive screening, was used to create an 8-day-protocol that steered hPSCs to the renal lineage by a step-wise process outlining the embryonic milestones in kidney organogenesis. Six days after growth factor treatment, a mixture of $SIX2^+$/$CITED1^+$ cells representing metanephric mesenchyme and an $HOXB7^+$/$GRHL2^+$ population indicative of ureteric bud progenitors was obtained that developed into $LGR5^+$/$JAG1^+$/$WT1^+$ renal vesicle cells by the day 8. Prolonged cultivation of these day 8 cells in three inductive media resulted in generation of $WT1^+$/$PODXL^+$/$SYNPO^+$ podocyte-precursors, PDGFRß$^+$/$DESMIN^+$/αSMA$^+$-mesangial cells and fractions of proximal, distal and collecting duct tubular epithelial cells *in vitro*. Moreover, day 8 cells differentiate spontaneously into renal organoids in culture. The hPSC-derived RP gave rise to tubular structures upon culture as a pellet in air-liquid interface and integrated into embryonic kidney re-aggregations. Thus, we demonstrate that our protocol generates RP reminiscent of nascent nephrons, which can be coaxed into specialized nephronal cell types *in vitro* after 14 days from hPSCs. This simple and rapid method to produce renal cells from a common precursor pool in 2D culture provides the basis for scaled-up production of tailored renal cell types, applicable for drug testing or cell therapies.

ZUSAMMENFASSUNG

Die Homöostase wird maßgeblich durch die Niere, bestehend aus Millionen funktioneller Untereinheiten, den Nephronen, aufrechtherhalten. Chronisch geschädigte Nephrone führen zur Entwicklung einer terminalen Nierenerkrankung (TNE). Die Erzeugung renaler Zellen aus humanen pluripotenten Stammzellen (hPSCs) stellt eine vielversprechende Strategie zur regenerativen Therapie und Behandlung von TNE dar. In der vorliegenden Arbeit wurde ein Protokoll zur Differenzierung von renalen Vorläufern (RV) aus hPSCs entwickelt, welches nephronale Zelltypen und Strukturen in vitro und ex vivo erzeugte. Eine selektierte Kombination von Faktoren wurde in diesem 8-Tage-Protokoll genutzt, um die schrittweise Differenzierung der hPSCs zu lenken, indem die embryonale Organogenese der Niere abgebildet wurde. Am Tag 6 der Differenzierung konnten SIX2+/CITED1+ Zellen des metanephrischen Mesenchyms und HOXB7+/GRHL2+ Zellen, welche auf Vorläufer der Ureterknospe hindeuten, nachgewiesen werden. Diese entwickelten sich am Tag 8 weiter zu LGR5+/JAG1+/WT1+ renalen Vesikelzellen. Weiterführende Kultivierung in drei verschiedenen induktiven Medien führte zu WT1+/PODXL+/SYNPO+ Podozytenvorläufern, PDGFRß+/DESMIN+/αSMA+ Mesangialzellen und epithelialen Zellen des proximalen und distalen Tubulus sowie des Sammelrohrs. Außerdem bildeten die Tag-8-Vorläuferzellen spontan 3D renale Organoide aus. Die RV induzierten tubuläre Strukturen an einer Luft-Flüssigkeits-Grenzfläche und integrierten sich in embryonale Nierenaggregate. Zusammenfassend konnte demnach ein Protokoll entwickelt werden, welches entstehenden Nephronen ähnliche RV generierte, die innerhalb von 14 Tagen in spezialisierte nephronale Zelltypen differenzierten. Diese einfache Methode, um renale Zellen aus einem gemeinsamen Vorläuferpool in einer 2D -Kultur zu erzeugen, schafft die Grundlage für eine Produktion im größeren Maßstab, sowie für Modellsysteme in toxikologischen Untersuchungen oder Zelltherapien

TABLE OF CONTENTS

1. INTRODUCTION

1.1. The Kidney: In high demand and low supply

Kidney diseases are a dominant problem with high morbidity and mortality rates as well as a very high financial burden to the society. Between 8 and 10% of the adult population have some form of kidney damage, and every year millions die prematurely of complications related to Chronic Kidney Diseases (CKD). This disease is a continuum of kidney dysfunction beginning from mild kidney damage culminating in kidney failure, referred to as end-stage renal disease (ESRD). At the end of 2013, there were around 3.2 million patients being treated for ESRD worldwide (Facts-European Renal Care Providers Association). In spite of the technological and pharmacological advances achieved in the last years for the treatment of ESRD patients, survival is still low. Cardiovascular disease has been considered the most common cause of death in these patients (Foley et al., 1998) and this may be connected with the high prevalence of classic cardiovascular risk factors, which include hypertension, diabetes mellitus, dyslipidemia, smoking, and advanced age (Sousa-Martins et al., 2016).

Hemodialysis, widely used during the past half-century, has offered a solution to lengthen the survival of ESRD patients. Nonetheless, it is associated with symptoms that affect the daily life, and there is evidence that patients consider the health-related quality of life more important than survival itself (Mazairac et al., 2012). Another option for ESRD patients is an organ transplant. Kidney transplantation offers patients with end-stage renal disease the greatest potential for increased longevity and enhanced quality of life; however, the demand for kidneys far exceeds the available supply. Dramatic shifts in baseline immunosuppression have resulted in early graft survival but do not necessarily benefit in the long term. However, death of transplant recipients from cardiovascular disease, infection and cancer remains an important limitation in kidney transplantation. Continued success in kidney transplantation will require increased numbers of donors, living and deceased, as well as reduction in the primary causes of late transplant loss, namely premature patient death with a functioning graft and chronic allograft nephropathy (Knoll, 2008).The increasing demand for kidneys provokes the quest for alternative renal therapies relying on concepts of regenerative medicine. Several strategies like stimulation of resident adult kidney stem cells, mobilization of stem cells from bone marrow to migrate into the injured kidney or injection of mesenchymal stem cells have been proposed or are currently studied.

1.1.1. Endogenous repair of the kidney

Kidneys regulate blood pressure through the renin–angiotensin–aldosterone system, erythrocyte production through production of erythropoietin, and circulating calcium and phosphate levels, in part through the activation of vitamin D. Many of these functions are required to be performed constantly and are accomplished by mechanisms of filtration, re-absorption, and secretion, which take place in the nephron, the functional unit of the kidney. Broadly, at one end of the nephron is the renal corpuscle (glomerulus), the filtration unit, followed by a segmented epithelial tubule devoted to the recapture of essential filtrate elements (Brunskill et al., 2008). Kidney epithelia are exposed to continuous passage of filtrate, and thousands of living cells from healthy humans are excreted daily. For instance, counts of exfoliated nephron tubular cells numbered ~78,000 cells per hour in men and ~68,000 cells per hour in women(Prescott, 1966). These cells need to be replenished regularly to maintain nephron function. Lineage tracing experiments show that a pool of renal tubular cells is poised for division and may serve to bastion against intermittent single cell loss or even more widespread, catastrophic insults(Vogetseder et al., 2008). In the recent years, several groups have isolated human tubule cells that exhibit impressive proliferation capacities *in vitro* and *in vivo* -when administered to mice with acute kidney injury (AKI), which they termed 'renal tubular progenitors' (Angelotti et al., 2012; Bussolati et al., 2005; Lindgren et al., 2011; Smeets et al., 2013). Bussolati *et al*. pioneered the use of the haematopoeitic stem cell antigen, cluster of differentiation 133 (CD133) in characterizing a fast cycling population contributing to repairing the tubule in concert with CD24 and transcription factor PAX2.

AKI causes nephron tubule cell death and local inflammation, followed by high cell proliferation of epithelial cells with or without mesenchymal transition, which restores tubule structure and function. While most post-AKI patients recover their baseline renal function, a significant number, approximately ~20% of those affected, will go on to develop long term illness characterized by an increase in late stage CKD, cardiovascular complications, and increased death rates(Palant et al., 2016).

While tubular progenitors are able to handle AKI, such a response is not suitable for CKD, which is characterized by escalating fibrosis initiated by a primary injury (cell loss/ abnormal cell behavior) at the glomerulus or tubule. The fibrotic lesions that result from excessive proliferation of cells of pericytic origin lead to the emergence of myofibroblasts that propagate over many years, causing nephron dysfunction, atrophy, and collapse, coincident with damage to the vasculature that magnifies fibrogenesis and propagates a vicious damage cycle (Li and

Wingert, 2013). Experimental evidence that abnormal PEC proliferation after glomerular injury can lead to maladaptive glomerular lesions that elicit CKD(Smeets et al., 2009a, 2009b). In other words, renal fibrosis is a wound injury response gone awry. Clinical administration of BMP-7 has been successful in reversing renal fibrosis(Zeisberg and Kalluri, 2008) and the administration of angiotensin-converting -enzyme (ACE) inhibitor reversed proteinuria and CKD progression in patients with non-diabetic chronic nephropathy(Ruggenenti et al., 1999). Evidence from animal models indicated ACE-inhibitor induced changes in glomerular structure including podocyte repopulation (Macconi et al., 2009).

1.1.2. Re-building nephrons for replacement therapy

As witnessed in the scenario of kidney maintenance and repair in acute or chronic injury, the human kidney displays a tendency of compensation by hypertrophy and hyperplasia rather than renewal of nephrons or nephrogenesis. Hence, endogenous regeneration cannot be solely relied upon for reviving kidney health during AKI/CKD. Although few populations of the nephron are regenerated by adult progenitors, is there a possibility to renew a complete nephron? Unlike single-cell disorders like diabetes or amyotrophic lateral sclerosis, the challenge with kidney failure is the creation of a functional organ composed of about 30 cell types organized in a precise three-dimensional structure (Humphreys, 2015). Even after this, how can the host blood supply integrate into the graft? How to plumb in the collecting system to existing ureters? In humans, as in most mammals, nephron formation is a fetal event with final nephron number set before or near birth. Human nephrogenesis ceases around week 36 of gestation (Potter and Thierstein, 1943). Moreover, there is a 10-fold variation in nephron number between individuals, no capacity to form new nephrons after birth and a clear inverse relationship between nephron number and renal disease (. A deeper look at the embryonic development of the kidney and its molecular and cellular basis could help understand these anomalies and how to build a nephron from the beginning.

1.2. Retracing the origin of the kidney

The kidney is embryonically derived by the reciprocal interactions of a nephric mesenchyme and epithelial tissue derived from a portion of the embryo called the intermediate mesoderm, which in turn arises from a mesendodermal population of the tri-laminar embryo. A detailed view of kidney organogenesis from the blastocyst stage of the embryo is described in the following sections.

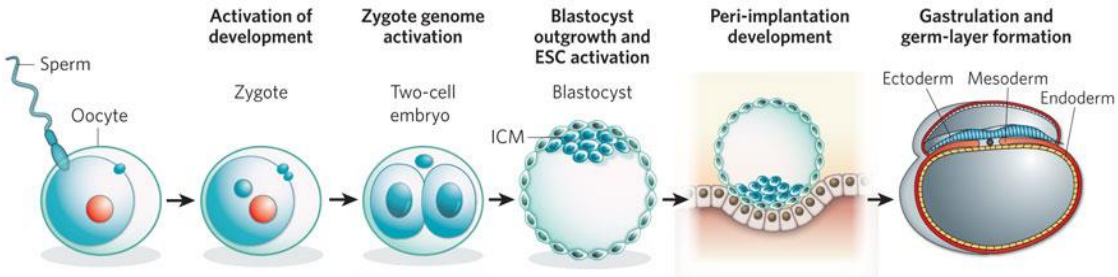

Figure 1: Embryonic events from fertilization to gastrulation (adapted from(Ho and Crabtree, 2010)**).**

1.2.1. The blastocyst: An embryo on the verge of organogenesis

Humans are triploblastic necessitating the generation of the germ layers: ectoderm, endoderm, and mesoderm, through a process called gastrulation. During gastrulation, pluripotent progenitors restrict their fate progressively to one of the three primary germ layers and kick-start organogenesis with the formation of organ primordia. The inner cell mass of the embryo, at the blastocyst stage **(Fig.1)**, forms a 2-layered disc where the lower cell layer is able to differentiate into endoderm and the upper layer into ectoderm without cell movement. Immediately after the formation of these two primary cell layers, the mesoderm arises by invagination and involution of cells from the upper layer. The cells at the surface begin moving to the midline where they involute and migrate laterally to form a mesodermal layer between the ectoderm and endoderm. A furrow along the longitudinal midline marks the site of this involution called the primitive streak (PS) **(Fig.1)**. During gastrulation, cells in the epiblast and their descendants are progressively displaced towards the PS where cellular ingression takes place (Lawson and Pedersen, 1992; Lawson et al., 1991) and are organized into layers of mesodermal cells that constitute the embryonic and extraembryonic mesoderm. The primary cell layer ectoderm gives rise to the epidermis, central nervous system, sense organs, neural crest and endoderm gives rise to the lining of the digestive and respiratory tracts; liver and pancreas. Lastly, the mesoderm gives rise to, the skeleton, muscles, blood vessels, heart, gonads and most importantly the kidney, our organ of interest. Therefore, we delve further into understanding the mesoderm and its derivatives.

1.2.2. Mesoderm

Fate-mapping studies of the mesoderm of a gastrulating embryo reveals that cells that are destined for the extraembryonic mesoderm constitute the major tissue type in the nascent mesodermal layer (Kinder et al., 1999). During embryonic trunk elongation, the nascent mesodermal cells divide, continually pushing out daughter cells toward the rostral region. After migration, these cells divide into paraxial mesoderm, lateral plate and intermediate mesoderm

(Takasato and Little, 2015).The precursors for cranial and heart mesoderm are present later in the mesodermal layer of the mid-streak stage embryo, but are ahead of those that contribute to the paraxial and lateral mesoderm of the trunk, which form the bulk of the embryonic mesoderm in the late-streak embryo (Parameswaran and Tam, 1995; Tam and Behringer, 1997). These studies also show that the various mesoderm precursors are distinctly regionalized in the mesodermal germ layer and their relative position is concordant with their final location in the fetal body. An examination of the regional distribution of PS-derived cells in the paraxial mesoderm has revealed that PS cells are allocated to the somites in a cranio-caudal manner(Tam and Beddington, 1987).

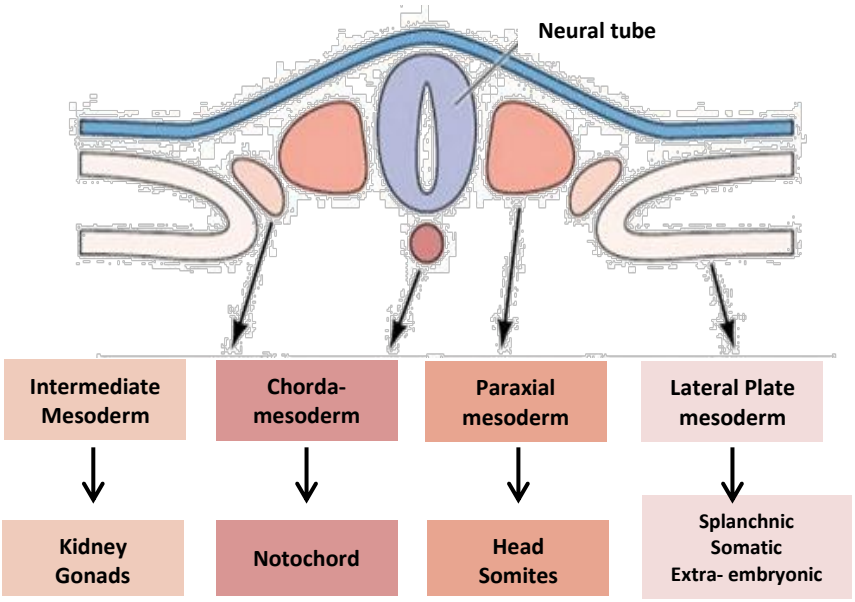

Figure 2: Constituents of the mesoderm and their derivatives (adapted from Scott.F.Gilbert 2000)

The trunk mesoderm of a neurula stage embryo can be subdivided into four regions (**Fig.2,**(Gilbert, 2000)):

- The central region of trunk mesoderm is the chorda-mesoderm. This tissue forms the notochord, a transient organ whose major functions include inducing and patterning the neural tube and establishing the anterior-posterior body axis.
- Flanking the notochord on both sides is the paraxial, or somitic, mesoderm (PM). The tissues developing from this region will be located in the back of the embryo, surrounding the spinal cord. The cells in this region will form somites—blocks of mesodermal cells on either side of the neural tube—which will produce muscle and many of the connective tissues of the back (dermis, muscle, and skeletal elements such as the vertebrae and ribs). The anterior-most PM does not segment; it becomes the head mesoderm, which (along with the neural crest) forms the skeleton, muscles, and

connective tissue of the face and skull.

- The intermediate mesoderm (IM) forms the urogenital system, consisting of the kidneys, the gonads, and their associated ducts. The outer (cortical) portion of the adrenal gland also derives from this region.
- Farthest away from the notochord, the lateral plate mesoderm (LPM) gives rise to the heart, blood vessels, and blood cells of the circulatory system, as well as to the lining of the body cavities. It gives rise to the pelvic and limb skeleton (but not the limb muscles, which are somitic in origin). LPM also helps form a series of extraembryonic membranes that are important for transporting nutrients to the embryo.

Along the medio-lateral (center-to-side) axis these four subdivisions are thought to be specified by increasing amounts of bone morphogenetic proteins (BMPs) (Pourquié et al., 1996; Tonegawa et al., 1997). The more lateral mesoderm of the chick embryo expresses higher levels of BMP4 than do the midline areas, and one can change the identity of the mesodermal tissue by altering BMP expression (Gilbert, 2000). During the development of IM, a low level of BMP signaling is required for the formation of the nephric duct and nodal/activin expressed by LPM is essential for IM specification (Fleming et al., 2013; Obara-Ishihara et al., 1999).The PM appears to be both necessary and sufficient for inducing kidney-forming ability in the IM, since co-culturing LPM with PM causes pro-nephric tubules to form in the LPM, and no other cell type can accomplish this(Mauch et al., 2000). Along the anterior-posterior axis, the determination of the rostral versus caudal fate of the IM is governed by opposing gradients of retinoic acid (RA) and fibroblast growth factor (FGF) signaling as studied in *Xenopus* and chick models (Amaya et al., 1993; Duester, 2008; Yatskievych et al., 1997).

1.2.3. Intermediate mesoderm

In the chick embryo, Pax2 and Lim1 are expressed in the IM, starting at the level of the sixth somite (i.e., only in the trunk, not in the head). If Pax2 is experimentally induced in the pre-somitic mesoderm, it converts that paraxial mesoderm into IM, causing it to express Lim1 and form kidneys(Mauch et al., 2000). In mice, Lim1 and Pax2 proteins appear to induce one another. The anterior border of the Lim1- and Pax2-expressing cells appears to be established by the cells above a certain region losing their competence to respond to activin, secreted by the neural tube. This competence is established by the transcription factor Hoxb4, which is not expressed in the anterior-most region of the intermediate mesoderm(Gilbert, 2000). The anterior boundary of Hoxb4 is established by a retinoic acid gradient, and adding activin locally

will allow the kidney to extend anteriorly(Barak et al., 2005; Preger-Ben Noon et al., 2009). In mice, the transcriptional regulator Osr1 is expressed broadly in the IM mesenchyme beginning at E7.5 and its activity is essential for development of multiple IM derived structures (James et al., 2006; Wang et al., 2005). Descendents of Osr1+ cells initially contribute to all kidney compartments and are restricted to nephron progenitors after E11.5 (Mugford et al., 2008). Careful lineage analysis in mouse suggests that the collecting ducts of the kidney arise from progeny of the anterior IM which form a Wolffian duct, whereas the nephrons arise from the progeny of the posterior IM, the metanephric mesenchyme (**Fig.3,**(Taguchi et al., 2014)). The origin of the vasculogenic endothelial progenitors and the surrounding stromal cells is less defined but is also likely to be IM, possibly from the posterior end. Importantly, cells present within these anterior and posterior regions are exposed to distinct spatio-temporal signals(Taguchi et al., 2014; Takasato and Little, 2015).

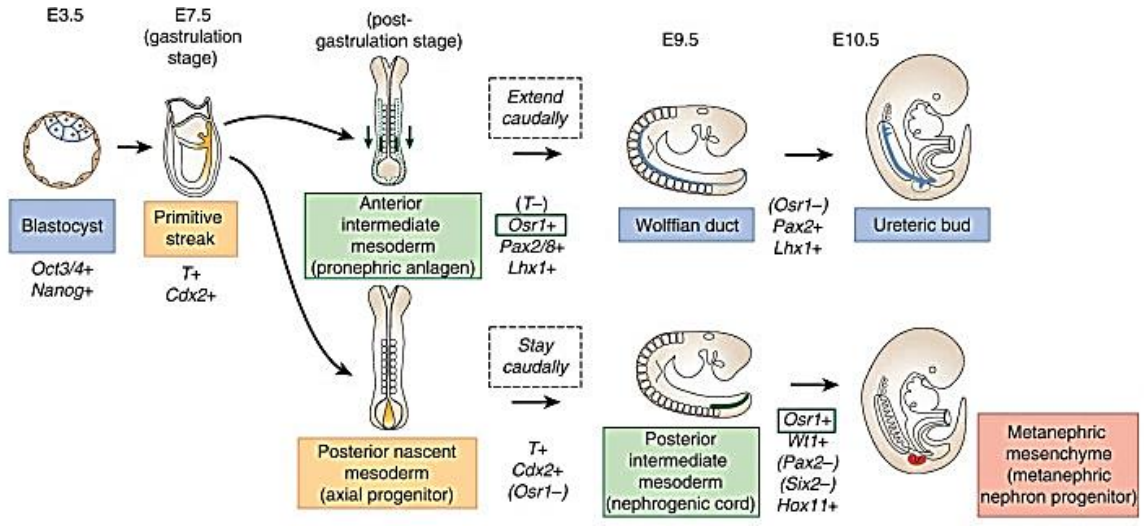

Figure 3: Novel model for lineage segregation of ureteric bud (UB) and metanephric mesenchyme (MM) proposed by Taguchi 2014.

1.2.4. Nephrogenesis

1.2.4.1. Nephric duct/Wolffian duct

The nephric duct (ND) is a tubular structure essential for the formation and function of the vertebrate excretory and reproductive systems. In mammalian and avian embryos, the ND is derived from the "duct primordium," an aggregate of mesenchymal cells that arises in the IM on both sides of the embryo at the axial levels of somites 6–10 (Attia et al., 2012)). Subsequently, the duct primordia elongate in a posterior (caudal) direction until they fuse

with the cloaca at the caudal end of the embryo. As the ND elongates, the cells that comprise it undergo mesenchymal to epithelial transition, and interactions between the duct and adjacent mesodermal cells induce formation of the mesonephros (the embryonic/fetal kidney) and the metanephros (the adult kidney). The ND itself gives rise to the collecting ducts of the kidney and the ureter, which drain urine from the kidney, and in males to the spermatic duct. If ND elongation is inhibited, none of these structures are formed (Soueid-Baumgarten et al., 2014; Waddington, 1938). FGF signaling is required for (non-directional) ND migration together with glial-derived neurotrophic factor (GDNF) (Attia et al., 2015; Drawbridge et al., 2000). Both FGF-receptors-2 and -3 are initially expressed in the duct, although in later embryos only FGFR2 expression can be detected, suggesting that FGFR2 is more likely to be critical for duct migration(Attia et al., 2015).

1.2.4.2. Pronephros and Mesonephros

Early in development (day 22 in humans; day 8 in mice), the pronephric duct arises in the IM just ventral to the anterior somites. The cells of this duct migrate caudally, and the anterior region of the duct induces the adjacent mesenchyme to form the pronephros, or tubules of the initial kidney (**Fig.4**(Romagnani et al., 2013)). The pronephric tubules form functioning kidneys in fish and in amphibian larvae, but they are not active in amniotes. In mammals, the pronephric tubules and the anterior portion of the pronephric duct degenerate, but the more caudal portions of the pronephric duct persist as the ND and serve as the central component of the excretory system throughout development (Saxén and Sariola, 1987). As the pronephric tubules degenerate, the middle portion of the ND induces a new set of kidney tubules in the adjacent mesenchyme. This set of tubules constitutes the mesonephros, or mesonephric kidney.

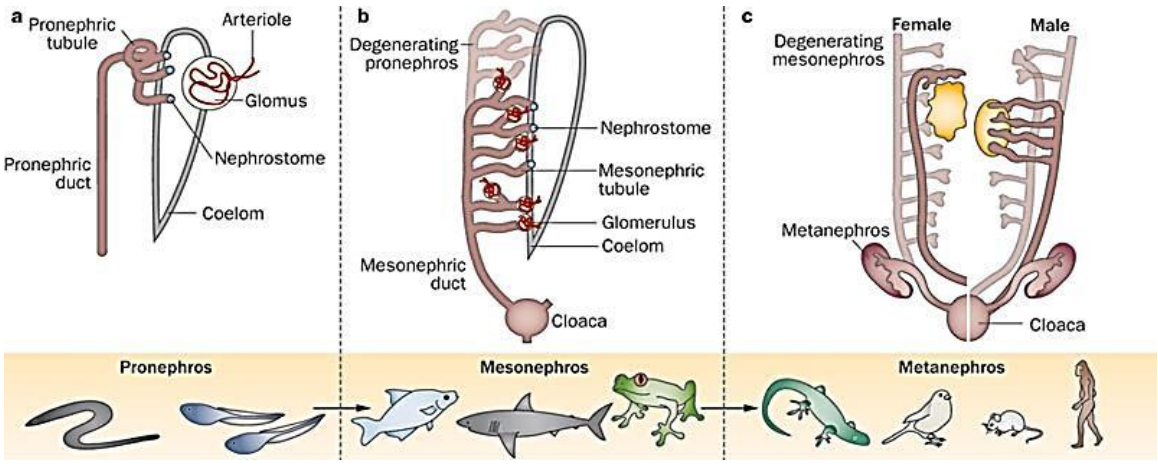

Figure 4: The kidney through evolution and maturation (Romagnani 2013).

The human mesonephros begins to develop in the fourth week of gestation and contains well-developed nephrons comprising vascularized glomeruli connected to proximal and distal type tubules draining into the mesonephric duct, itself a continuation of the pronephric duct. The mesonephric duct extends to fuse with the cloaca, the urinary bladder precursor, at the end of the fourth week. In some mammalian species, the mesonephros functions briefly in urine filtration, but in mice and rats it does not function as a working kidney. In humans, about 30 mesonephric tubules form, beginning around day 25(Woolf and Pitera, 2009). The pronephros and mesonephros can be regarded as a single unit, and as the wave of differentiation spreads caudally, the cranial end of this organ complex begins to regress. While it remains unknown, whether the human mesonephros actually filters blood and makes urine, it is one of the main sources of the hematopoietic stem cells necessary for blood cell development(Medvinsky and Dzierzak, 1996; Wintour et al., 1996). Second, in male mammals, some of the mesonephric tubules persist to become the tubes that transport the sperm from the testes to the urethra (the epididymis and vas deferens (Gilbert, 2000).

1.2.4.3. Metanephros

The metanephros is the last embryonic kidney to develop and represents the functioning kidney in humans. It consists of two components. These are the ureteric bud (UB) epithelium, which branches from the caudal part of the mesonephric duct around 4 weeks of gestation, and the metanephric mesenchyme (MM), which condenses from the IM around the enlarging tip, or ampulla, of the bud (Potter 1972,(Woolf and Pitera, 2009)). In humans, the metanephric kidney can be identified as an entity around week 5–6 of gestation. The UB and its branches form epithelia of the collecting ducts, renal pelvis, ureter and bladder trigone, whereas the MM differentiates into nephron tubules (glomerular, proximal tubular, and loop of Henle epithelia). The metanephric (permanent) kidney develops by means of a series of iterative branching and inductive events between the UB and adjacent MM. Repeated rounds of branching morphogenesis and nephron induction occur within the nephrogenic zone, the birthplace of a nephron, located at the tip of every ureteric branch (**Fig.5**).

Three major cellular compartments are represented within the nephrogenic zone:

(i) A nascent Wnt11^{+} ureteric tip epithelium which undergoes successive rounds of branching, elongation, and differentiation to form the collecting ducts;

(ii) A multipotent, self- renewing, nephrogenic progenitor $Six2^{+}$; $Cited1^{+}$ cell population (Kobayashi et al., 2008; Rothenpieler and Dressler, 1993) (cap mesenchyme) that is induced to condense along the surface of the ureteric tips, undergo a mesenchymal-to-epithelial transition (MET) and form the nephron epithelium; and

(iii) An outer layer of $Foxd1^{+}$ mesenchymal stromal/interstitial cells that contribute to the renal capsule and the interstitium interspersed with $Flk1^{+}$ vascular progenitors.

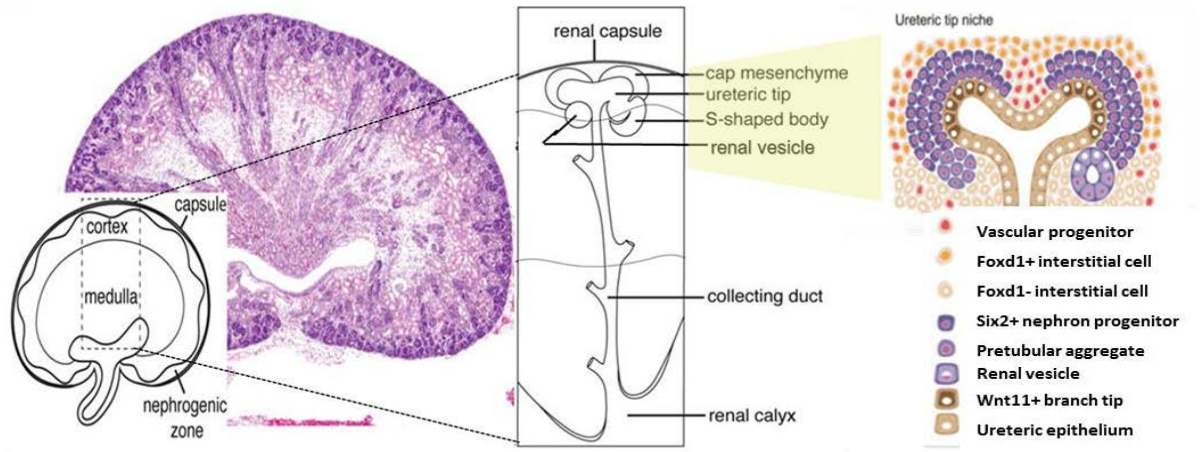

Figure 5: Detailed view of a mouse metanephros. The developing metanephros consists of discrete compartments. The renal capsule envelops the kidney and contains capsular stromal cells. The outer cortex (nephrogenic zone) beneath the capsule is the site where nephrogenesis is initiated. The inner cortex consists of maturing nephrons. The medulla lies interior to the cortex and contains developing tubules that penetrate deep into the kidney tissue. Cellular and molecular organization of collecting duct (Wnt11+), nephron (Six2+), interstitial (Foxd1+), and vascular progenitors within a ureteric tip niche.(Adapted from (Li et al., 2014; McMahon, 2016))

Successive waves of nephron induction in the nephrogenic zone propagate centrifugal growth and expansion of the kidney, inwardly displacing older generations of ureteric tips, renal vesicles, and stromal progenitors. The nephrogenic progenitor $Six2^{+}$ cell population also called the uninduced MM (uiMM) is highly proliferative and responsive to Fgf9/Fgf20 and Bmp7 **(Fig. 6)**. These cells are called induced MM (iMM) once they attain a Cited1+ state, and are responsive to Wnt9b that coaxes a mesenchymal-epithelial transition generating a $Lef1^{+}/Six2^{-}$ population, a pre-tubular aggregate (PTA) stage(Brown et al., 2013). Wnt9b signaling activates expression of secondary signals, Fgf8 and a second Wnt member, Wnt4, within PTAs triggering the formation of an epithelial structure with a lumen -the precursor of the nephron epithelial tube and is called the renal vesicle (RV). (*Genes important in these morphogenic events are listed in a separate table- Table 15*).

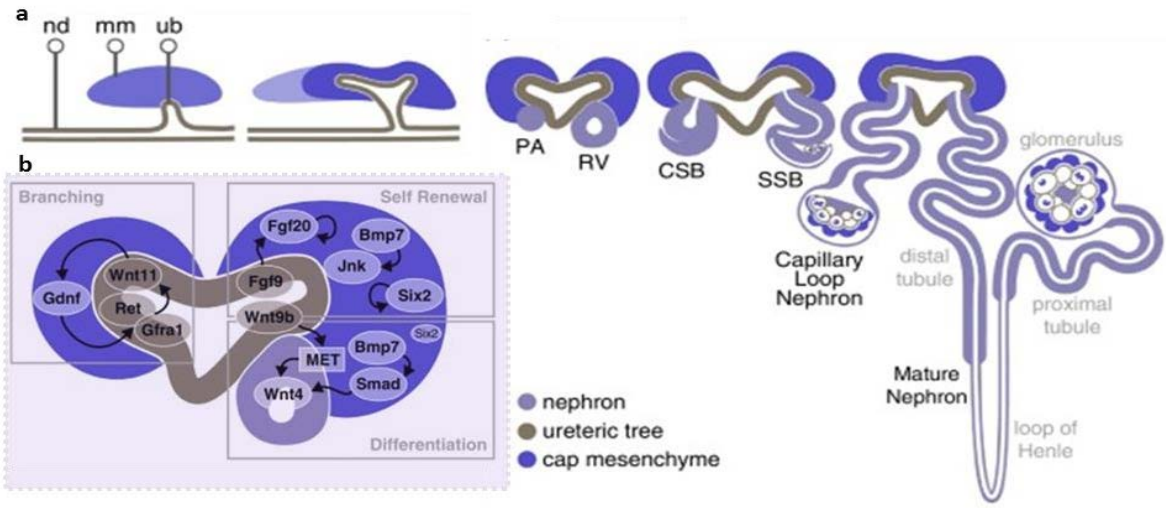

Figure 6: Key inductive events in mammalian kidney morphogenesis Diagram showing the formation of the UB as a swelling of the ND which grows towards the MM before undergoing initial bifurcation and the stages of nephron maturation from PTA through RV, CSB(Comma-shaped body), SSB (S-shaped body), capillary loop nephron and mature nephron. b) Diagram of a nephrogenic niche illustrating the signaling pathways critical for branching (left) versus cap mesenchyme self-renewal (top right) and differentiation (bottom right). (Adapted from Little 2015)

1.2.4.4. Stage I and II nephrons: Renal vesicle and S-shaped body

The RV represents the point of transition from mesenchyme to a polarized epithelial state. Because the kidney expands as a sphere from a central starting point, researchers consider the center to peripheral axis as the proximal–distal axis in describing the relative position of emerging structures within the MM. Thus, peripheral structures become distal and closer to the cortex than to the medulla. Nascent epithelial structures always appear on the proximal side of the UB tip, and their own proximal–distal axis remains aligned, with the duct tip marking the distal end (Kopan et al., 2007). Proximal–distal polarity within nascent nephrogenic bodies is morphologically apparent in the comma-shaped body, formed because the first cells to elongate, change shape, and form a "slit" are located at the proximal end, farthest from the ureteric bud (Saxén and Sariola, 1987). Proliferation and differential adhesion may be the drivers that contort the comma-shaped body into an S-shaped structure that fuses at its distal end with the UB while podocyte precursors emerge at its most proximal end. Variations in the levels of β-catenin activity in the nephron, within a gradient are directly responsible for correct patterning, controlled by the intermingling Wnt and Notch signaling pathways (Lindström et al., 2014).

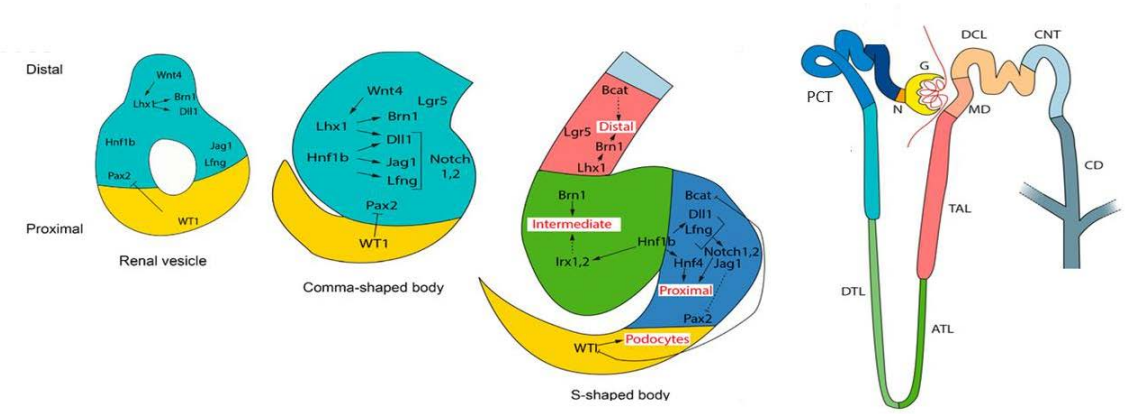

Figure 7: Genetic pathways of nephron segmentation in mice. Genes described in Appendix-Table, right panel nephron showing G: glomerulus; N: neck; PS1, PS2, and PS3: segments of the proximal tubule, DTL: descending thin limb, ATL: ascending thin limb; TAL, thick ascending limb, MD: macula densa, DCT: distal convoluted tubule, CNT: connecting tubule; CD: collecting duct (Adapted from (Desgrange and Cereghini, 2015)**)**

Several distinct cell-populations form and these produce the different segments of the adult nephron(Saxén and Sariola, 1987) as seen in **Fig.7**; a Wt1+ cell population gives rise to proximal structures including the glomerulus and a segment of proximal tubules, a Jag1+ population to the medial part- proximal tubules and loop of Henle; and Lgr5+ cells generate the distal nephron segments - distal convoluted tubules (Barker et al., 2012; Chen and Al-Awqati, 2005; Cheng et al., 2007; Kreidberg, 2010). These segments are in turn further subdivided into functionally specialized portions of the adult nephron, which express specific combinations of transmembrane transporters/channels for salts, glucose, and metals (Raciti et al., 2008).

1.2.5. Stage IV: Adult nephron

1.2.5.1. Corpuscle

The renal corpuscle is composed of two parts: a tuft of capillaries and mesangial cells called glomerulus and a double-walled epithelial capsule called Bowman's capsule. The interior of Bowman's capsule (Bowman's space) is continuous with the proximal convoluted tubule. The glomerular capillary tuft in each glomerulus arises from the afferent arteriole that brings blood to the glomerulus and eventually coalesces to form the efferent arteriole that takes blood away from the glomerulus(Kriz and Kaissling, 2013).

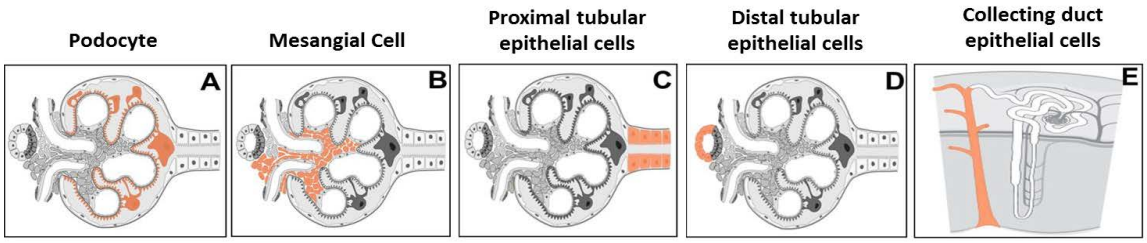

Figure 8: Constituent cell types of the nephron [Source: Cellfinder.de]

Mesangial cells are modified smooth muscle cells, and lie in between the glomerular capillaries (Fig.8 B). They generate extracellular matrix, regulate capillary flow and ultrafiltration surface and produce prostaglandins and cytokines. The outer layer of the Bowman's capsule is the outer boundary of the renal corpuscle and formed by a single layer of squamous epithelial cells called parietal cells. The inner visceral layer of the Bowman's capsule is composed of modified epithelial cells known as podocytes, which have foot-like processes called pedicels that wrap themselves tightly around endothelial cells of the glomerular capillaries which are fenestrated. These pedicels inter-digitate, to form filtration slits, leaving small gaps between the digits to form a sieve. The association of the glomerular capillary endothelial cells and podocytes leads to the formation of the glomerular filtration barriers (also referred to as the blood-to-urine barriers). The filtration barrier is formed by three components: the diaphragms of the filtration slits, the thick glomerular basement membrane, and the glycocalyx secreted by podocytes. Overall, filtration is regulated by fenestrations in capillary endothelial cells, podocytes with filtration slits, membrane charge, and the basement membrane between capillary cells. Any proteins that are roughly of molecular weight 30 kDa or under, can pass freely through the filtration barrier. Between the visceral and parietal layers is a Bowman's space, into which the filtrate enters after passing through the filtration slits of podocytes. Any small molecules such as water, glucose, salt (NaCl), amino acids, and urea pass freely into the Bowman's space, but cells, platelets and large proteins do not. As blood passes through the glomerulus, 10 to 20 percent of the plasma filters at the filtration membrane to be captured by the Bowman’s capsule and funneled to the proximal convoluted tubule as the glomerular ultra-filtrate(Kriz and Kaissling, 2013).

1.2.5.2. Tubulus

The first part of the renal tubule is called the proximal convoluted tubule (PT), which has convoluted early and intermediate segments S1 and S2 in the renal cortex and a straight segment S3 that enters the outer medulla. Water and solutes that have passed through the proximal convoluted tubule enter the Loop of Henle, which consists of two portions - first the descending limb of Henle, then the ascending limb. In order to pass through the Loop of Henle (LOH), the water (and substances dissolved in it) pass from the renal cortex into the renal medulla, and then back to the renal cortex. When this fluid returns to the renal cortex (via the ascending limb of Henle) it passes into the distal convoluted tubule (DT). The fluid that has passed through the distal convoluted tubules is drained into the collecting duct. The distal convoluted tubules of

many individual kidney nephrons converge onto a single collecting duct that drains into the calyces.

The PT is composed of a single layer of cuboidal epithelial cells equipped with microvilli that aid in re-absorbing approximately two-thirds of the filtered salt and water and all filtered organic solutes (primarily glucose and amino acids) from the ultra-filtrate into the peritubular capillaries. The primary role of the LOH is to concentrate the salt in the interstitium, the tissue surrounding the loop. While the descending limb is impermeable to salt, allowing water to be transported over the osmotic gradient, the ascending limb is impermeable to water and actively pumps sodium out of the filtrate, generating the hypertonic interstitium that drives countercurrent exchange. By the time the filtrate reaches the DT, it is hypotonic as a huge amount of sodium was lost. Although composed of the same cuboidal epithelial cells as the PT, cells of DT have fewer microvilli and mitochondria and are susceptible to endocrine regulation. Aldosterone increases the amount of Na+/K+ ATPase in the basal membrane of the DT and collecting duct thereby causing sodium to move out of the filtrate. Aldosterone is secreted by the adrenal cortex in response to angiotensin II stimulation. Receptors for parathyroid hormone (PTH) are found in DT cells and when bound to PTH, induce the insertion of calcium channels on their luminal surface thus recovering calcium from the filtrate. Regulation of urine volume and osmolarity are major functions of the collecting ducts. By varying the amount of water that is recovered, the collecting ducts play a major role in maintaining the body's normal osmolarity, regulated by the anti-diuretic hormone (ADH or vasopressin) secreted by the posterior pituitary. When stimulated by ADH, aquaporin channels are inserted into the apical membrane of principal cells, which line the collecting ducts allowing water to be osmotically extracted from the collecting duct (CD) into the surrounding interstitial space and into the peri-tubular capillaries, thereby concentrating the filtrate into urine(Matlin and Caplan, 2013).

In humans, nephrogenesis is complete by 36 weeks. Furthermore, there is no evidence to suggest that new nephrons can be formed after this time point. The above sections have defined the key steps in nephron development. In order to generate kidney replacements, we need to recapitulate nephrogenesis *in vitro*. Producing all cell types that lead to nephronal cell types necessitate the use of stem cells which are described in the sections that follow.

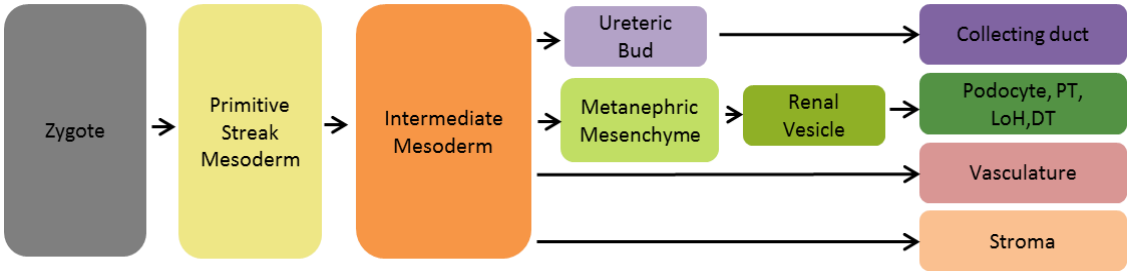

Figure 9: Developmental milestones in kidney organogenesis.

1.3. A Toolbox for human embryology – Pluripotent stem cells

While our knowledge on the structure and function of mature organs is mostly derived from animal models, human cadavers, or biopsies, the information we have on embryonic organ development is largely derived from various model organisms and from technologies that study human embryogenesis *in vitro*. In 1944, the first human egg was fertilized *in vitro*(Rock and Menkin, 1944). Edwards and Steptoe implanted a fertilized egg into a woman's uterus in 1977(Steptoe and Edwards, 1978) giving the world its first test tube baby. These scientists were also paving the way for a closer observation of human embryonic development. Edwards and his team had worked on growing human embryos *in vitro*, until the blastocyst stage (Edwards et al., 1981)before re-implanting the embryo into the uterus. Knowing that *in vitro* culture was a suitable interim step in producing a viable organism spurred the goal of replacing damaged organs by transplanting organoids produced *in vitro*. Key advances in this field included the derivation of human embryonic stem cells (hESCs) from the inner cell mass of normal human blastocysts(Thomson et al., 1998) and the generation of induced pluripotent stem cells (iPSCs)(Takahashi and Yamanaka, 2006; Takahashi et al., 2007). These cells demonstrate evidence of stable developmental potential even after prolonged culture forming derivatives of all three embryonic germ layers from the progeny of a single cell. A huge advantage of iPSCs over ESCs is the possibility to have pluripotent stem cells from every individual, providing an opportunity to study and repair genetic disorders at a personal level. Pluripotency has been exploited to recapitulate many embryonic processes *in vitro*, including primitive streak formation, neural tube induction, and trophoblast formation, extending to the generation of functioning neurons, beating cardiomyocytes, and insulin producing beta cells of the pancreas. Major achievements in the field of stem cell biology have been the derivation of a multitude of differentiated cell types morphologically similar to their terminally differentiated counterparts *in vivo*, but functionally immature *in vitro*, that have been intended to be used as regenerative cell sources in degenerative disease conditions.

1.3.1. Breaking pluripotency

Humans are triploblastic and thus, develop a tri-laminar embryo upon gastrulation, consisting of ectoderm, endoderm, and mesoderm. Several groups have cultured PSCs in a feeder free matrix-coated surface and promoted differentiation by adding growth factors and inhibitors to this 2D system, while other groups applied inductive media to a 3D system, after the generation of a sphere of PSC cells known as an embryoid body (EB). Protocols applying defined time periods and concentrations of exposure to inductive agents have allowed for the differentiation of endo-, ecto-, or mesodermal lineages and specific cell types. For example, activin signaling leads to 80% efficient induction of SOX17+/GSC+/FOXA2+/MIXL1+ definitive endoderm in hESC cultures after 5 days of differentiation in 100 ng/ml activin A (D'Amour et al., 2005). In another seminal study, sequential treatment of high-density undifferentiated monolayer hESC cultures with activin A for 24 h and bone morphogenetic protein 4 (BMP4) for 4 days consistently yielded >30% cardiomyocytes (Laflamme et al., 2007). For neural induction of hESCs, the growth factors insulin, epidermal growth factor (EGF) and basic fibroblast growth factor (bFGF) were added in a chemically defined medium, giving rise to up to 90% PAX6+ neural progenitors(Joannides et al., 2007). These studies have proved that while a spontaneously differentiating mass of PSC can generate varying proportions of endo- and ecto- and mesoderm, targeting signaling pathways prominent in the development of an organ of interest in a temporal fashion can promote that particular lineage. Over the years, researchers have tested various combinations of cell signaling modifiers to achieve enrichment of tissue-specific cell types in a heterogeneous population of differentiated PSC progeny (reviewed by (Murry and Keller, 2008)). Moreover, the level of enrichment varies with the iPSC or ESC used. iPSC that are reprogrammed from a somatic cell type originating from an organ and are differentiated to a cell type of the same organ, show higher efficiencies owing to epigenetic memory of the source (Hiler et al., 2015). This highlights the need for standardization of protocols with certain PSC lines for certain lineages.

1.3.2. State of the art in developing kidney cells from PSC

Unlike other organs, few protocols have been established for the kidney. The kidney exhibits a remarkable architectural complexity coupled with the presence of at least 26 different specialized cells (Al-Awqati and Oliver, 2002). Based on earlier studies that highlighted important molecules and pathways that drive mesodermal and nephron differentiation in model

organisms, initial studies of differentiation toward the renal lineage were performed on mouse ESC-EBs treated with media containing serum together with multiple combinations of factors including activin A, BMP4, BMP7, RA, leukemia inhibiting factor (LIF), and GDNF or UB-derived conditioned media. These protocols led to the generation of cells expressing markers of differentiation, e.g., Pax2 (kidney tubules), Aquaporin-2 (collecting duct principal cells), Wt1 (metanephric mesenchyme and podocytes), or Ksp-Cadherin (distal nephron tubules), within EBs, which provided evidence of successful renal lineage induction (Bruce et al., 2007; Kobayashi et al., 2005b; Morizane et al., 2009; Nishikawa et al., 2012; Ren et al., 2010; Vigneau et al., 2007). Although a renal identity was achieved in the examples mentioned before, the desired cell types could not be isolated owing to low and varying frequencies of occurrence and their functionality was not demonstrated.

Meanwhile, genetic lineage tracing demonstrated that the induced Six2-expressing cap mesenchyme represents a nephron progenitor population that gives rise to all cell types of the nephron (Kobayashi et al., 2008). Also, the intermediate mesodermal origin of kidney cells was confirmed when Mugford *et al.,* used molecular fate mapping to demonstrate that the majority of cell types within the metanephric kidney arise from an Osr1-expressing population within the intermediate mesoderm (Mugford et al., 2008). These new findings were considered in differentiation protocols to distinguish the exact mesodermal cell sub-type required to enrich cultures of PSC-derived renal progeny. For instance, Mae *et al* developed a robust protocol using activin A and Wnt-agonist CHIR99021 for 2 days and sequential treatment with BMP7 and CHIR99021 for 8 days to obtain 90% OSR1+ cells (Mae et al., 2013). Despite such an efficient protocol, the dependence on OSR1 as a population identifier created ambiguity, since even though OSR1 is expressed in the intermediate mesoderm, it is also expressed in the earlier mesoderm prior its subdivision into paraxial and intermediate domains (Guillaume et al., 2009). Moreover, OSR1 is expressed in both the intermediate mesoderm and lateral plate (James and Schultheiss, 2003; Wilm et al., 2004).

Additional protocols were developed to induce different cell types within the nephron. Human PSC derived podocytes expressing Podocin, Nephrin, and Synaptopodin were generated from EBs using treatment with activin A, RA, and BMP7 and plating on gelatin (Song et al., 2012). In another study, ~90% AQP1+ proximal tubule cells were obtained by treating a monolayer PSC culture with media containing renal epithelial growth medium for 9 days (Kandasamy et al., 2015). Recent reports demonstrated stepwise induction of UB and/or MM through systematic induction of primitive streak alone, followed by intermediate mesodermal

specification (Lam et al., 2014; Taguchi et al., 2014; Takasato et al., 2014; Xia et al., 2013, 2014). These studies performed thorough characterization of cell types obtained at every stage; focusing on obtaining PAX2+ GATA3+ LHX1+ UB cells(Xia et al., 2013) and SIX2+ PAX2+GDNF+ HOX11+ WT1+ MM cells(Taguchi et al., 2014). Takasato et al. were able to generate UB and MM between 14 and 18 days, whereas Lam et al generated SIX2+ SALL1+ WT1+ cap mesenchyme by 8 days and showed the potency of PAX2+ LHX1+ IM cells to generate tubule structures that express Lotus lectin and Ksp-Cadherin after 9 days of differentiation (Lam et al., 2014; Takasato et al., 2014).

Table 1 : Methods of differentiation to renal cell types

CELL TYPE	GROWTH FACTORS	MARKERS /STAGE OF RESULTING POPULATION	REFERENCE
mESC (Rosa26)	RA , Activin-A, BMP RA+ActA+BMP4 [RA4 cocktail] and RA+ActA+BMP7 [RA7 cocktail]	Pax2, Wt1, Lim1, Gdnf and Cdh6	Kim and Dressler 2005
mESC , miPSC	Activin A, GDNF , BMP7 , LIF , Gremlin , Gdf11 Wnt4 Conditioned medium from CMV-Wnt4 transfected NIH3T3 cells	Pax2,Wt-1,KSP	Morizane 2009
mESC	RA and Activin-treated EBs and Conditioned medium from fetal ureteric bud cell culture	Pax2, Brachury	Ren 2010
hESC	Reduction of serum concentration and feeder layer density reduction cultures	Pax2, Lhx1, Wt1	Lin.2010
hiPSC	RA+ActA+BMP7	Synaptopodin, Nephrin , WT1	Song, 2012
hiPSC	ActA/Wnt3A/BMP7	Osr1 – capable of embryonic kidney repopulation	Mae, 2013
hESC	REGM+B7, B2, ActA, R.A	Ksp-Cadherin, transporters	Narayanan 2013
hPSC	BMP4+ FGF2, RA+ Activin A+ BMP2	UB progenitors in 4 days	Xia. 2013
hPSC	CHIR99021, FGF2 + RA, FGF9+ Activin	MM progenitors in 7 days	Lam 2014
hPSC	CHIR99021, FGF9	Mixture of UB and MM in 12-18 days	Takasato 2014
hiPSC	BMP4, Activin A, RA, FGF9, high to low CHIR99021	MM in 14 days	Taguchi 2014
hiPSC	CHIR99021+ AM580/TTNPB, AM580/TTMPB	IM cells in 5-14 days	Osafune 2014
hiPSC	REGM	PT cells in 9 days	Kandasamy 2015

Partial self-organization of mouse embryonic kidney cells upon their re-aggregation, after dissociation was first achieved by Unbekandt and Davies (2010) – an example of an architecturally intact kidney *in vitro*. The novelty of this system was the introduction of a ROCK inhibitor, which prevented the dissociation-induced apoptosis within single cell suspensions

and facilitated a significant recovery of re-aggregated tissues. The Unbekandt re-aggregation method has since then been used as a test system to check the capacity of cells (e.g., PSC-derived cells) to integrate into forming tubules or glomeruli of the mouse nephron. While this method proves the property of test cells to contribute to kidney formation, it cannot provide proof of self-organization of PSC-derived renal progenitors.

Table 2: Status of lab-grown kidney organoids(Hariharan et al., 2015)

CELL SOURCE	DESCRIPTION	REFERENCE
In vitro		
Embryonic cells	Suspension culture of dissociated-reaggregated chick mesonephric cells.	Moscona 1952
	Culture at air–medium interface of dissociated- reaggregated mouse metanephric cells.	Unbekadnt 2010
Adult cells	Collagen matrix embedded murine and human renal cells	Joraku 2009 and Guimaraes-Souz 2012
PSC- derived cells	2-D culture of 18 day differentiated hPSC.	Takasato 2014
	14-day differentiated EBs induced with mouse embryonic spinal cord.	Taguchi 2014
	3-D nephron organoids after 25 days of differentiation in a pellet.	Takasato 2015
	3-D kidney organoids in suspension	Lam 2015
	3-D kidney organoids in matrigel sandwich culture from epiblastoid spheres.	Freedman 2015
In vivo		
Embyonic cells	Mouse metanephric cells cultured on CAM of avian embryos.	Preminger 1980
	Rat metanephroic cells transplanted in the omentum of a rat.	Hammerman 2002
	Mouse metanephric cells cultivated in mouse lymph node.	Francipane 2015
PSC-derived cells	Mouse embryonic spinal cord-induced EBs transplanted under the kidney capsule of mice	Taguchi 2014
	Sall1- deficient mouse blastocyst, complemented with wildtype mouse PSCs.	Usui 2012

To this end, kidney organogenesis from PSC have been reported by Takasato et al., where 18 days of differentiation of PSC seeded initially on Matrigel, develop an ECAD+ ureteric epithelium surrounded by clumps of SIX2+ WT1+ PAX2+ MM cells or JAG1+ CDH6+ renal vesicles (Takasato et al., 2014). Lam *et al.* also observed appearance of tubule-like structures positive for Lotus lectin (a proximal tubule marker) from SIX2+ cap mesenchyme cell cultures, obtained on day 7 of their differentiation procedure, upon treatment with CHIR99021(Lam et al., 2014). This was reminiscent of induced metanephric mesenchyme that responds to Wnt signals to undergo mesenchymal-epithelial transition and form renal vesicles *in vivo* (Park et al., 2007; Schmidt-Ott et al., 2007). Meanwhile, the group of Nishinakamura also obtained evidence of a slightly different nature. They used PSC in the form of EBs for a differentiation protocol that took 8.5 days in mouse ESCs and 14 days in human iPSCs, resulting in SIX2+ WT1+ SALL1+ PAX2+ MM cells that could give rise to tubules and podocytes when induced

by mouse embryonic spinal cord(Taguchi et al., 2014). These studies are evidence that a systematic mirroring of embryonic kidney development in PSC derivatives can lead to the formation of organo-typical structures, as summarized in **Table 2**.

1.4. Research gap

The last five years have brought us a step closer to develop nephrons *in vitro*, yet, there is clearly a need to enhance protocols to achieve full maturation of nephrons that have on one hand a filtering unit and on the other hand an optimal spatial orientation of tubules that trigger their functionality in terms of electrolyte transport. Together, these important studies provided proof of principle that most, if not all components of the kidney can be induced from PSCs. The PSC-derived UB cells can be utilized to generate a ureteric tree or PSC-derived MM cells can be coaxed to produce S-shaped bodies that undergo proximal distal patterning initiating tubulogenesis, giving rise to fetal nephrons in culture. It would also be interesting to use cells derived from the Xia and Taguchi protocols to obtain reciprocally interacting UB & MM and investigate if they interact in a similar manner as they do *in vivo*. Since most kidney diseases involve the damage and loss of podocytes or hypertrophy of tubular epithelial cells, these cell types have a high priority of being derived. On the other hand, the big picture of nephron reconstruction requires other specialized cells including mesangial cells, glomerular endothelial cells, epithelial cells of the loop of Henle, principal cells and intercalated cells that have not yet been procured from PSCs. Induction of terminal differentiation, recapitulation of the architectural context and building of functional nephrons of the kidney are key challenges to be mastered.

1.5. Objective of this study

The aim of this project was to establish a rapid and efficient step-wise protocol for directing the differentiation of human pluripotent stem cells towards the renal lineage.

- Screening of factors (e.g. growth factors, small molecules, extracellular matrix) to identify concentrations, combinations and timely order that direct human pluripotent stem cells towards the renal lineage.
- Characterizing the renal cells derived from the treatment of the newly developed protocol.
- Testing the potency of candidate cell populations that exhibit characteristics of renal progenitor cells to form renal tissue/ nephron

2. .MATERIALS

List of materials

Table 3: List of antibodies used for immunoflourescence and flow cytometry

Name	Species	Clone	Description	Company	Cat.Nr
AQP 2	Rabbit polyclonal		Collecting duct	Novus Biologicals	NB110-74682
SLC12A3	Rabbit polyclonal		Distal tubule and collecting ducts	Novus	NBP1-59699
CK19	Mouse monoclonal	A53-B/A2	Loop of Henle	Santa Cruz	SC-6278
NKCC2	Rabbit polyclonal		Loop of Henle	Santa Cruz	SC-133823
Uromucoid	Mouse monoclonal		Loop of Henle (Descending)	Abcam	AB167678
CDH16	Rabbit polyclonal		Loop of Henle in medulla	Proteintech	15107-1-AP
PDGFRß	Rabbit polyclonal		Mesangial cells	Santa Cruz	SC -432
SYNPO	Mouse monoclonal	G1D4	Podocyte- actin-binding protein	Progen	65294
PODXL	Mouse monoclonal	222328	Podocyte membrane	R&D Systems	MAB1658
NPHS1	Goat polyclonal		Podocyte marker, filtration barrier	SantaCruz	SC -19000
WT1	Mouse monoclonal	6F-H2	Podocytes, metanephric mesoderm	Dako, Carpinteria, CA	M3561
WT1	Rabbit polyclonal		Podocytes, metanephric mesoderm	Santa Cruz	SC-192
VILLIN	Mouse monoclonal		Proximal tubule	Millipore	MAB1671
Na+/K+-ATPase	Rabbit polyclonal		Proximal tubule	Abcam	AB58475
AQP 1	Rabbit polyclonal		Proximal tubule	Proteintech	20333-1-AP
CK8	Rabbit polyclonal		Whole nephron	Santa Cruz	SC -134484
CK18	Mouse monoclonal	DC-10	Whole nephron	Santa Cruz	SC -6259
MIXL1	Mouse monoclonal	319919	Definitive mesoderm	R&D Systems	MAB2610
SIX2	Mouse monoclonal	3D7	Embryonic cap mesenchyme	Abnova (tebu-bio)	H00010736-M01
Brachyury(T)	Rabbit polyclonal		Definitive mesoderm	Santa Cruz	SC -20109
GSC	Goat polyclonal		Definitive mesoderm	R&D	AF4086
OSR-1	Rabbit polyclonal		intermediate mesoderm	LifeSpan BioSciences	LS-C37923
PAX2	Rabbit polyclonal		intermediate mesoderm/metanephros	Invitrogen	71–6000
LIM1	Mouse monoclonal		intermediate mesoderm/nephricduct	Novus Biologicals	NBP2-01926
ITGA8	Mouse monoclonal	481709	Metanephric mesenchyme	R&D	FAB6194A
CITED1	Rabbit polyclonal		Embryonic cap mesenchyme	Pierce	PA1-24469
CDH1	Mouse monoclonal		Embryonic cap mesenchyme	BD Biosciences	610181
OCT4	Rabbit polyclonal		Pluripotency	CellSignaling technology	2840S

Table 4: List of primers used for gene expression analysis

GENE	SEQUENCE (5'->3') FORWARD PRIMER	SEQUENCE (5'->3')REVERSE PRIMER	MARKER FOR
OCT4	TGTCTCCGTCACCACTCT	TTCCCAATTCCTTCCTTA	Pluripotency
CMYC	GGCTCCTGGCAAAAGGTCA	AGTTGTGCTGATGTGTGGAGA	Pluripotency
KLF4	CCCACATGAAGCGACTTCCC	CAGGTCCAGGAGATCGTTGAA	Pluripotency
NANOG	AAGGTCCCGGTCAAGAAACAG	CTTCTGCGTCACACCATTGC	Pluripotency
SOX2	TGGACAGTTACGCGCACAT	CGAGTAGGACATGCTGTAGGT	Pluripotency
FOXA2	GGAGCAGCTACTATGCAGAGC	CGTGTTCATGCCGTTCATCC	Endoderm
SOX17	GTGGACCGCACGGAATTTG	GGAGATTCACACCGGAGTCA	Endoderm
NESTIN	TTGCCTGCTACCCTTGAGAC	GGGCTCTGATCTCTGCATCTAC	Ectoderm
SOX1	CAGTACAGCCCCATCTCCAAC	GCGGGCAAGTACATGCTGA	Ectoderm
ZIC1	CACGCGGGACTTTCTGTTC	TGCCCGTTGACCACGTTAG	Ectoderm
T	AATTGGTCCAGCCTTGGAAT	CGTTGCTCACAGACCACA	Mesoderm
GSC	AACGCGGAGAAGTGGAACAAG	CTGTCCGAGTCCAAATCGC	Mesoderm
MIXL1	CTGTTCCCCTCTCTCTGAAGA	GGCAGAAAAGATGTGTTCCTCC	Mesoderm
OSR1	GCTGTCCACAAGACGCTACA	CCAGAGTCAGGCTTCTGGTC	Intermediate Mesoderm
PAX2	AGATTCCCAGAGTGGTGTGG	GGGTATGTCTGTGTGCCTGA	Intermediate Mesoderm
LHX1	TCATGCAGGTGAAGCAGTTC	TCCAGGGAAGGCAAACTCTA	IM, Nephricduct
RET	TATCCTGGGATTCCTCCTGA	TCTCCAGGTCTTTGCTGATG	Uretericbud
HOXB7	GTGGACTGTGGGTCTGGACT	GAACACGCGAGTGGTAGGTT	Uretericbud
HOXD11	TGGAACGCGAGTTTTTCTTT	CTGCAGACGGTCTCTGTTCA	Metanephricmesenchyme
SIX2	AGGAAAGGGAGAACAACGAGAA	GGGCTGGATGATGAGTGGT	Metanephricmesenchyme
FOXD1	TGCGGGTCCCTCTATTTATG	TAACGCCTGGACCTGAGAAT	Stromalcomponentof MM
EYA1	GGACAGGCACCATACAGCTACC	ATGTGCTGGATACGGTGAGCTG	Cap mesenchyme
WT1	GGCAGCACAGTGTGTGAACT	CCAGGCACACCTGGTAGTTT	IM, podocyte

Table 5: List of materials used in this study

BUFFER FOR ICC-STAINING	MANUFACTURER/SUPPLIER
BD Perm/Wash™	BD Biosciences, Franklin Lakes (USA)
BD Cytofix™	Biochrom AG, Berlin (Germany)
Donkey Serum	Sigma Aldrich, St. Gallen (Switzerland)

CHEMICALS/REAGENTS	MANUFACTURER/SUPPLIER
4', 6-diamidino-2-phenylindole (DAPI)	Life Tecnologies GmbH, Darmstadt (Germany)
Agarose Standard	Carl Roth GmbH, Karlsruhe (Germany)
Dimethyl sulfoxide (DMSO)	Sigma Aldrich, St. Gallen (Switzerland)
DNA-Ladder 100 bp (0.1 µg/µl)	Solis BioDyne Tartu, (Estonia)
Ethanol	Carl Roth GmbH, Karlsruhe (Germany)
Formaldehyde	Carl Roth GmbH, Karlsruhe (Germany)
Glutamax	Gibco®, Life Technologies GmbH, Darmstadt (Germany)
Gel Red	Biotium, Inc. (USA)
Gentle Dissociation Reagent	StemCell™ Technologies, Grenoble (France)
Hank´s Balanced Salt Solution (HBSS)	Sigma Aldrich, St. Gallen (Switzerland)
HEPES Buffer	Lonza (Switzerland)
Lithium Chloride	Carl Roth GmbH, Karlsruhe (Germany)
PBS (Dulbecco's Phosphate Buffered Saline) with or without Mg2+/Ca2+	Gibco®, Life Technologies GmbH, Darmstadt (Germany)
TritonX	Sigma Aldrich, St. Gallen (Switzerland)
Trypan blue	Gibco®, Life Technologies GmbH, Darmstadt (Germany)

CULTURE DISHES	MANUFACTURER/SUPPLIER
Falcon tubes	BD Biosciences, Heidelberg (Germany)
BD Falcon™ 6-well Multiwell Plate	BD Biosciences, Heidelberg (Germany)
BD Falcon™ 12-well Multiwell Plate	BD Biosciences, Heidelberg (Germany)
BD Falcon™ 24-well Multiwell Plate	BD Biosciences, Heidelberg (Germany)
BD Falcon™ 96-well Multiwell Plate, flat bottom	BD Biosciences, Heidelberg (Germany)
CellCarrier® 96-well Multiwell Plate	Perkin Elmer, Waltham (USA)
Falcon tubes	BD Biosciences, Heidelberg (Germany)
Transwell plates (6- and 24 well format)	Costar, Corning Inc. (USA)

ENZYME	MANUFACTURER/SUPPLIER
Dispase in DMEM/F-12 (1mg/ml)	StemCell™ Technologies, Grenoble (France)
DNase	Roche AG (Switzerland)
StemPro® Accutase®	Gibco®, Life Technologies GmbH, Darmstadt (Germany)
Trypsin/EDTA, 0.05 %/0.02 %	Biochrom AG, Berlin (Germany)

EQUIPMENT	MANUFACTURER/SUPPLIER
Agarose gel chamber	Peqlab, Erlangen (Germany)
Allegra™ Centrifuge X-22	Beckman Coulter GmbH, Krefeld (Germany)
BD FACSAria™ III	BD Biosciences, Heidelberg (Germany)
BD LSR Fortessa	BD Biosciences, Heidelberg (Germany)
Cell Scraper	TPP® Techno Plastic Products AG, Trasadingen (Switzerland)
Centrifuge Allegra X15R	Beckman Coulter, Krefeld (Germany)
Cryovials	Sigma Aldrich, St. Gallen (Switzerland)
Gel electrophoresis equipment	Peqlab, Erlangen (Germany)
Freezing Container, Nalgene® Mr. Frosty	Thermo Scientific, Dreieich (Germany)
Heraeus Fresco 211 centrifuge	Thermo Scientific, Dreieich (Germany)
Heraeus Multifuge X3R centrifuge	Thermo Scientific, Dreieich (Germany)
Heraeus Pico 17 centrifuge	Thermo Scientific, Dreieich (Germany)
Incubator 11-13625	BINDER GmbH, Tuttlingen (Germany)
Mastercycler epgradient S	Eppendorf, Hamburg (Germany)

Microtubes	Eppendorf, Hamburg (Germany)
NanoDrop 1000 spectrophotometer	Peqlab Biotechnology GmbH, Erlangen (Germany)
Neubauer cell counting chamber	Celeromics, Grenoble (France)
Operetta High Content Screener	Perkin Elmer, Waltham (USA)
PCR cycler Gene Amp PCR System 9700	Peqlab, Erlangen (Germany)
Phase-Contrast Microscope: Axiovert 40CFL	Zeiss, Jena (Germany)
pH-measurement PB11	Sartorius Stedim Biotech GmbH, Göttingen (Germany)
Real time-PCR –QuantStudio	Applied Biosystems®, Life Technologies GmbH, Darmstadt (Germany)
Stem cell cutting tool	Vitrolife (United Kingdom)
Stereo microscope SMZ 1000	Nikon GmbH, Düsseldorf (Germany)
Thermomixer 5436	Eppendorf, Hamburg (Germany)
UV-Gel documentation system NightHawk	Berthold Technologies GmbH & Co. KG, Bad Wildbad (Germany)
Vortex-2 Genie	Scientific Industries, Inc, Ney York (USA)
Waterbath	GFL, Burgwedel (Germany)
Workstation L226IVF	HD Scientific, Wetherill Park (Australia)

MEDIA	**MANUFACTURER/SUPPLIER**
DMEM/F12	Gibco®, Life Technologies GmbH, Darmstadt (Germany)
Knockout™ DMEM/F-12 (1X)	Gibco®, Life Technologies GmbH, Darmstadt (Germany)
mTeSR™1	StemCell™ Technologies, Grenoble (France)
TeSR-E8	StemCell™ Technologies, Grenoble (France)
REBM (Basal medium+ Bullet kit)	Lonza (Switzerland)
RKCM	RNL Bio (Korea)
StemDiff APEL	StemCell™ Technologies, Grenoble (France)
OptiMEM	Life Technologies GmbH, Darmstadt (Germany)

KITS	**MANUFACTURER/SUPPLIER**
Rneasy®Micro/Mini Kit (Qiagen)	Qiagen®, Hilden (Germany)
CrimsonTaq™MasterMixKit	New England Biolabs (USA)
SuperScript® III First-Strand Synthesis System	Invitrogen™, Life Technologies GmbH, Darmstadt (Germany)
SYBR® Green-ROX, PCR Master Mix	Applied Biosystems®, Life Technologies GmbH, Darmstadt (Germany)

SUPPLEMENTS	**MANUFACTURER/SUPPLIER**
β -2-Mercaptoethanol	Invitrogen™, Life Technologies GmbH, Darmstadt (Germany)
Glutamax	Invitrogen™, Life Technologies GmbH, Darmstadt (Germany)
Hydrocortisone	Sigma-Aldrich, St. Gallen (Switzerland)
Insulin-Transferrin-Selenium	Sigma Aldrich, St. Gallen (Switzerland)
Fetal calf serum	Biochrom AG, Berlin (Germany)
Pen Strep 10000 Units/ml	Gibco®, Life Technologies GmbH, Darmstadt (Germany)
ActivinA	PeproTech, Hamburg (Germany)
BIO	InSolution™ GSK-3 Inhibitor IX , Calbiochem, Merck KGaA, Darmstadt (Germany)
rhBMP4	PeproTech, Hamburg (Germany)
rhBMP7	PeproTech, Hamburg (Germany)
rhbFGF/FGF2	PeproTech, Hamburg (Germany)
rh GDNF	PeproTech, Hamburg (Germany)
rhHGF	PeproTech, Hamburg (Germany)
Retinoic Acid	Stemgent (USA)
Y27632	Wako Chemicals Inc.(USA)

SOFTWARE	**MANUFACTURER/SUPPLIER**
Columbus Image Data System	Perkin Elmer, Waltham (USA)

FlowJo Version 8.8.2	Tree Star, Inc., Ashland (USA)
GraphPad Prism	GraphPad Software, California (USA)
QCapture	QImaging (Canada)
Volocity	Perkin Elmer, Waltham (USA)

3. METHODS

3.1. Culture and maintenance of human pluripotent stem cells (PSCs).

3.1.1. hPSC culture conditions

The hPSC were tested in various conditions to find the best suited culture media for the colonies to remain undifferentiated and healthy. Broadly, the conditions can be classified as feeder cell co-culture and feeder free culture (Figure 10).

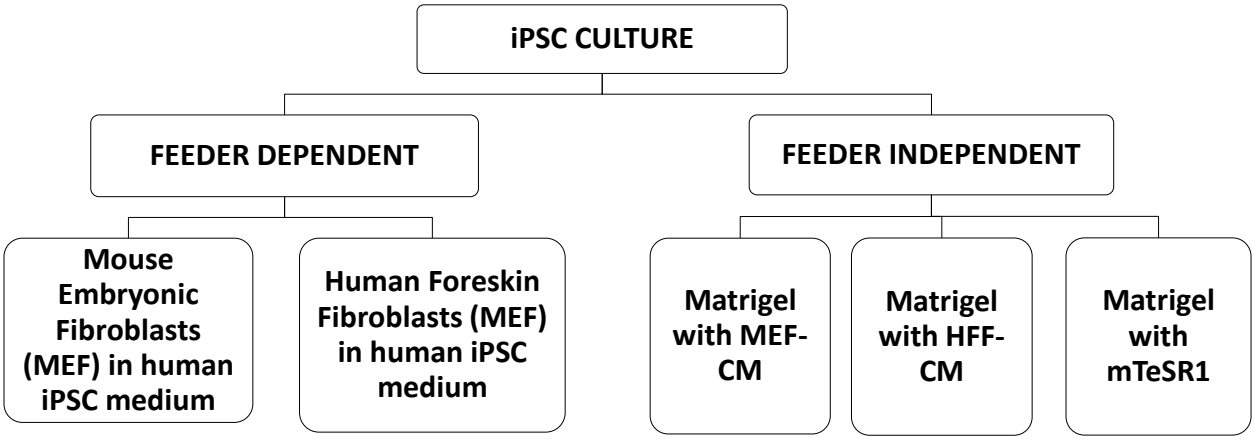

Figure 10: Different conditions of iPSC culture

3.1.2. Preparation of feeder cell cultures

Human embryonic and induced pluritpotent stem cells have been classically cultivated on feeder layers of mouse embryonic fibroblasts (MEF) or human foreskin fibroblasts (HFF). MEF (CF-1 strain) were cultured in Dulbecco's Modified Eagle Medium (DMEM) containing 10% fetal calf serum (FCS), 1% glutamax, 1% Non-Essential Amino Acids (NEAA), 1% penicillin/streptomycin and HFF were cultured in Iscove's Modified Dulbecco's Medium (IMDM) containing 10% FCS and 1% penicillin/streptomycin. Stocks of both the cell types were prepared for future cultivation of pluripotent stem cells. MEFs/HFFs were thawed and plated and cultured for several days. During these days cell numbers increased while MEFs still had growth potential. After 3 expansions (passages), the cells were trypsinized and the cell suspension was exposed to gamma irradiation (30 Gray) to inactivate the fibroblasts, impairing mitosis and avoiding further growth. Inactivated MEFs were washed and frozen in a solution containing 40% DMEM basic medium, 50% FBS, 10% DMSO and stored in liquid nitrogen. When hPSCs need to be cultured, feeder cell plates are prepared by thawing MEFs/HFFs the day before on gelatin coated dishes and incubated in iPSC medium for acclimatisation.

3.1.3. Preparation of conditioned medium

Conditioned media was harvested from confluent monolayers of γ-irradiated MEF and HFF in a T175 flask cell culture system (MEF-CM and HFF-CM respectively). Irradiated fibroblasts were plated in MEF medium and from the following day for a week, the cells were provided human iPSC medium (30 ml). Every day, the conditioned media was collected, filtered to remove cellular debris, and frozen at -20℃.

3.1.4. Subcultivation of hPSCs on feeders

In feeder cell co-cultures the used iPSC medium was composed of Knockout DMEM/F12 and Knockout Serum Replacer (KSR), NEAA, glutamax, β-Mercaptoethanol, bFGF and gentamycin. During thawing of the iPSC master culture, ROCK inhibitor- Y27632 was added to prevent apoptotic loss of cells.

Table 6: Standard iPSC medium

COMPONENT	CONCENTRATION	FOR 500 ML:
Knockout DMEM/F12		388ml
Nonessential amino acids (100x)	0,1 mM	5 ml
GlutaMax –I, Solution (100x), 200 mM		5 ml
Gentamycin	50 µg/ ml Med.	2 ml (of 12,5 mg/ ml)
Knockout Serum Replacer (KSR)	20%	100 ml
Sterile filtration 0,22 µm		
ß Mercaptoethanol	0,1 mM	1 ml
bFGF	10 ng/ ml	500 µl (of 10 µg/ ml)
ROCK Inhibitor (Thawing medium only)	5mM	1ml

Two kinds of subcultivation techniques were utilized to expand iPSC cultures - mechanical and enzymatic. Human iPSC colonies cultivated on feeder layers were preferentially passaged mechanically using a Stem Cell Cutting Tool. Briefly, the cutting tool was used to mark the borders of the undifferentiated colony with the sharp edge and gently loosened with the blunt side to let them float. The floating colonies were collected using the pipetting function of the tool and transferred onto new feeder plates in a desired ratio. Enzymatic passaging was performed using Dispase or Collagenase IV. The spent medium was aspirated and washed with KO-DMEM/F12. The enzyme collagenase IV was added and incubated for 7-10 minutes until the edges of the colonies seemed separate; at this point the enzyme was removed. The cells

were rinsed with KO-DMEM/F12 and the colonies were collected, centrifuged and replated on fresh feeders at the desired ratio.

3.1.5. Feeder free culture of iPSC

To culture the iPSC in feeder free conditions mTeSR-1 medium was tested other than MEF-CM and HFF-CM. mTeSR-1 is a complete serum-free, defined formulation designed for the feeder independent maintenance and expansion of human embryonic stem cells (hESCs) in the undifferentiated state (Ludwig et al., 2006). Complete mTeSR-1 medium (Basal Medium + 5X Supplement) contains recombinant human basic fibroblast growth factor (rh bFGF) and recombinant human transforming growth factor β (rh TGFβ). In the feeder free culture system, cells were cultured in Matrigel coated flasks. Enzymatic passaging was performed using dispase as in the procedure mentioned before. This enzyme allowed cells to remain in clumps, which has been shown to be essential for hPSC propagation. After cells have been incubated for 7 min at 37 °C with dispase, the enzyme is removed and cell clumps were washed and detached from the plate using a scraper and suspended in 2 mL medium to wash the dispase. Cells were centrifugated at 300 x g for 5 minutes. The supernatant was removed and cell pellet was was re-suspended and plated onto a new culture dish.

The feeder-free culture conditions were eventually shifted to TeSR-E8 medium (Stemcell Technologies) on Geltrex (Life technologies) coated dishes following the determination of essential eight components of pluripotent stem cell culture. Cultures were fed daily and passaged every 4–6 days with gentle cell dissociation reagent (Stemcell technologies) for 5 min at 37°C and then manually detached from the dish using a cell scraper. The resulting clumps of cells were plated in a ratio of 1:6.

3.1.6. Morphological distinction between hPSCs and differentiated cells

Due to high nuclear cytoplasmic ratio, the hESC colonies form ordered, flat, tight colonies with sharp borders, with low light scattering properties while the differentiating colonies are apparently disordered or irregular with uneven edges or transparent centers and exhibit high light-scattering property. Also the differentiated cells look bigger than undifferentiated cells due to the reduced nuclear-cytoplasmic ratio.

3.1.7. Single cell preparation of hPSCs

Although regular expansion of PSC colonies was performed as mentioned above, when cells were required in a standard fashion for experiments, they were preferred as single cells in order to be quantified for seeding. For this procedure, the enzyme mixture Accutase was added to the

cells and incubated at 37°C for 7 minutes. This enzyme mixture cannot be neutralized and therefore was diluted with twice the volume of medium. The cells suspended in this enzyme-medium mixture are centrifuged at 300xg for 5min. The supernatant was discarded and the pellet is re-suspended in medium containing ROCK-inhibitor. Cells are seeded at a required density and maintained in medium containing ROCK-inhibitor for 24 hours after which it was replaced by the test medium.

3.1.8. Cryopreservation of hPSCs

The procedure for freezing human PSCs is identical to that of passaging these cells till the final step of re-suspending the cell clumps. Shortly, colonies were incubated with dispase, washed with KO-DMEM/F12 and gently lifted out with a cell scraper. Then the clumps were collected, centrifuged for sedimentation and re-suspended gently in pre-cooled freezing medium (60% FBS, 20% DMSO and 20% culture medium). Usually cells clumps collected from one well of a 6-well plate were suspended in 1ml of freezing media and accommodated in a 1 ml cryovial, which was placed in a freezing container (Nalgene) and stored at -80°C overnight were transfered to liquid nitrogen for long-term storage the following day.

* To obtain higher efficiency during thawing, cells clumps for freezing should be slightly larger than those used for splitting.

3.1.9. List of PSCs utilized.

Table 7: Human PSCs utilized in this study

CELL LINE	SOURCE	VECTOR	FACTORS	REFERENCE
WAe001-A (WA01)	Human embryo	-	-	Thomson et al.
WISCi004-A (IMR90-4)	Lung fibroblasts(female)	Lentivirus	Oct4, Sox2,Nanog, Lin28	Yu Junying et al. 2007
BCRTi004	Urinary cells	Sendai virus	Oct4, Sox2, Klf4, cMyc	Rossbach et al. 2016a
BCRTi005	Urinary cells	Sendai virus	Oct4, Sox2, Klf4, cMyc	Rossbach et al. 2016b

3.2. Stem cell Differentiation

3.2.1. Media

The basal medium used for differentiation during screening experiments was prepared in the lab by adding B.S.A (1.8%) and NEAA (0.1mM) to DMEM/F12 with high glucose containing Glutamax and Sodium Pyruvate. On obtaining 4 candidate growth factor combinations, the basal medium was switched to xeno-free, serum free defined APEL medium (Ng et al., 2008).

3.2.2. Extracellular matrices

Tissue culture and tissue multiwell plates used for iPSC cultivation where pre-coated with Geltrex^{TM} Matrix 1:30 in Knockout DMEM for one hour at RT or at 4 C, overnight. Other matrices used for differentiation include Collagen A (diluted 1:1) and rhLaminin521 (10µg/ml) both dissolved in PBS containing Calcium and Magnesium.

3.2.3. Growth factors

Table 8: Concentration of growth factors used

CATEGORY	SYMBOL	GROWTH FACTOR	CONCENTRATION USED	VOLUME FOR 10ML APEL
Meso factors :	A	ActivinA (2ng/µl Stock)	10ng/ml	50µl
	B4	BMP4 (2ng/µl Stock)	30ng/ml	150µl
	RA	Retinoic Acid	1µM	1µl
	BIO	BIO	1µM	1µl
Nephro factors :	B7	BMP7 (2ng/µl Stock)	15ng/ml	75µl
	F2	FGF2 (2.5ng/µl)	10ng/ml	40µl
	G	GDNF (5ng/µl)	150ng/ml	300µl
Podo factor	HGF	HGF(10ng/µl)	50ng/ml	50µl

3.2.4. Optimal protocol

For differentiation experiments, a single cell suspension was prepared by treating a confluent PSC culture with Accutase (Life Technologies) and seeding in stem cell culture medium containing 10µM Y27632(Wako) at a density of 10,000cells/cm2 for 24 hours. The seeded cells are maintained in stem cell culture medium until attainment of 75% confluency when induction factors are applied for specified time periods. Differentiation media used in all stages was prepared using STEMdiff APEL Medium (Stemcell technologies) as a base medium, to which growth factors and inhibitors were added as required. During Stage I, 10ng/ml Activin A (Peprotech), 30ng/ml rh-bone morphogenetic protein 4 (BMP-4; Peprotech) with either 10 µM

all-trans-retinoic acid (RA; Sigma-Aldrich) or 10 ng/ml basic fibroblast growth factor (bFGF, Peprotech) or 15ng/ml rh-BMP7 (Peprotech) or 3μM (2′Z, 3′E)-6-Bromoindirubin-3′-oxime (BIO; Sigma-Aldrich) was added to APEL base. Stage II media were composed of 150ng/ml Glial-Derived Neurtrophic Factor (GDNF, Peprotech) or alternatively a combination of 15ng/ml BMP7 and 10ng/ml bFGF. During the course of differentiation, medium was replenished every 48 hours.

For the terminal differentiation, cells obtained at the end of day 8 were replated on Laminin521 (BioLamina) and treated with medium containing 50ng/ml rh-Hepatocyte Growth Factor (HGF; Peprotech) for podocyte differentiation or alternatively Renal Epithelial Growth Medium (REGM; Lonza) for tubular epithelial differentiation and in a medium containing 15ng/ml BMP7 and 10ng/ml FGF2 for mesangial cells.

3.3. Characterization of PSC-derived cells.

3.3.1. Gene expression analysis

Relative gene expression analysis was performed by semi-qualitative reverse transcriptase PCR (RT-PCR), quantitative real-time PCR (qPCR) and RNA-Seq analysis.

3.3.1.1. **RNA ISOLATION**:

RNA isolation from cell lysates was performed using the RNeasy® Mini Kit (Qiagen) following the manufacturer's instructions, including the optional step of DNase I treatment of the samples on column to get rid of trace amounts of genomic DNA. This technology combines the selective binding properties of a silica-based membrane with centrifugation which enables the capture and purification of up to 100 μg of RNA longer than 200 bases by binding to the silica membrane in a column. The procedure provides enrichment for mRNA since most RNAs <200 nucleotides (such as 5.8SrRNA, 5S rRNA, and tRNAs, which together comprise 15–20% of total RNA) are selectively excluded.

First, the cells were briefly rinsed with pre-warmed PBS (37°C) and RLT lysis buffer (highly denaturing guanidine-thiocyanate–containing buffer) to which β-mercaptoethanol was added at the rate of 10 μl per 1 ml RLT Buffer prior to use. 600 μl Then the cells were scraped out using a cell scraper and collected in a 1 ml microcentrifuge tube, followed by thorough vortexing for 1 minute to ensure proper cell lysis. Then the lysates were transferred to RNeasy-columns and further RNA isolation was carried out according to the manufacturer's instructions. RNA was

eluted into RNAsefree tubes using 22 µl of RNAse-free sterile water, out of which 2 µl was used for quality check by agarose gel electrophoresis and quantification.
The quantity and quality of RNA and cRNA was determined using a spectrophotometer (NanoDropTechnologies, Wilmington, DE, USA). This technology combines fibre optics and surface tension to measure small amounts of sample. 1µl of sample was loaded onto the optical pedestal of the NanoDrop and its arm is closed. The sample is held by surface tension as a column during the measurement. If the concentration exceeded saturation limits, the samples were diluted by adding RNAse-free sterile water.

3.3.1.2. RT-PCR

Reverse transcription was performed using the SuperScript® III First-Strand Synthesis System. Whole volume of isolated RNA was used to generate cDNA. 50µM OligodT and 10mM dNTPs were added to the RNA samples and made up with sterile distilled H2O to a volume of 13 µl. The samples were incubated at 65°C for 5 minutes and then placed on ice for 1 minute. A mixture of 4µl 10x RT buffer, 1µl 0,1M DTT, 1µl RNaseOut and 1µl Superscript III RT were added to the samples, making it a 20µl reaction volume. The reverse transcription reaction was performed at 50°C for 1h and inactivated at 70°C for 15 minutes. Generated cDNA was measured with the NanoDropTM Spectrophotometer at 260nm and stored at -20°C for further use.

Specific genes were amplified from the obtained cDNA by the application of certain primers listed in **Table 4**. The components of the CrimsonTaq Master Mix Kit (New England Biolabs), were mixed with the yielded cDNA as depicted in **Table 8**. For each primer an additional negative control was applied (without cDNA). GAPDH (Housekeeping gene) was used as the positive control.

Gels of 1-3% were prepared by mixing agarose (Life Technologies, Paisley, Scotland) in 1x TAE buffer. 1µl of GelRed was added directly to the gel and mixed before solidifying. To assign the length of the amplicons the GeneRuler^{TM} 1kb DNA ladder (Fermentas, St. Leon-Rot, Germany) was used. Gels were run in an electrophoresis chamber with 90V for 30 to 60min. Nucleotides were visualized with a UV transilluminator.

Table 9: PCR amplification Mix

Component	Concentration	1x Sample
5X Reaction buffer	1X	5µl
cDNA Template	1µg	*n* µl
dNTP Mix (10mM)	200µM	0.5µl
Forward Primer (10µmol)	0.2µM	0.5µl
Reverse Primer (10µmol)	0.2µM	0.5µl
TopTaq DNA Polymerase	1.25 units	0,125µl
RNase free H_2O		Fill up to 25µl

Table 10: Thermocycling conditions.

Step	Temperature	Time	Cycles
Initial melting	95° C	5 min	
Melting	95° C	30 sec	30
Primer annealing	n° C	30 sec	
Elongation	72° C	30 sec	
Final elongation	72° C	10 min	
Cooling	4°C	∞	

3.3.1.3. RNA-Seq library preparation and NGS

For Illumina HiSeq 2000 RNA sequencing, RNA-Seq library preparation and NGS: cDNA libraries from poly-A-tail enriched RNA were prepared from 3 biological replicates for each timepoint, using TruSeq mRNA sample prep kit v.2 (Illumina). Sequence alignment and RNA-Seq analysis: Bcl to fastq conversion was performed using Illumina software (Illumina). Fastq files were aligned to build 19 of the human genome provided by the Genome Reference Consortium (GRCh19). Transcript alignment was performed using TopHat. Analysis (Trapnell et al., 2009) of differential expression and transcript abundance was performed using Cuffdiff (Trapnell et al., 2010) from the Cufflinks analysis package (version 2.1.1). The transcript levels (expressed as Fragments per Kilobase of transcript per Million mapped reads; FPKM) of the samples were used to plot heatmaps based on Pearson correlation, using R (R Development Core Team (2011)) (version 3.1 or greater).The data (significantly impacted pathways,

biological processes, molecular interactions, miRNAs, SNPs, etc.) were also analyzed using Advaita Bio's iPathwayGuide(Draghici et al., 2007).

RNA-Seq data for 22 samples has been deposited at the GEO database with the accession number GSE75711.

Table 11: Details of sequenced samples

SAMPLE NAME	TITLE	CHARACTERISTICS : TIMEPOINT	DESCRIPTION
D14-1	D14-1	Day 14 of nephron cell induction	IPS cells exposed to 4 days of ActivinA,BMP4,Retinoic acid, 4 days of GDNF and 6 days of HGF
D14-3	D14-3	Day 14 of nephron cell induction	IPS cells exposed to 4 days of ActivinA,BMP4,Retinoic acid, 4 days of GDNF and 6 days of HGF
D2-1	D2-1	Day 2 of nephron cell induction	IPS cells exposed to 2 days of ActivinA,BMP4,Retinoic acid
D2-2	D2-2	Day 2 of nephron cell induction	IPS cells exposed to 2 days of ActivinA,BMP4,Retinoic acid
D2-3	D2-3	Day 2 of nephron cell induction	IPS cells exposed to 2 days of ActivinA,BMP4,Retinoic acid
D4-1	D4-1	Day 4 of nephron cell induction	IPS cells exposed to 4 days of ActivinA,BMP4,Retinoic acid
D4-2	D4-2	Day 4 of nephron cell induction	IPS cells exposed to 4 days of ActivinA,BMP4,Retinoic acid
D4-3	D4-3	Day 4 of nephron cell induction	IPS cells exposed to 4 days of ActivinA,BMP4,Retinoic acid
D6-1	D6-1	Day 6 of nephron cell induction	IPS cells exposed to 4 days of ActivinA,BMP4,Retinoic acid and 2 days of GDNF
D6-2	D6-2	Day 6 of nephron cell induction	IPS cells exposed to 4 days of ActivinA,BMP4,Retinoic acid and 2 days of GDNF
D6-3	D6-3	Day 6 of nephron cell induction	IPS cells exposed to 4 days of ActivinA,BMP4,Retinoic acid and 2 days of GDNF
D8-1	D8-1	Day 8 of nephron cell induction	IPS cells exposed to 4 days of ActivinA,BMP4,Retinoic acid and 4 days of GDNF
D8-2	D8-2	Day 8 of nephron cell induction	IPS cells exposed to 4 days of ActivinA,BMP4,Retinoic acid and 4 days of GDNF
D8-3	D8-3	Day 8 of nephron cell induction	IPS cells exposed to 4 days of ActivinA,BMP4,Retinoic acid and 4 days of GDNF
H1_d8-1	H1_d8-1	Day 8 of nephron cell induction	IPS cells exposed to 4 days of ActivinA,BMP4,Retinoic acid and 4 days of GDNF
H1_d8-2	H1_d8-2	Day 8 of nephron cell induction	IPS cells exposed to 4 days of ActivinA,BMP4,Retinoic acid and 4 days of GDNF
T315615; C1-undiff i PSC	undiff-1	NA	no treatment
T315716; C2-undiff i PSC	undiff-2	NA	no treatment
T315817; C3-undiff i PSC	undiff-3	NA	no treatment
T315918; U1-Strati-I	D8-4	Day 8 of nephron cell induction	IPS cells exposed to 4 days of ActivinA,BMP4,Retinoic acid and 4 days of GDNF
T316019; U2-Strati-II	D8-5	Day 8 of nephron cell induction	IPS cells exposed to 4 days of ActivinA,BMP4,Retinoic acid and 4 days of GDNF
T316120; U3-Strati-V	D8-6	Day 8 of nephron cell induction	IPS cells exposed to 4 days of ActivinA,BMP4,Retinoic acid and 4 days of GDNF

3.3.2. Detection of proteins by Immunocytochemisty

3.3.2.1. Immunofluorescence staining of cells and tissues

For immunofluorescence staining, cultured cells were washed with phosphate-buffered saline (PBS) and fixed with *BD Cytofix* for 10 min. If necessary, cells were then permeabilized with BD Perm/Wash for 15 min. Cells were washed twice with PBS and blocked with 10% secondary antibody host serum in washing buffer for 30 min at 37°C. Cells were incubated overnight at 4°C with primary antibodies (Table 3) diluted in Perm/Wash buffer. Cells were then washed three times (5 min each) and incubated with fluorescence-labeled secondary antibodies in washing buffer at room temperature for an hour and rinsed three times (5 min each) with PBS. For negative controls, only the secondary antibody was used (results not shown). The fluorescent dye 4′, 6-diamidino-2-phenylindole (DAPI; Sigma-Aldrich, D-8417) was used for staining nuclei. Images were obtained using the Operetta High content imaging system (Perkin Elmer) and analysed using Columbus (Perkin Elmer) software.

3.3.2.2. Flow cytometry

Cells were detached to a single-cell suspension using trypsin and stained for LIVE/DEAD™ Fixable Blue (ThermoFisher Scientific) for 30 min. For labeling of intracellular antigens, cells were permeabilized by incubation with Phosflow Perm Buffer II (BD Biosciences) for 15 min. Cells were incubated with primary antibody (Table 3) diluted in ice-cold buffer (1% (vol/vol) Fetal calf serum in PBS) for 30min. Cells were incubated with appropriate secondary antibodies (donkey anti-mouse IgG Alexa 647 or donkey anti-donkey IgG Alexa 488) if they were not conjugated with a fluorophore. Cell labeling was measured using a LSR Fortessa cell analyzer (BD Biosciences) and analyzed with FlowJo software (FLOWJO LLC).

3.3.3. Assays demonstrating potency, tubulogenic and angiogenic capacities of cells.

3.3.3.1. Pellet culture assay

The pellet culture was adapted from Takasato 2014. PSC-derived cells were harvested and dissociated into single cells using Accutase (ThermoFisher Scientific) at day 8-9 of the differentiation. Around 3-5x10 ^{5} cells were spun down at ×400*g* for 5 min to form a pellet and

then placed onto a transwell filter membrane (0.4μm polyester, Greiner bio-one) on the culture media of 10% FCS/DMEM for 4 days.

3.3.3.2. Mouse embryonic kidney re-aggregation assay

The re-aggregation assay was performed as described by Xia et al. 2013. Briefly, embryonic kidneys from 12.5-dpc (days post coitum) mice were digested with Accutase for 10 minutes and washed with KCM containing 10% FCS and placed in a low-binding eppendorf vial together with $3x10^5$ day 8 hiPSC-derived renal cells; the tubes were centrifuged at 190g for 5 min. The supernatant was removed, and the pellet was re-suspended in 120 µl KCM (MEM supplemented with 10% FBS) supplemented with 10 µM ROCK inhibitor (Sigma). The cells were pelleted in the same PCR tube at 190*g*, 4 °C for 5 min. The PCR tube was placed upright in the incubator for 12 h. The aggregates were then transferred onto transwell filters (0.4μm polyester, Greiner bio-one) with KCM in the lower chamber. Following 4 days of culture, the whole aggregates from both the pellet culture and embryonic re-aggregation were fixed and stained by immunofluorescence. The samples from this study were imaged using Leica S450 two-photon microscope.

4. RESULTS

4.1. Development of a protocol for differentiation of pluripotent stem cells towards the renal lineage.

The strategy- Screening of growth factors in a chemically defined medium initially involved two broad steps, the first being mesodermal induction and the second specifying cells to the nephric lineage. hPSCs have been used to generate several mesodermal lineages *in vitro*, including heart, bone and cartilage and hematopoietic system. This information indicates that steering a PSC to the mesodermal lineage through the primitive streak (PS) is feasible, although the path to intermediate mesoderm and further to urogenital systems has yet to be uncovered.

4.1.1. Literature mining for potential modifiers of stem cell fate.

The balance of BMP and Activin/Nodal signaling with canonical Wnt signaling has been known to specify the cell fate of hPSC-derived-nascent PS into mesoderm or endoderm progenitors (Sumi et al., 2008). FGF2 can switch the fate of BMP4-induced human PSC, to mesendoderm, which is characterized by the uniform expression of T (Brachyury) and other primitive streak markers, by acting through the MEK-ERK pathway (Yu et al., 2011). Wnt3 and beta-catenin play an important role in vertebrate axis formation (Liu 1999), and when applied in conjugation with activinA, this combination induced hPSCs to form T+ mesendoderm cells (Lam et al., 2014). Also, RA is a morphogen specifying the anterio-posterior axis, a caudalizing agent that influences HOX genes during embryonic development (Durston et al., 1989; Mavilio et al., 1988). A combination of activinA and RA induces pronephric markers *in vitro* in *Xenopus* and mESCs (Kim and Dressler, 2005; Osafune et al., 2002). In addition, it is known that BMP7-deficient mice die shortly after birth due to impaired kidney development, since BMP7 affects the expression of key signaling components in nephrogenesis, such as Pax-2 and Wnt-4 between 12.5 and 14.5 days post-coitum (dpc) (Luo 1995, Dudley et al., 1995; Torban et al., 2006). Considering this evidence, we used activinA and BMP4 (AB4) as a constant base to initiate nephrogenesis in combination with either FGF2 (F2) or BMP7 (B7) or retinoic acid (RA) or the Wnt agonist BIO. Human PSC were exposed to these factor combinations for 4 days (**Fig.11**).

To spur nephrogenesis further *in vitro*, we attempted to derive early stages of renal cell specification by supporting mesenchyme growth and branching morphogenesis. MM-derived GDNF was shown to promote UB differentiation and branching, and provide a positive feedback to MM cells (Majumdar et al., 2003; Sainio et al., 1997). Dudley et al. have demonstrated that BMP7 signaling can prevent apoptosis in explants of mouse MM and in

conjunction with FGF2; BMP7 promotes growth and maintains competence of the mesenchyme *in vitro* (Dudley et al., 1995, 1999). A biphasic role for BMP7 has been proposed where BMP7 elicits MAPK-dependent cap mesenchyme (CM) proliferation and regulates cell survival and interstitial progenitor phenotype via SMAD signaling(Oxburgh et al., 2011). Therefore, in a second step, we selected GDNF and BMP7-FGF2 to elucidate their effect on differentiation of AB4RA, AB4F2, AB4BIO and AB4B7 induced cells for four further days (**Fig.11**).

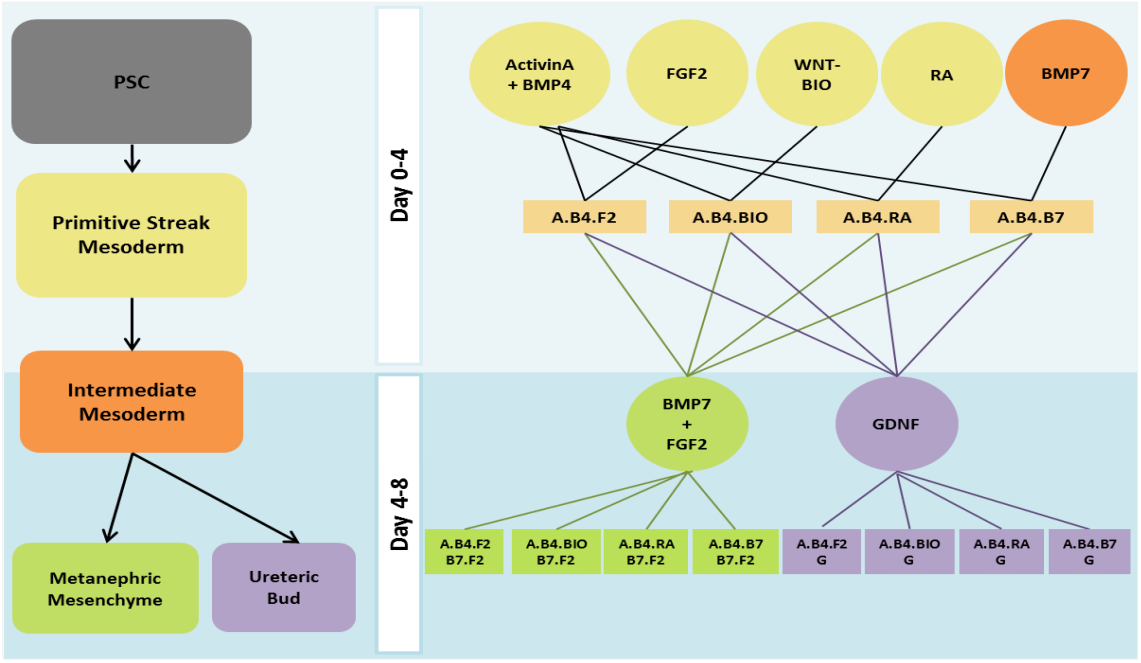

Figure 11: Strategy of the screen and combination of growth factors corresponding to the developmental milestones described in literature for renal linage specification. FGF-Fibroblast growth factor, BIO- (2'*Z*, 3'*E*)-6-bromoindirubin-3'-oxime, RA- Retinoic Acid, BMP- Bone morphogenetic protein, GDNF- Glial-derived Neurotrophic Factor.

4.1.2. Gene expression pre-screen identifies 4 promising growth-factor combinations to induce renal lineage.

The resulting 15 combinations were subjected to an initial screen based on RT-PCR of samples at the end of 8 days of treatment. Renal progenitors have transcription factor signatures that allow their identification, ranging from IM to MM and ND. Based on the loss-of-function phenotypes and expression patterns in various mutants, the early patterning genes appear to fall into two groups: 1) genes that specify the intermediate mesoderm along the mediolateral axis, such as Lim1, Odd1, Pax2/8; and 2) genes that specify the intermediate mesoderm along the anterior-posterior axis, such as the Hox11 group, Eya1, Six, and Wt1(Dressler, 2006). Therefore, we chose SIX2, LHX1, OSR1, PAX2, EYA1 and WT1 (S.L.O.P.E.W) as candidates to check the successful steering of PSCs to the renal lineage. (*A description of the roles played by these genes and the phenotype caused by their loss of function can be found in the appendix*).

An evaluation of the expression profile generated by RT-PCR allowed the shortlisting of combinations AB4B7, AB4BIO-B7F2, AB4F2-G and AB4RA-G, as they possessed a minimum S.L.O.P.E.W score – 4/6 **(Fig.12)**.

Table 12: Expression of developmentally significant transcription factors during differentiation evaluated based on RT-PCR.

		Combination of growth factors applied for 4+4 days														
		1	2	3	4	5	6	7	8	9	10	11	12	13	14	15
Time frame	d0-d4	AB4	AB4 BIO	AB4 F2	AB4 RA	AB4 B7	AB4	AB4 BIO	AB4 F2	AB4 RA	AB4 B7	AB4	AB4 BIO	AB4 F2	AB4 RA	AB4 B7
	d4-d8	AB4	AB4 BIO	AB4 F2	AB4 RA	AB4 B7	B7 F2	B7 F2	B7 F2	B7 F2	B7 F2	G	G	G	G	G
Transcription factors	**Eya1**	+	+	-	+	+	-	+	+	-	-	-/+	-	+	+	+
	Six 2	-	-	+	-	-	+	-	-	-	-	-	-	+	+	-
	Pax 2		-	+	-	-	-	+	-	+	+	-	-	+	+	-
	Wt1	+	-	-	-	+	-	+	+	+	+	-	-	-	+	-/+
	Lhx 1	-	-	-	+	+	-	+	+	+	-	-	+	-	+	+
	Osr1	-/+	-	-/+	-	+	-	+	+	+	+	-	+	+	-	+

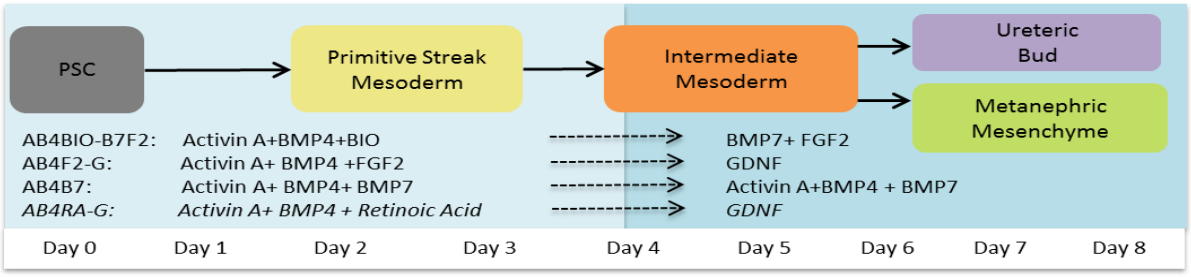

Figure 12: The 4 selected growth factor combinations with respect to approximate developmental stage and time.

4.1.3. AB4RA-G treatment for 8 days is highly efficient in generating the renal progenitor population.

Further screening was performed by means of high-content screening of the transcription factors important in the developmental cascade, as detected by immunofluorescence. The first time point, day 4, was chosen to check for the induction of mesoderm and specification into intermediate mesoderm. The indication of S.L.O.P.E.W signature by RT-PCR experiments led to the selection of day 8 as a second time point. The assay was performed to visualize the disappearance of OCT4, marking the loss of pluripotency and the subsequent appearance of T^{+}

cells representing a mesendodermal commitment of stem cells. SOX17 was used to identify nascent definitive endoderm cells, a population of a contaminating nature as we aim to achieve maximum induction of mesoderm. Also, SIX2, LHX1, OSR1, PAX2, WT1 and CDH1 were investigated. Evaluation of the extent of differentiation by day 4 shows the co-expression of OCT4 and T in conditions AB4B7, AB4BIO and AB4F2 while AB4RA treated cells lost OCT4 and express T in isolation (**Fig.13**). In line with the observation by Keong Teo *et al*. that OCT4 and BRACHYURY are still co-expressed in hESCs grown for 24 h in endoderm-promoting conditions, remarkably high numbers of SOX17+ cells are seen in AB4BIO and AB4F2 samples (Teo et al., 2011). Although AB4B7 did not show induction of SOX17, as previously shown in RT-PCR studies, this combination was rather inefficient in inducing PAX2, OSR1 or SIX2 after 4 days of treatment. AB4BIO and AB4F2 triggered higher intensities and lower number of PAX2 and SIX2 expressing cells while AB4RA on the other hand induced highest numbers of SIX2 and PAX2+ cells (**Fig.13**). None of the combinations seemed to display OSR1. The morphology of cells in all 4 combinations varied considerably; cells with expanded cytoplasm and large nuclei were seen in AB4B7, AB4BIO and AB4F2. The AB4RA cells were much smaller and numerous in comparison to the other 3 combinations, which can be attributed to the lower intensity of signal from the nuclei of these cells.

Completion of the 8-day treatment resulted in total loss of OCT4 confirming differentiation of all PSCs. The sustained expression of T together with SOX17 in combinations AB4BIO-B7F2 and AB4F2-G suggest the lack of developmental progression into the nephric lineage although a considerable number of OSR1, PAX2 and SIX2 + cells were observed (**Fig.14**). AB4B7 improved its performance in terms of SIX2+ and OSR1+ cells but was contaminated by the presence of SOX17+ cells. AB4RA showed some remnant populations of T+ cells, the highest number of SIX2 and PAX2 cells faring well among the all the combinations (**Fig. 14**).

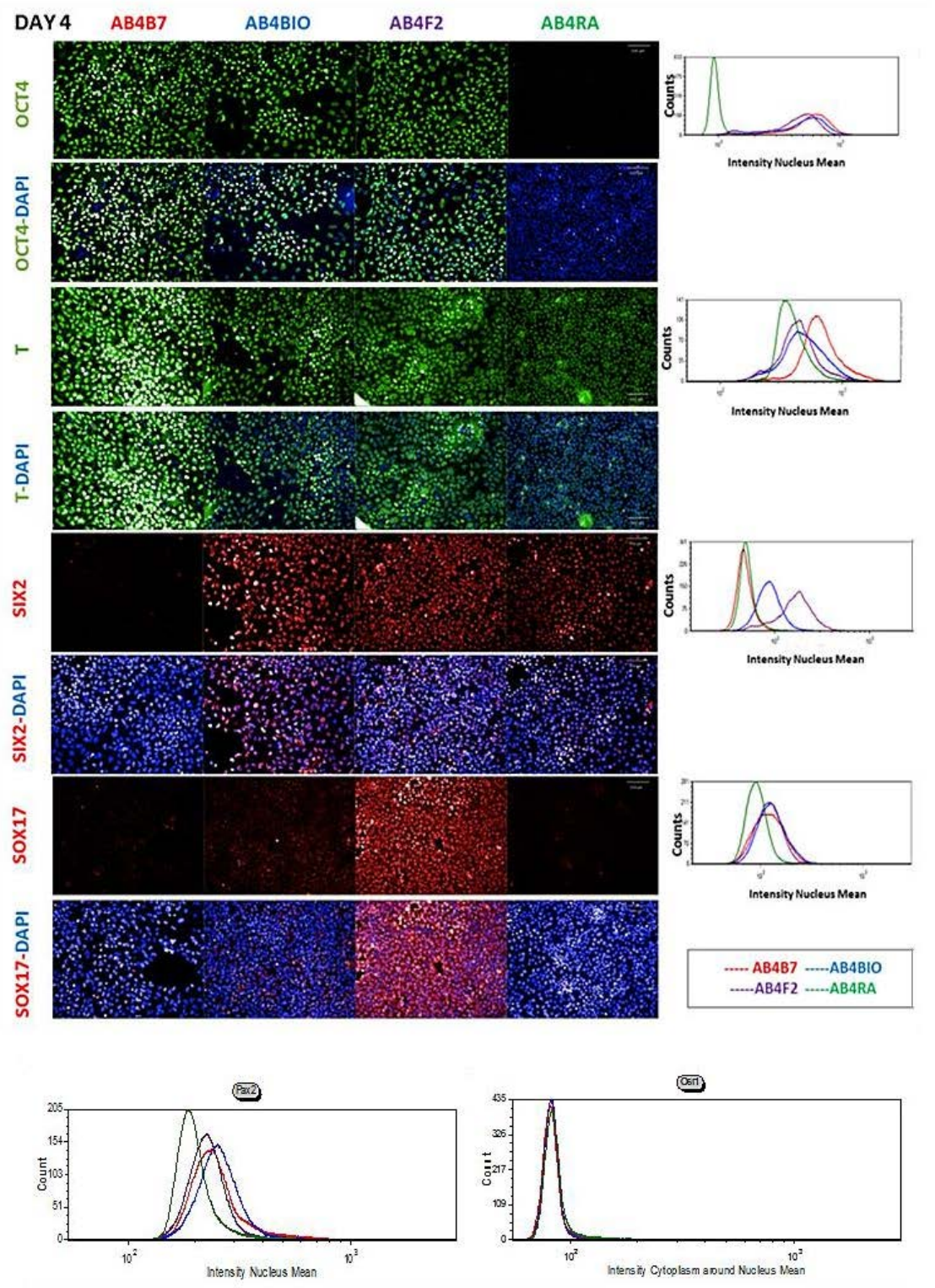

Figure 13: Screening of the optimal growth factor combination for renal progenitor generation after 4 days. The number of nuclei expressing the transcription factors OCT4, T, SIX2, SOX17, PAX2 and OSR1 out of 1000 nuclei in every combination were quantified using high content image analysis as shown in the accompanying graphs portraying count (each cell = 1 count) versus intensity of fluorescence of the nuclei. Scale bar = 50µm.

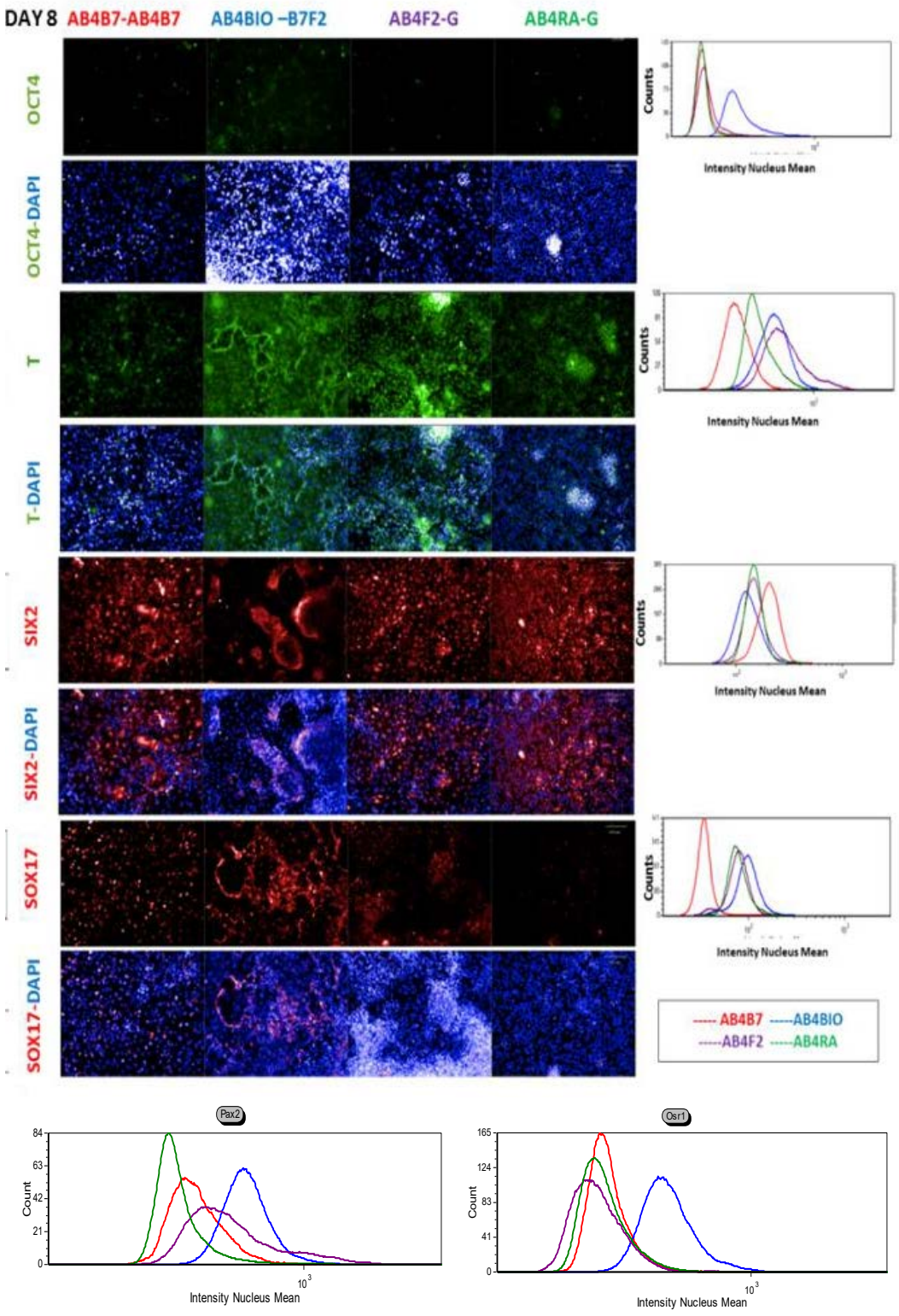

Figure 14: Screening of the optimal growth factor combination for renal progenitor generation after 8 days. The number of nuclei expressing the transcription factors OCT4, T, SIX2, SOX17, PAX2 and OSR1 out of 1000 nuclei in every combination were quantified using high content image analysis as shown in the accompanying graphs portraying count (each cell = 1 count) versus intensity of fluorescence of the nuclei. Scale bar = 50µm.

Testing the best performer AB4RA-G on several PSC lines indicated a high efficiency of renal progenitor generation within 8 days. While the cell line IMR90-iPS showed 60% efficiency, two urinary cell-derived induced PSC-lines generated in our lab: BCRTi004 and BCRTi005 attained 75-80% efficiency in terms of SIX2 expression (**Fig.15**). The occurrence of LHX1 in a majority of the cells at this stage in conjunction with PAX2 corresponds to the manifestation of nephric duct as well as representative of RV cells. Moreover, association of LHX1 cells and CDH16 demonstrates the synchronous development of the ureteric epithelium(Karavanov et al., 1998; Shen et al., 2005). Therefore, AB4RA-G was verified to be the optimal protocol for deriving major renal progenitor populations including MM, ND and RV.

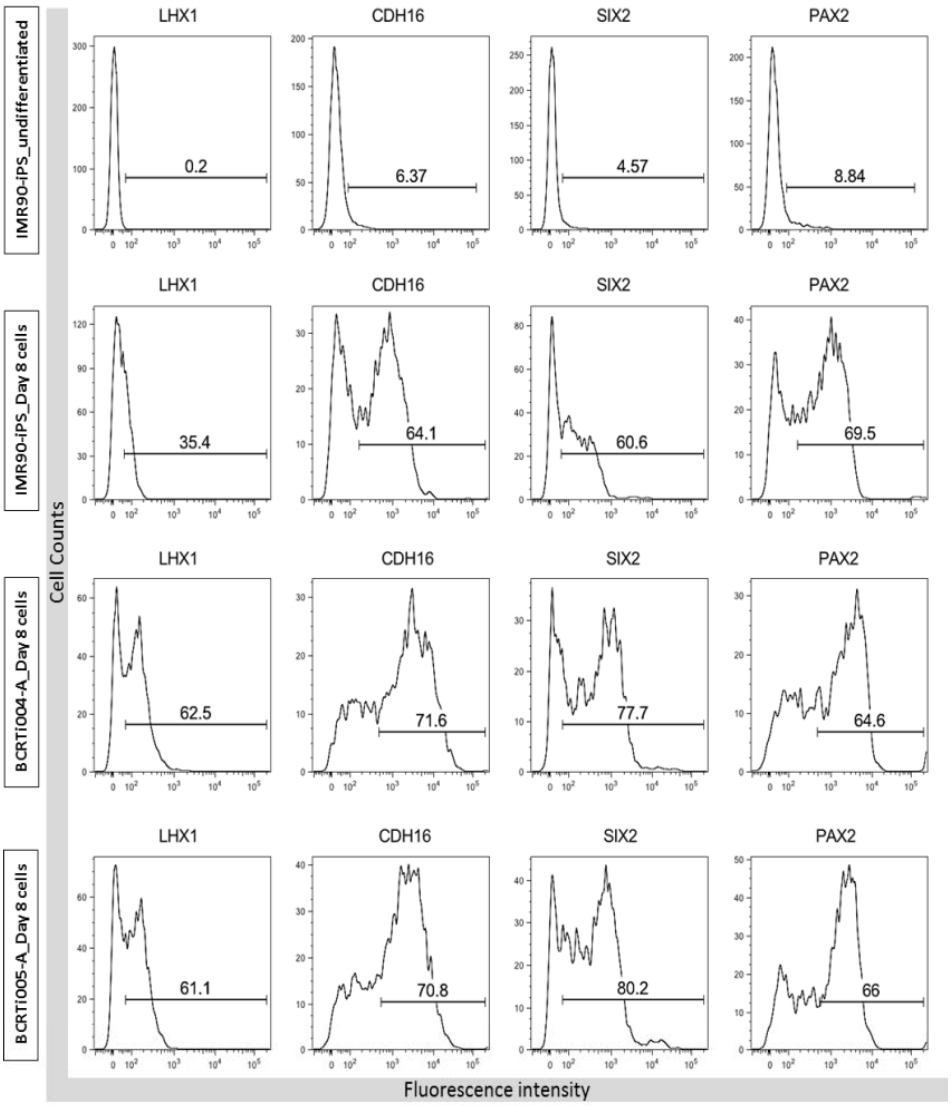

Figure 15: Efficiency of generation of renal progenitors. Flow cytometric analysis of day-8 cells generated shows SIX2⁺/PAX2⁺ cells representative of MM. LHX1⁺/PAX2⁺ cells representative of pre-tubular aggregate and together with CDH16 indicative of ND cells. Day 8 cells were generated from the human pluripotent stem cell lines IMR90-4-iPS and lab-derived iPSC lines BCRTi004 and BCRTi005.

4.1.3.1. Morphological characteristics

The process of differentiation was accompanied by marked morphological changes of the cells. In AB4RA for 2 days, hPSCs began losing their compact structure and spread out throughout the culture surface accompanied by cell proliferation and considerable amount of cell death. Following two further days of AB4RA, the differentiating cells began forming dome-like structures in culture (**Fig.16**). Removal of AB4RA and addition of GDNF for the next 4 days lead to a loss of dome-like structure and cessation of massive cell death. A heterogeneous cell mass characterized by epithelial islands surrounded by mesenchymal cells was observed by the eighth day of differentiation (**Fig.16).** A starting culture of hPSCs (~ 800,000 cells) yields around 4 million cells (up to 5-fold increase).

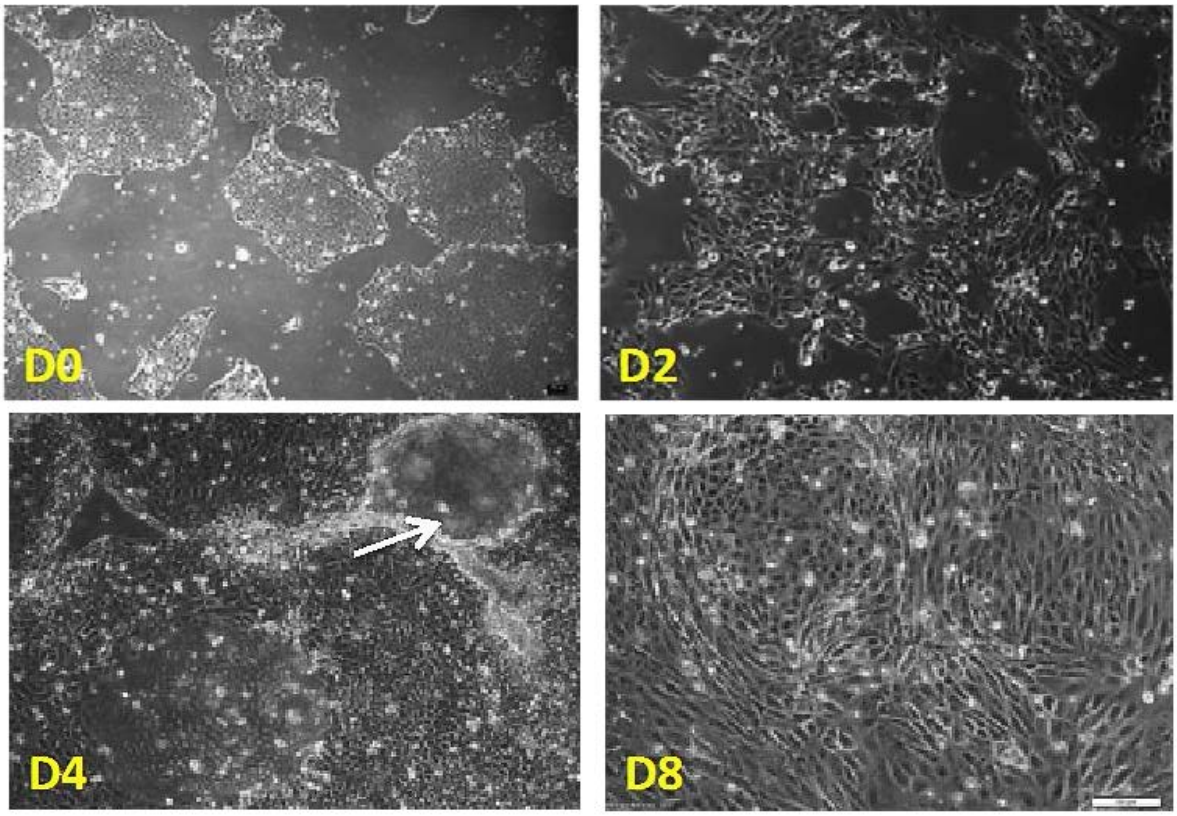

Figure 16: Morphological characteristics of AB4RA-G. Pluripotent stem cells colonies (D0) exposed to AB4RA form confluent cultures exhibiting dome formation (arrowhead) by D4. GDNF treatment is followed by rapid proliferation and formation of islands of mesenchymal cells surrounded by epithelial cells (D8).

4.2. Dissecting the molecular signatures of renal progenitors derived from hPSC.

4.2.1. AB4RA effectively breaks pluripotency coaxing the appearance of mesendodermal cells in 2 days.

iPS cells are generated by reprogramming somatic cells back to pluripotent state with defined reprogramming factors, OCT4, SOX2, KLF4 and C-MYC (also known as Yamanaka factors). These transcription factors and their downstream target genes coordinately promote self-renewal and pluripotency hence the first step of differentiation involves the disruption of this state. When PSCs are treated with the activinA-BMP4-RA combination for 48 hours, OCT4, NANOG and cMYC are down-regulated, promoting germ layer formation (**Fig. 17).** KLF-4 on the other hand was up-regulated, concurring with evidence from *Xenopus* suggesting the involvement of Klf-4 as a competence factor in early embryonic cells to be responsive to inducing signals for germ-layer differentiation and body axis patterning (Cao et al., 2012).

An increase in the expression of ACVR1 indicates a response to activinA provided in the induction medium. Also, notable changes are the upregulation of BMP4 and WNT3 that help in defining mesodermal identity. While BMP4 was provided in the induction medium and activation of its downstream SMADs or feed forward loop is obvious, the WNT and FGF pathway have likely been switched on by reciprocal signaling of cells creating several different cell populations (**Fig.17** bar graph). Existence of all three germ layers can be marked by the appearance of several early lineage signatures. For example, Dlx5 is one of the earliest known markers for the most rostral ectoderm, before the formation of an overt neural plate(Yang et al., 1998). Meis1 and Pax6 are involved in early neural and later pancreatic development (Cerdá-Esteban and Spagnoli, 2014).

Among the genes that are commonly accepted as mesoderm markers and key players in mesoderm specification and patterning, are those coding for the transcription factors, TWIST, SNAIL, GATA factors and Brachyury (T). GATA factors appear to play crucial roles in specifying mesendoderm in early development, later specifying endoderm, when mesoderm separates from endoderm(Technau and Scholz, 2003). The conserved chromosomal organization of Hox genes in clusters (four in vertebrates) is intimately linked to regulatory constraints, which couple Hox gene expression to the progression of embryonic patterning.

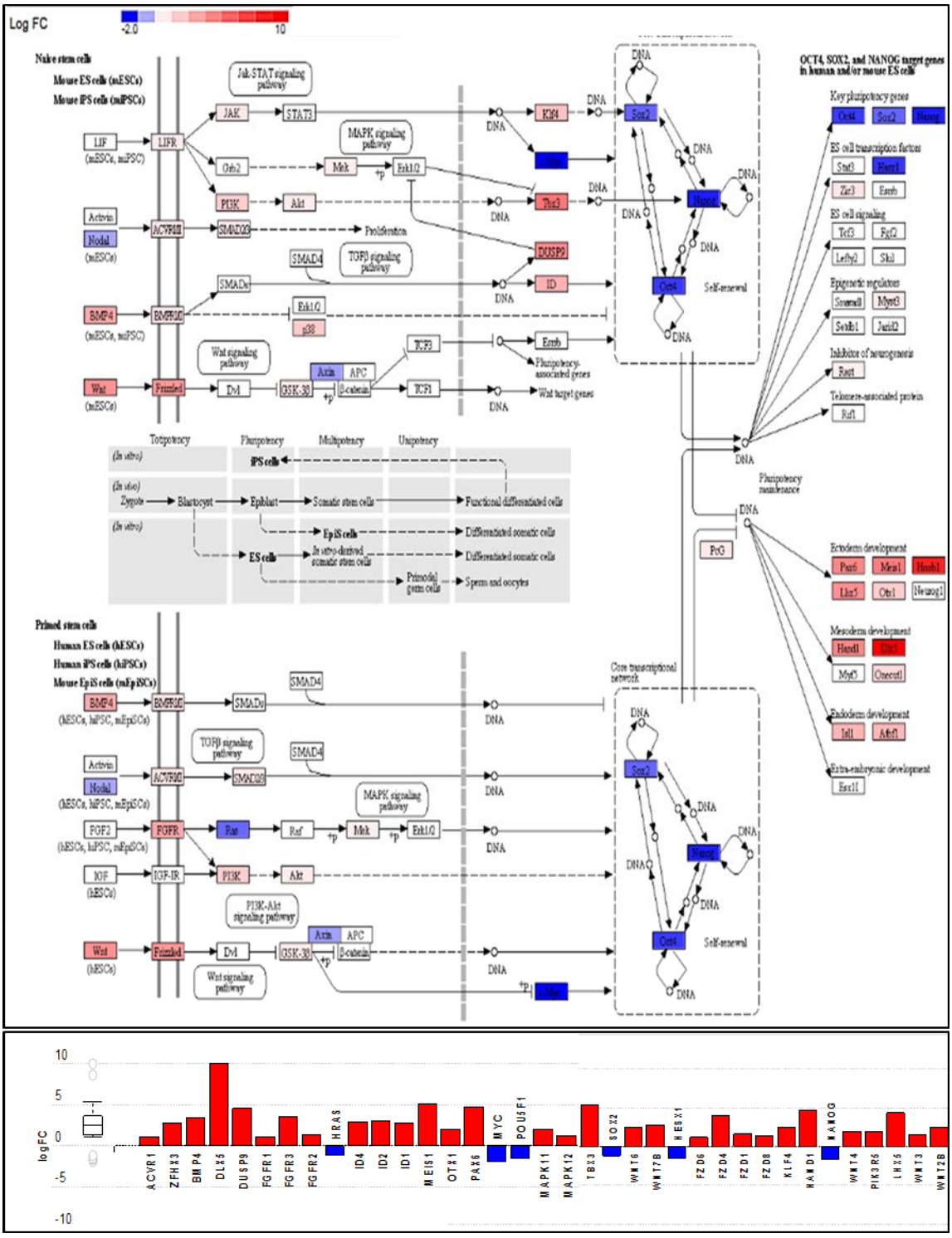

Figure 17: Signaling pathways regulating pluripotency of stem cells (KEGG: 04550): The pathway diagram is overlaid with the computed total perturbation of each gene. The highest negative perturbation is shown in dark blue, while the highest positive perturbation in dark red. The legend highlights the different gradients in between.

Embryonic mouse and chick studies suggested that mesoderm acquires positional information when emerging from the primitive streak (Tam and Beddington, 1987), and Frohman et al. proposed that differential Hox gene expression is established at that moment(Frohman et al., 1990). Concurrent with literature, HOXA1, HOXA3 and HOXB1-2 are elevated after 48 hours of AB4RA treatment as seen in **Table 13**.

Around 5-fold increase is seen in the case of TBX3 and HAND1 **(Fig.17)**. TBX3 orchestrates a complex network of downstream effects within the T-box family members to direct pluripotent cells toward a mesendodermal fate (Weidgang et al., 2013). HAND1 belongs to the basic helix-loop-helix family of transcription factors and regulates cardiac morphogenesis(Riley et al., 1998). MEOX1 is important for somitic development (Mohamed et al., 2013) and PAX genes, also involved in organ development, are highly up-regulated **(Table 13)**. Altogether, AB4RA treated PSCs were successfully coaxed to different lineages by 2 days and began to show commitment towards specific parts of the mesoderm including LPM and PM together with HOX delineated anterio-posterior patterning.

Table 13: Genes expressed differentially between Day 0 and Day 2 of AB4RA treatment.

Gene symbol	Gene name	Log-FC	P-value
GATA3	GATA binding protein 3	6.920	1,89E-04
GATA2	GATA binding protein 2	6.394	1,89E-04
GATA6	GATA binding protein 6	4.691	1,89E-04
GATA4	GATA binding protein 4	4.287	1,89E-04
TWIST1	Twist family bhlh transcription factor 1	3.930	1,89E-04
SNAI2	Snail family transcriptional repressor 2	2.455	1,89E-04
SNAI1	Snail family transcriptional repressor 1	1.116	1,89E-04
MEOX1	Mesenchyme homeobox 1	7.221	1,89E-04
GSC	Goosecoid homeobox	3.503	0.022
PAX6	Paired box 6	4.725	1,89E-04
PAX7	Paired box 7	3.116	3,61E-04
HOXA1	Homeobox A1	10.000	1,89E-04
HOXB1	Homeobox B1	8.612	0.008
HOXA3	Homeobox A3	8.480	0.007
HOXB2	Homeobox B2	6.896	1,89E-04
HOXB3	Homeobox B3	4.867	8,33E-04

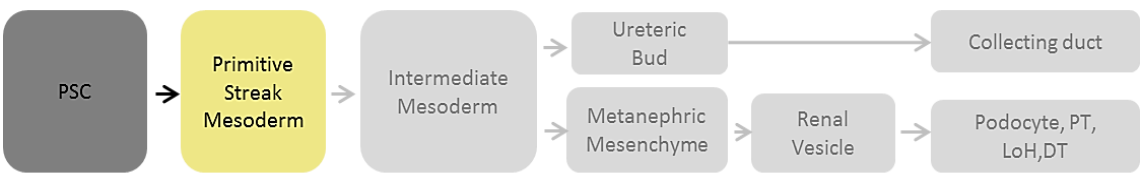

Figure 18: Progress in embryonic development in vitro.

4.2.2. Intermediate mesoderm cells pave the way for metanephric and ureteric cells by day 4.

Two days of AB4RA exposure resulted in heterogenous PSC-derived progeny that represented a post-gastrulation embryo. According to the protocol, AB4RA treatment for sustained for two more days until day 4. It can be hypothesized that the developmental stage of the day 4 cells were specified to IM.

Table 14: Genes expressed differentially between Day 2 and Day 4 of AB4RA treatment.

Gene Symbol	Gene Name	Log FC	P-value
DCN	Decorin	10.000	4,07E-04
OSR1	Odd-skipped related transciption factor 1	6.453	4,07E-04
HOXB4	Homeobox B4	4.873	4,07E-04
HOXB7	Homeobox B7	3.863	4,07E-04
EYA1	EYA transcriptional coactivator and phosphatase 1	2.906	4,07E-04
AQP3	Aquaporin 3	2.044	4,07E-04
KIF26B	Kinesin family member 26B	1.901	4,07E-04
NPNT	Nephronectin	1.690	4,07E-04
SIX2	SIX homeobox 2	1.631	4,07E-04
LHX1	LIM homeobox 1	-1.783	4,07E-04
OTX2	Orthodenticle homeobox 2	-2.072	4,07E-04
RET	Ret proto-oncogene	-3.451	4,07E-04
DAZL	Deleted in azoospermia like	-4.180	4,07E-04
TDRG1	Testis development related 1	-4.242	7,60E-04
EGR3	Early growth response 3	-5.080	4,07E-04

Comparison of gene expression between day 2 and day 4 cells (**Table 14**) revealed an up-regulation of OSR1 marking the IM accompanied by an increase in HOXB4 that marks the anterior boundary of IM in chick, regulated by RA signaling, causing LHX1 expression (James and Schultheiss, 2003; Preger-Ben Noon et al., 2009). Although the level of LHX1 was down-regulated at day 4 (compared to day 2), this gene was active and was visualized in cells by immunofluorescence (**Fig.19**). No significant change was seen in the level of PAX2 between day 2 and day 4. Also, the presence of $LHX1^{+}$-$PAX2^{+}$ cells **(Fig.19)** represents a nephric duct-like population. An approximately3-fold up-regulation of EYA1 in an $OSR1^{+}$ context suggests a parallel development of nephrogenic mesenchyme, a stage similar to E9.0 in embryonic mice.

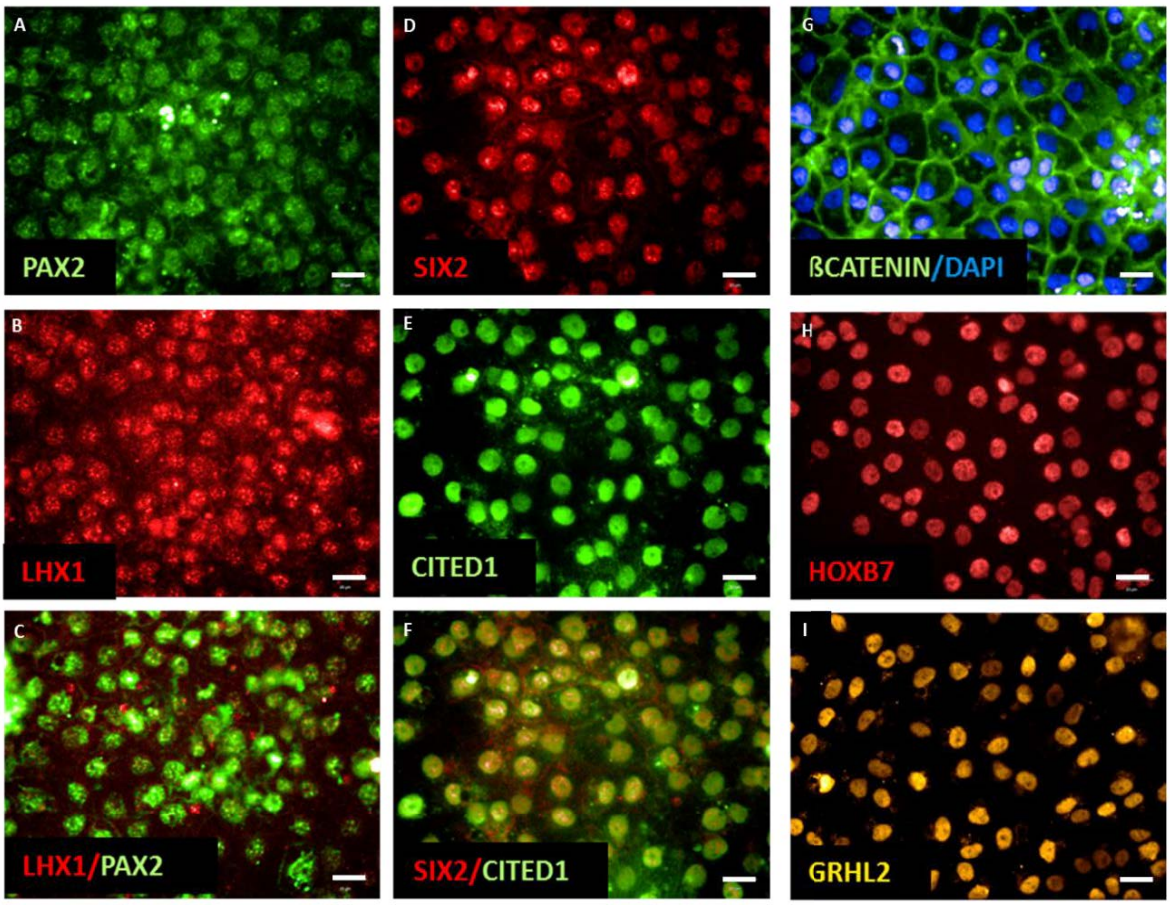

Figure 19: Expression of IM, MM and UB related transcription factors in PSC-derived cells. Exposure to AB4RA-G induces expression of intermediate mesoderm and metanephric mesenchyme markers PAX2, LHX1, SIX2, and CITED1 by day 4. (A-F). Expression of ß-CATENIN (G) and ureteric progenitor markers HOXB7 and GRHL2 (H, I) were seen by day 8. Scale bar = 50µm.

The simultaneous up-regulation of HOXB7 (4.8 fold) and SIX2 (1.6 fold), however, points to the further development of ND to UB and nephrogenic mesenchyme to MM. This was also supported by the immuno-histochemical observation of these transcription factors (**Fig. 19**). In contrast to our hypothesis, the cells are more advanced in development than IM. Appearance of higher levels of DCN, NPNT and KIF26B illustrated the possible establishment of a niche for $SIX2^{+}$ cells. The decrease in OTX2 and EGR3 suggests a reduction in neural development. Since IM cells are progenitors of kidney and gonads, the presence of TDRG1 and DAZL is unavoidable, but their down-regulation together with the emergence of MM and UB hints at the inability of the cell mixture to advance gonadal development. A morphological characteristic of AB4RA cultures at day 4 is the manifestation of domes due to fluid retention in the cell layer. RNA-Seq data indicate significant up-regulation of AQP3, SLC10A4 and SLC23A3 and several other solute career family members that actively transport electrolytes upon formation of a polarized epithelial layer.

Kinetics of IM and MM markers were investigated by immunofluorescence as the data from screening experiments with only 2 time points (day 4 and day 8) did not correlate with RNA-seq. The transcription factor expression was quantified by high-content analysis of the image data. As seen at the RNA level, the markers initially appeared at day 2, rising steadily until day 6 after which they were sustained till day 8 (SIX2) or died down by day 8 (PAX2, CITED1, LHX1). The efficiency of the protocol was measured in earlier experiments **(Fig. 15)** towards the regression of these markers and need to be reconsidered by their expression at day 4, which for IMR90-iPS-derived cells was ~85% (**Fig.20**).

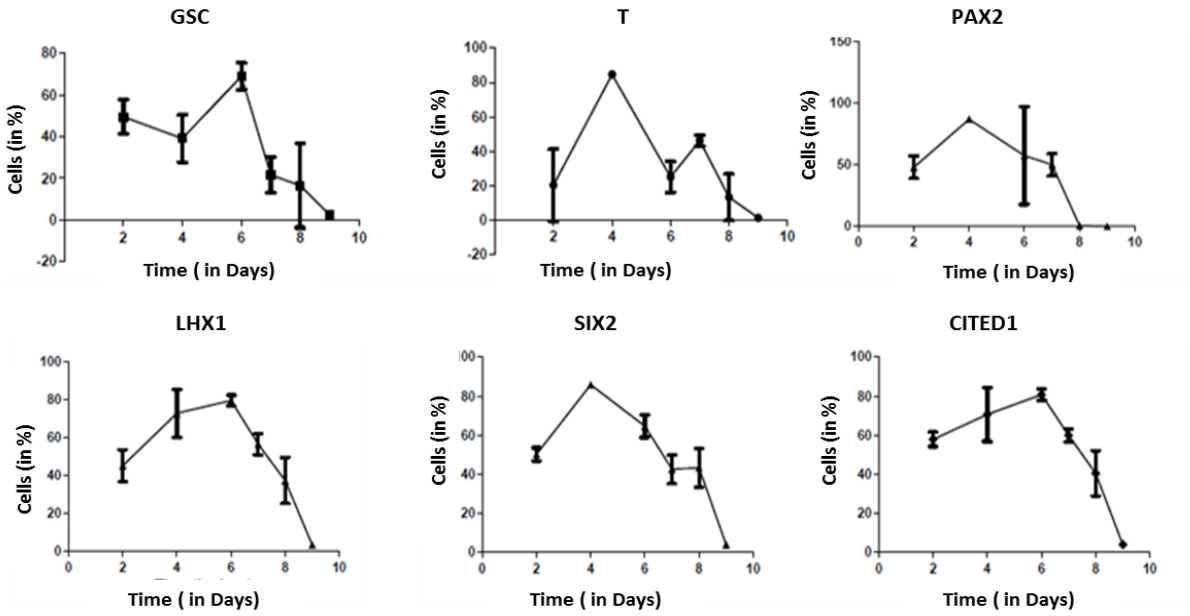

Figure 20: Quantification of developmental stage-specific transcription factors of AB4RA-G protocol..The number of nuclei positive for the desired markers was assessed by high-content image analysis every other day of differentiation. (n=3)

The best recorded data of nephrogenesis in mammals is in the mouse model, making it a gold standard to assess the extent of renal differentiation. The top 198 differentially expressed genes (upregulated in day 4 versus day 2) were used to investigate the extent of enrichment of renal pathways by matching them to publicly available RNA-seq transcription profiles obtained from stage-specific embryonic kidney cells of the mouse (GUDMAP). Single cells were isolated based on different subsets in the nephrogenic zone. Significant correlations were obtained for 3 major populations: MM, ureteric epithelium (UE) and stromal mesenchyme (SM). The genes most strongly representing this link as identified by Toppgene enrichment analysis (Chen et al., 2009) are summarized in **Fig. 21**. While MM was majorly represented by transcription factors, the presence of genes KRT7 and EML5 are cytoskeletal and DCN, COL5A2, LUM are extra-

cellular matrix organization, respectively for UE and SM, suggesting a more dynamic nature of the former and stabilized existence of the latter populations.

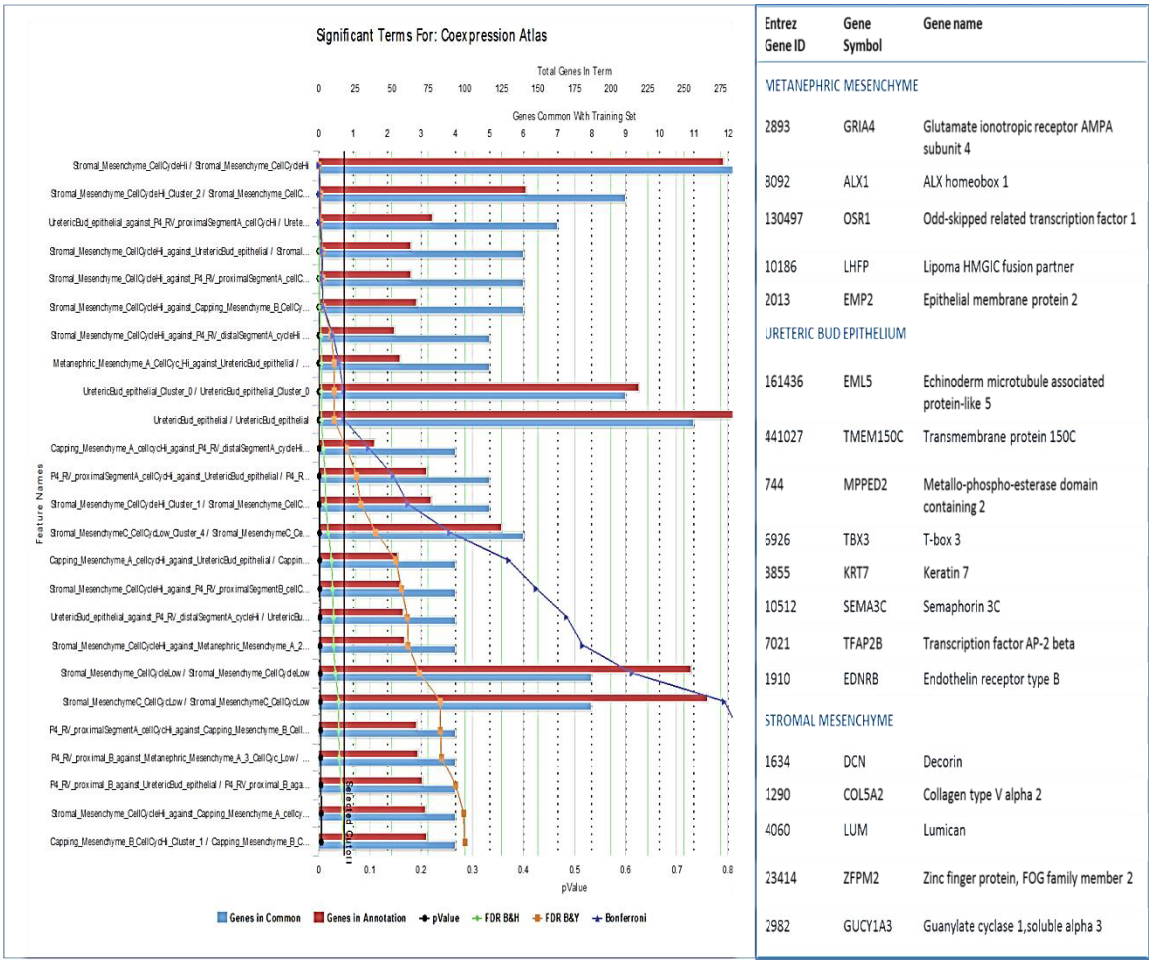

Entrez Gene ID	Gene Symbol	Gene name
METANEPHRIC MESENCHYME		
2893	GRIA4	Glutamate ionotropic receptor AMPA subunit 4
3092	ALX1	ALX homeobox 1
130497	OSR1	Odd-skipped related transcription factor 1
10186	LHFP	Lipoma HMGIC fusion partner
2013	EMP2	Epithelial membrane protein 2
URETERIC BUD EPITHELIUM		
161436	EML5	Echinoderm microtubule associated protein-like 5
441027	TMEM150C	Transmembrane protein 150C
744	MPPED2	Metallo-phospho-esterase domain containing 2
5926	TBX3	T-box 3
3855	KRT7	Keratin 7
10512	SEMA3C	Semaphorin 3C
7021	TFAP2B	Transcription factor AP-2 beta
1910	EDNRB	Endothelin receptor type B
STROMAL MESENCHYME		
1634	DCN	Decorin
1290	COL5A2	Collagen type V alpha 2
4060	LUM	Lumican
23414	ZFPM2	Zinc finger protein, FOG family member 2
2982	GUCY1A3	Guanylate cyclase 1,soluble alpha 3

Figure 21: Assessment of the association of genes highly regulated in PSC-derived cells and mouse embryonic kidney. Co-expression data illustrating the association of genes up-regulated in PSC-derived cells to different subsets occurring in embryonic kidney cells, their counterparts *in vivo* with the mouse embryonic kidney atlas (GUDMAP).

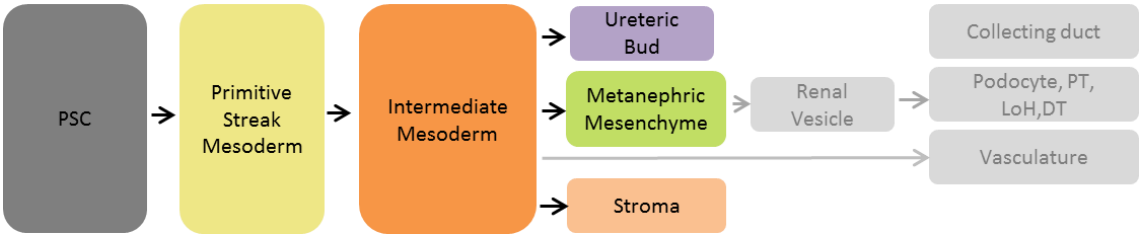

Figure 22: Progress in embryonic development *in vitro*

4.2.3. GDNF activates UB, reciprocally inducing MM to form nephron epithelia

The two important populations for the formation of the nephron and the collecting duct tree, which are the MM and UE respectively, are available by the end of day 4. The renal lineage is now specified and needs to be advanced to generate kidney cells. As per evidence from our screening to get maximal renal progenitors, following the exposure of PSC to AB4RA for 4 days, they were treated with GDNF for the next four days. In mice, GDNF is generated by MM and promotes ureteric morphogenesis by priming the nephric duct for bud initiation and secretion of WNT11 (*Appendix-Table*). We have already seen the occurrence of LHX1+/PAX2+ cells accompanied by GATA3 expression in the previous result **(Fig.19, 20 and Table 9)**. These cells represent the responder population of GDNF secreted by MM cells. We hypothesized that strengthening UB activation will lead to formation of ureteric epithelia that naturally induce condensation of MM and its subsequent epithelialization. Changes in cell identity due to this treatment are dissected with the help of RNA-seq data of cells harvested at day4, day 6 and day 8.

At day 4, cells show highest expression of SIX2-SIX1-SALL1 re-confirming the presence of MM **(Fig.23).** Sall1 is expressed in Six2-positive progenitors as well as differentiating nascent nephrons. Although in the mouse, the related transcriptional regulators Six1 and Six2 play non-overlapping roles in nephron progenitors: transient Six1 activity prefigures, and is essential for, active nephrogenesis; by contrast, Six2 maintains later progenitor self-renewal from the onset of nephrogenesis. In humans, an auto/cross-regulatory loop drives continued SIX1 and SIX2 expression during active nephrogenesis. (O'Brien et al., 2016). This population expresses KIF26B, produces NPNT (**Table 9**) and has the ability to secrete GDNF. The presence of RET (**Fig.23**) hints the readiness of the LHX-PAX2 expressing cells to receive the GDNF signal and activate UB formation indicated by the gradual appearance of CDH1 and SOX9 at day 6 that is prolonged till day 8. Expression of SOX9 can be found from the earliest stages of renal development within the ureteric tip, the ureter mesenchyme and in a segment-specific manner during nephrogenesis. SOX8/9 are required downstream of GDNF signaling for the activation of RET effector genes such as Sprouty1 and Etv5 (*Appendix-Table*). The presence of HOXB7 was sustained and not significantly altered between Day 4 and Day8 as indicated by absolute FPKM values. Day 8 marks the highest expression of WNT11 and WNT9b demonstrating a functional UB, producing signals to regulate itself and the surrounding mesenchyme as is seen *in vivo*.

The expression of several growth factors including FGF8, BMP7 and BMP2 are seen to increase until Day 8 along with the WNTs secreted by the UB population. The fate of SIX2+ MM cells to either maintain stemness and self-renewal or epithelial transition to form the renal vesicle is a decision based on the balance between BMP-FGF-WNT controlled ß-catenin (CTNNB1) gradient(Lindström et al., 2014). BMP7 activates CITED1 in SIX2+ cells, marker of the iMM. Concurrent with the sequence of embryonic events, we also observe a shift from CITED1+ cells at day 6 (CM) to the $LEF1^{+}$, WNT4, FGF8 and HEY1 expressing population characteristic of the pre-tubular aggregate. (*A description of the roles played by these genes and the phenotype caused by their loss of function can be found in the appendix, Appendix-Table*)

Surprisingly, the presumptive PTA also expressed several genes associated with stage I nephrons – the renal vesicle. Broadly, markers common to the proximal and distal RV-like stage, including JAG1, CCDC86, CDH6, WNT4, PAX8, NPY and CDH4 showed elevated expression at day 8. The distal expression of Notch (Dll1, Jag1), Bmp (Bmp2), and Wnt (Wnt4, Lef1, and Dkk1) pathway genes implies different cellular identity and activity along the proximal–distal axis ((**Fig.23, 24**) (Georgas et al., 2009; Kopan et al., 2007). Many of these genes are critical for specification of specific nephron segments. WT1 was also expressed at day 8 marking proximal RV. LHX1, POU3F3 (Brn1), GREB1 and DLL1 were expressed at day 2 with a higher expression at day 4 already. Genes such as Lhx1 and Pou3f3 occupy distal RV domains, whereas Wt1 expression becomes restricted to proximal regions. Notch signaling, predominantly Notch2, is critical for the elaboration of proximal nephron fates (podocytes and proximal tubules) whereas Lhx1 regulates patterning of distal tubular structures. Lhx1 is upstream of Notch2, which in turn regulates the onset of expression of another distal RV gene, Cdh6. Although we detected the up-regulation of CDH6 at day 8, we were not able to observe NOTCH2 expression. Instead, NOTCH1 expression was recorded. Chen *et al*. report strong Notch1 expression in capillary loop vascular wall including glomerular mesangial and endothelial precursors, whereas nothing was detected in the podocytes (Chen and Al-Awqati, 2005). Interaction of the highest up-regulated genes reveals their heavy interdependence in regulating proximal-distal polarity (**Fig.25 left**).

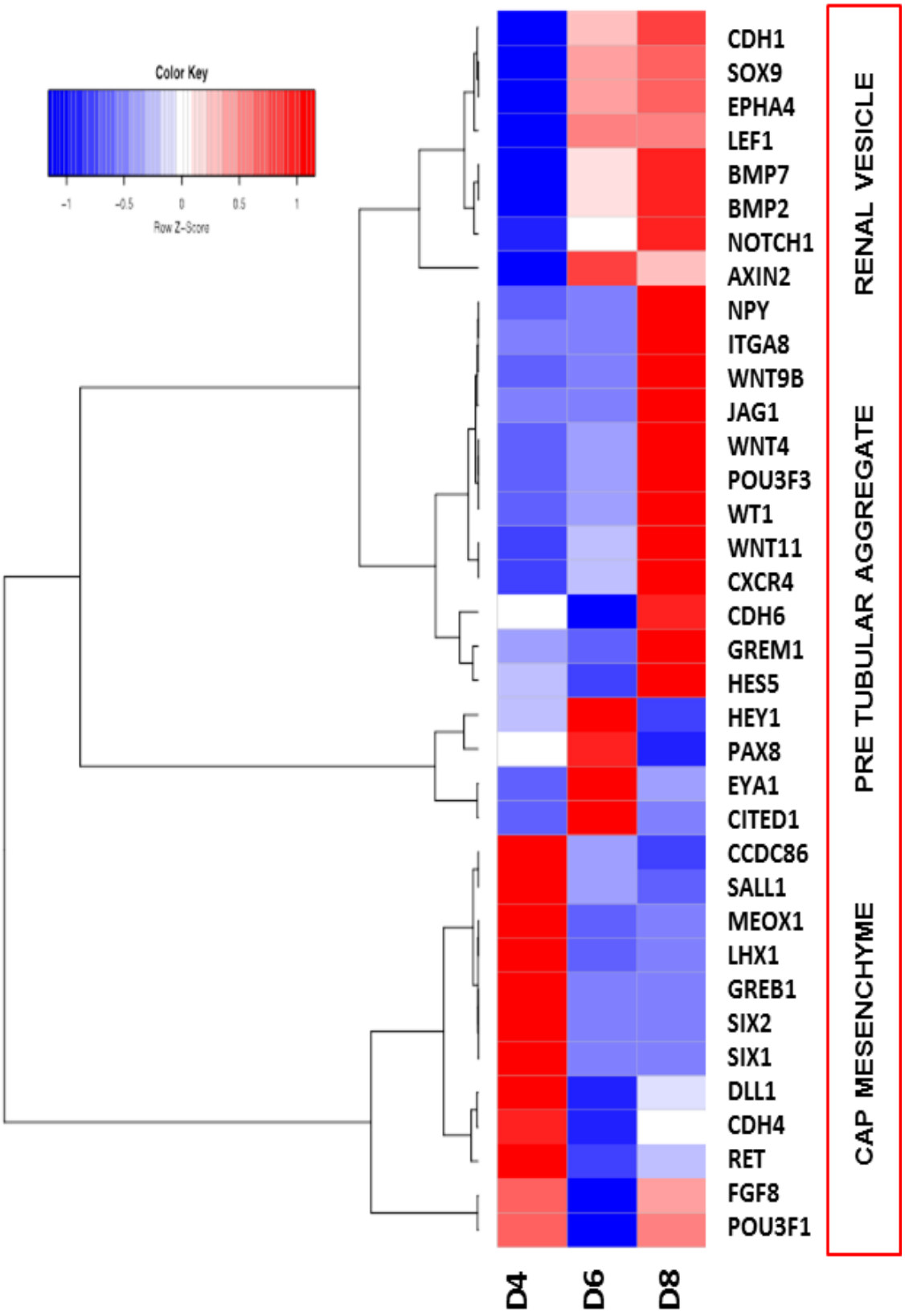

Figure 23: Mesenchymal epithelial transition of MM to renal vesicle stage. Heatmap showing the expression pattern of major genes involved in pre-tubular aggregate formation and RV development during nephrogenesis.

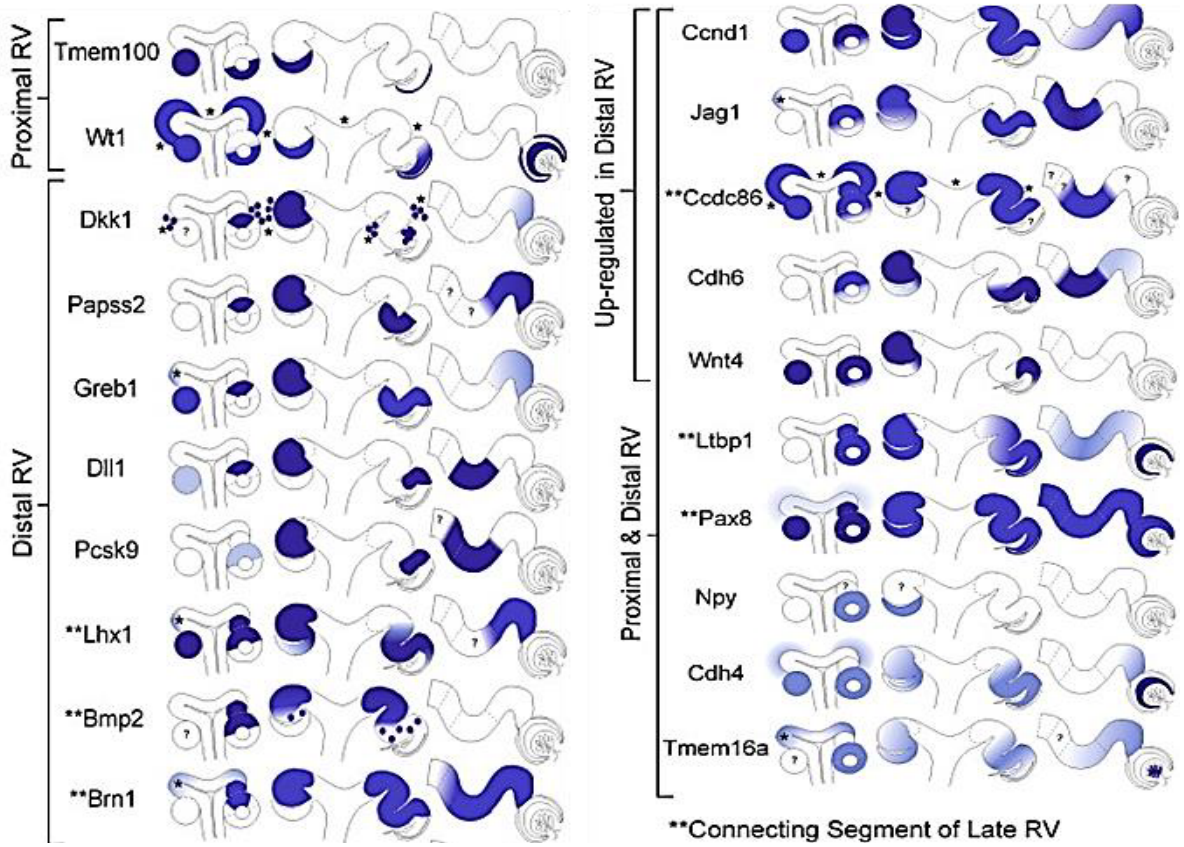

Figure 24: Expression of the desired genes mapped as per their occurrence in embryonic mouse kidney development (Georgas 2009).

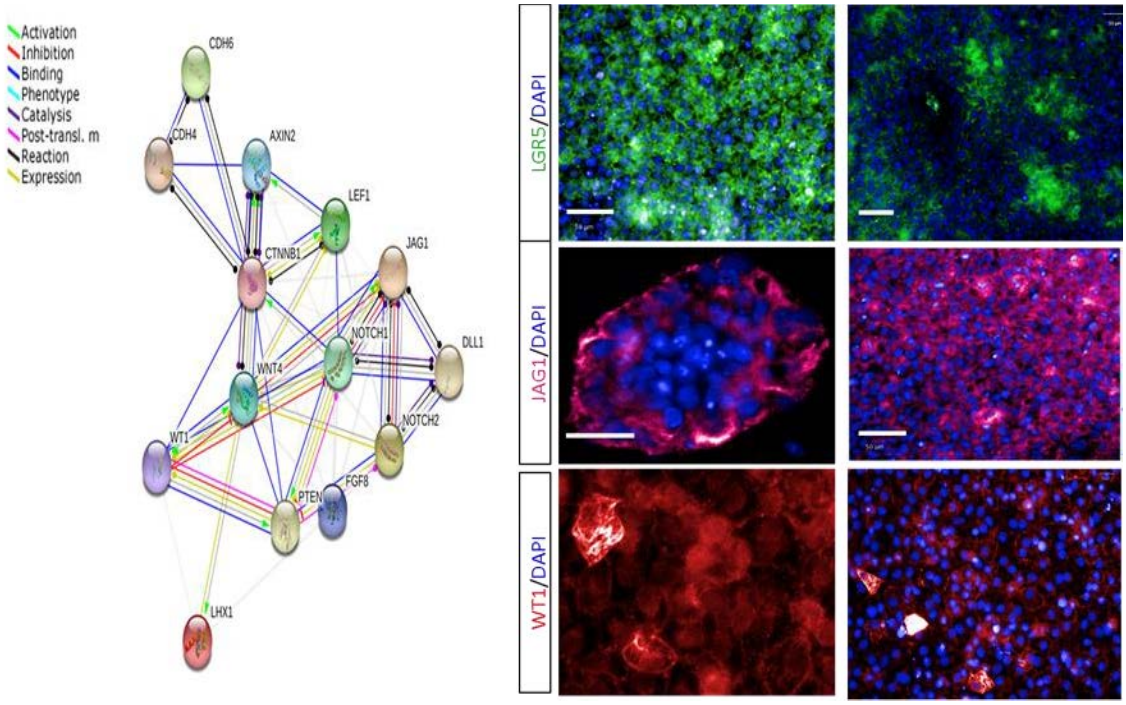

Figure 25: (Left) Interaction of highly up-regulated genes on day 8. (right) Segmentation genes of RV Immunofluorescence staining shows protein expression of JAG1 and LGR5 (medial and distal RV markers) in day 8 cells.

Distinct cell-populations form after polarization and these produce the different segments of the adult nephron; a Wt1+ cell population gives rise to proximal structures, a Jag1+ population to the medial part and Lgr5+ cells generate the distal nephron segments. The strong evidence of segmentation prompted us to investigate protein localization of 3 of these genes WT1, JAG1 and LGR5, in day 8 cells (**Fig.25**). Indeed their presence was detected but with no particular pattern of organization as observed *in vivo*.

Thus, the cell mass obtained at day 8 is poised to segment and elongate into different compartments of the nephron together with ureteric epithelia primed for collecting duct formation.

4.2.4. Autonomous renal precursor interactions lead to development of kidney organoids.

After completion of 4 days of AB4RA and 4 days of GDNF treatment, cells were rested without medium change for 2 additional days. This resulted in the spontaneous appearance of compound structures spanning 200-500 μm with multiple columnar epithelial rings (50-100 μm) bounded by a common basal membrane (**Fig.28)**. While in the case of WA01- ESC by the end of 8 days of induction, for the IMR90- iPSC- line, these structures appeared only when the day 8 cells were left in culture for 2 more days without dissociation into single cells. These structures were classified as organoids and occurred on an average at a rate of 6 organoids per cm^2 (n=5) for all cell lines. Thus, the ESC at day 8 and iPSC at day 10 seem to be equivalent in developmental maturity.

In order to understand why the spontaneous event of organoid formation happened in the case of ESCs on day 8 while at the same time point the iPSC lines did not form organoids, we investigated the gene expression. Comparing the gene expression of ESC- derived day 8 organoids to the same set of genes discussed before, spanning between MM to a polarized renal vesicle, we found interesting patterns **(Fig.26)**.

The organoids showed the highest expression of WNT9B, BMP2 and BMP7, which are all required for inducing CM and its priming for epithelialization. Furthermore, all day 8 cells shared the high expression pattern of LEF1, WNT4, NOTCH1, JAG1, CDH6 and HES5. Although the pattern was similar, the organoids show a higher tendency of genes responsible for a more medial and distal segment of the nephron. Prominently, the set of genes grouped together included CDH6, JAG1, POU3F3 and WNT4.

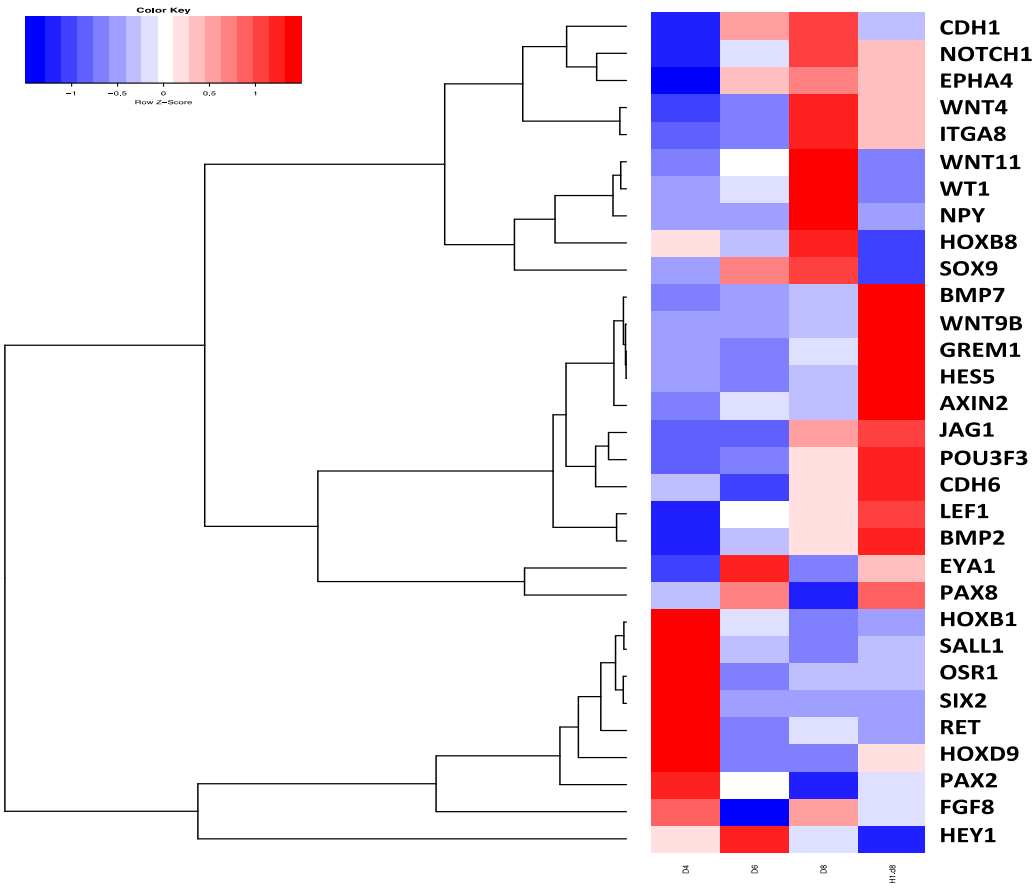

Figure 26: Mesenchymal-epithelial transition of MM to renal vesicle stage in organoids. Heatmap showing the expression pattern of major genes involved in pre-tubular aggregate formation and RV development during the course of organoid formation obtained by RNA-Seq.

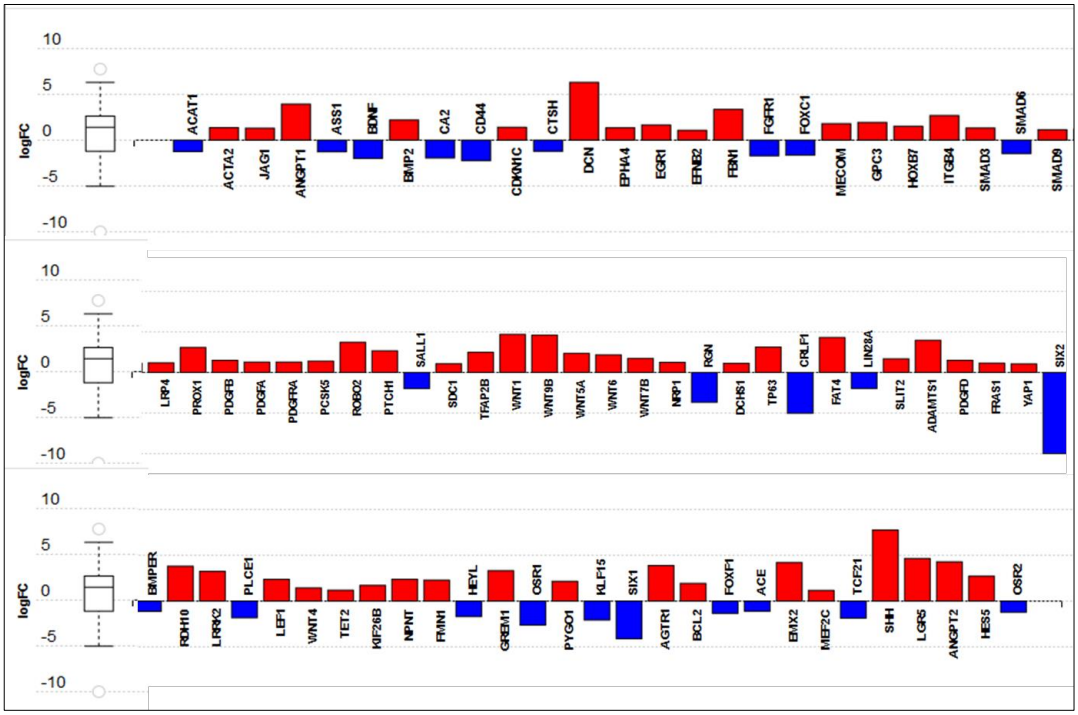

Figure 27: Differential expression of day 4 and organoid with respect to renal system development genes obtained by RNA-Seq.

Interestingly, even though most genes correlated to nephron segmentation, a synchronous occurrence of EYA1-PAX8 and HOXD9 hints at the possibility that a lingering metanephric progenitor population can probably act as a source of nascent nephrons as the previous ones mature. As the orchestration of the EYA-PAX-HOX was observed in the organoids **(Fig.26)**, they were compared to MM cells of day 4 **(Fig.27)**. As seen previously, the renal vesicle associated WNT and segmentation genes were higher than day 4. Importantly, OSR1, OSR2, SIX1 and SIX2 were down-regulated but UB related genes HOXB7, GPC3, SHH and PTCH1 were up-regulated. Shh is secreted from the medullary collecting duct and ureteric stalk and signals to the Ptch1 receptor in the surrounding interstitium (Yu et al., 2002). A rather regular expression of HOXB7 in the pseudostratified epithelium of organoids was seen using immunofluorescence **(Fig.28)**. The manifestation of AGTR2, ANGPT1 and ANGPT2 together with a higher expression of PDGFA, B and D suggests a tendency towards mesangial and vascular differentiation.

An abundance of the nephronal segmental genes in the organoids highlights the question if signatures of mature nephrons are present. Gene expression data of ESC-derived organoids present high FPKM values of AQP3 and Na+/K+ ATPase reflected by the reactivity to *Lotus tetragonolobus* Lectin (LTL) and Cytokeratin18 (CK18/KRT18), known to have a high affinity to proximal tubules and whole nephron respectively (**Fig.28** E,F). Occurrence of Laminin indicates the formation of basement membranes in these structures. Thus, kidney organoids containing tubular and glomerular segments were obtained by 8-10 days of differentiation of hPSCs.

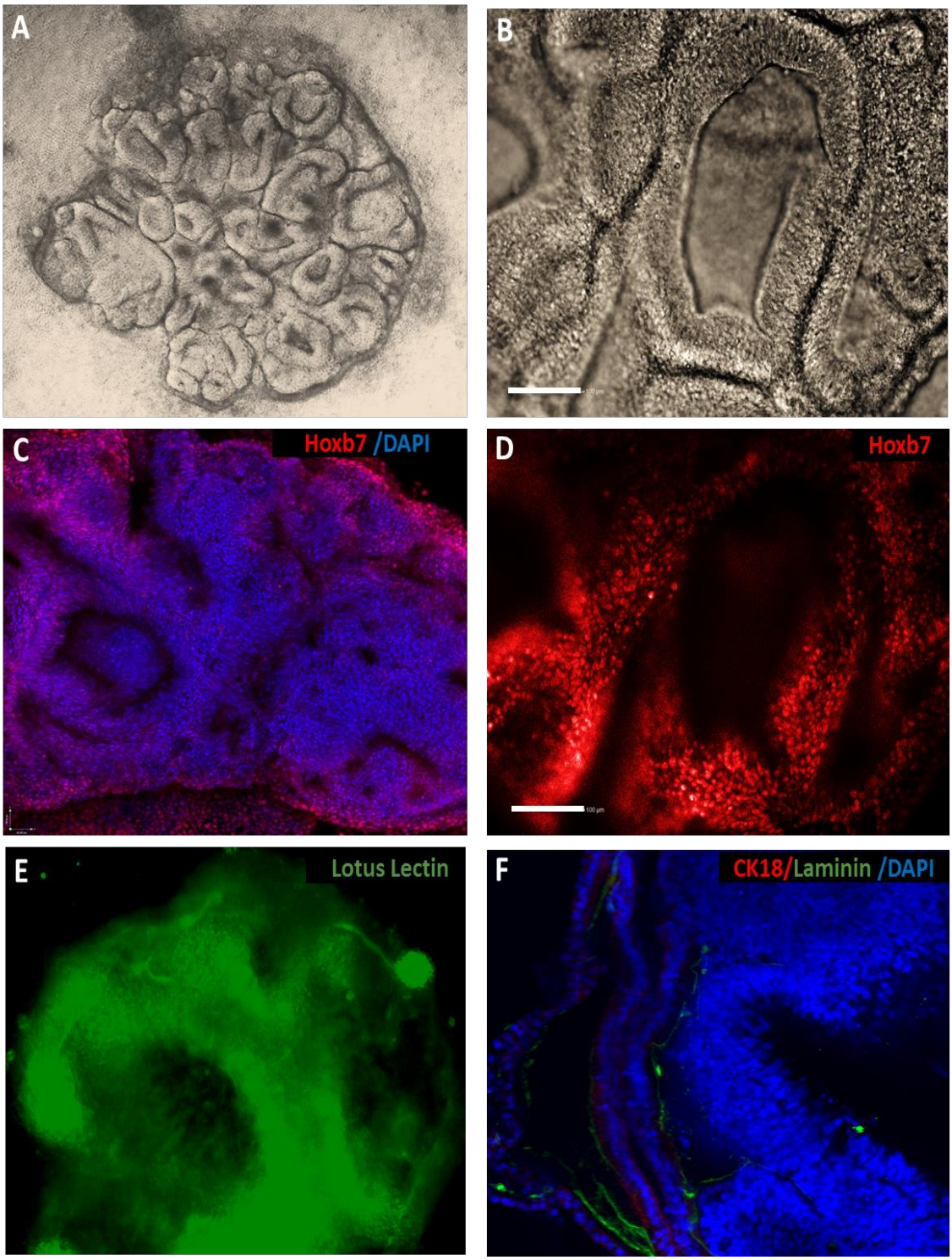

Figure 28: Organoid-like structures after 10-days of-AB4RA-G treatment on hPSCs. A, B- Phase contrast images, C- Hoxb7 stained nuclei of the organoid, D- higher magnification of C; E- Lotus lectin stained organoid, F- Organoid showing regions of Laminin (green) and Cytokeratin 18 (CK18 in green). C-F were obtained by multi-photon microscopy. Scale bar = 100µm.

4.3. hPSC-derived renal progenitors give rise to constituent cell types of the nephron *in vitro* –

4.3.1. Day 8 cells associate with reorganizing embryonic mouse kidneys

A classic method to demonstrate the renal competence of a progenitor population in question is to test for functional integration into kidney tissue(Takasato et al., 2014; Xia et al., 2013). In this assay, embryonic kidneys of mice were used that characteristically reorganize themselves after dissociation into single cells when cultured in an air-liquid interface (Fig 29: A). To test this with the progenitor cells generated by the AB4RA-G protocol, we condensed day 8 renal differentiation cells into a pellet together with dissociated e12.5 mouse kidney cells. After 4 days, tubular connections formed that ramified the aggregate (Fig.29: E, F) containing islands of human cells among murine embryonic kidney cells (Fig.29: G, H). Thus, day 8 precursor cells are successful in giving rise to nephronal aggregates in the absence of external induction factors.

4.3.2. Nephron developmental programs advance in RV-like cells without the requirement of external elements.

Molecular and immune-histochemical analysis of day-8 cells, indicate their poised state for nephronal development. To elucidate their inherent potency to generate different lineages of the nephron, day 8 RV-like cells were allowed to differentiate in the absence of induction factors post dissociation. Pellets of dissociated day 8 cells were prepared and placed on a trans-well membrane, an air-liquid interface facilitating movement of solutes through a membrane. The specific transport properties of epithelia are accomplished by the expression of proteins (co-transporters, exchangers, channels) governing the movement of ions on either cell side (Bachmann et al., 1999). Five days of pellet culture resulted in a 3D tubular network of cells, which showed the presence of transporters characteristic of the different tubular compartments of the nephron (**Fig 30**). Enriched occurrence of $AQP1^{+}$ and $Na/K\text{-}ATPase^{+}$ indicated the presence of proximal tubule-like cells. Also present were SLC12A3 (Sodium chloride transporter-NCCT), characteristic of the distal part of the nephron tubule, and UMOD (Tamm Horsfall protein-THP), which is a protein localizing to the thick ascending loop of Henle. This experiment demonstrates the potency of day 8 cells to spontaneously generate three types of nephron epithelia with characteristic transporters without the requirement of external stimuli like embryonic cells and growth factors.

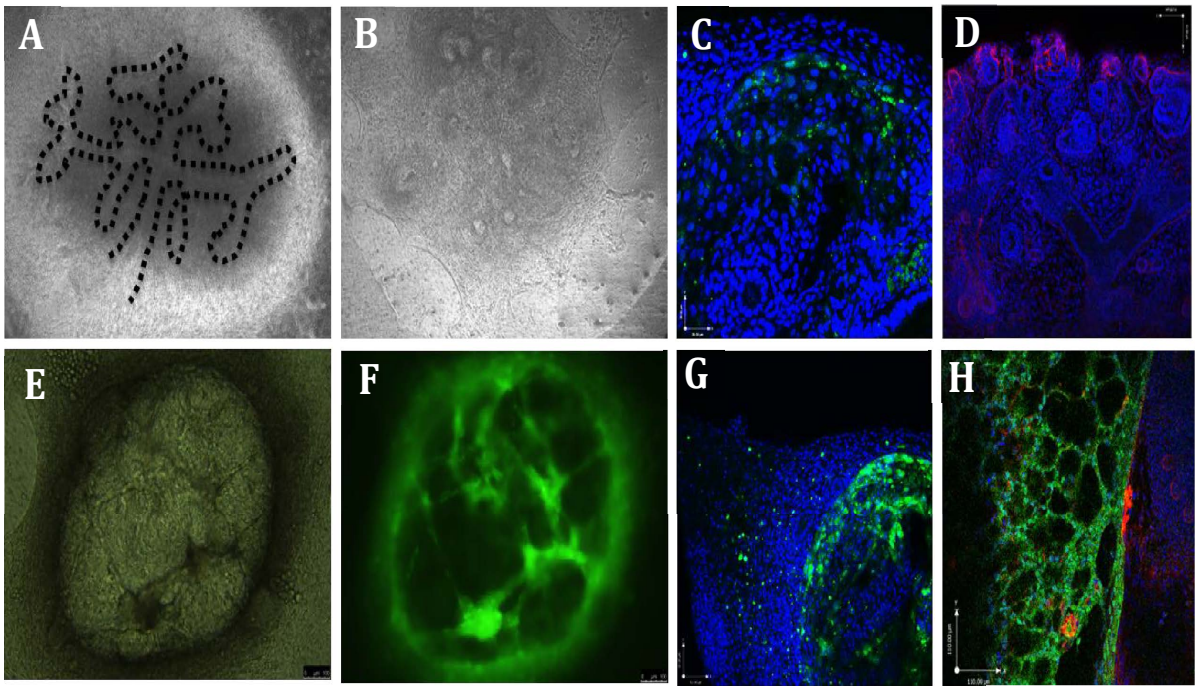

Figure 29: Embryonic mouse kidney re-aggregation assay with PSC-derived cells A, B: show phase contrast images of control E12.5 mouse kidney and a mixture of E12.5 mouse kidney cells and PSC-derived renal cells re-aggregated after dissociation. C, Confocal microscopy of aggregates reveals the presence of few human cells (Celltracker-Green) integrated, but no definite kidney structure as in (D) E12.5 mouse kidney aggregate showing the presence of a ductal tree and surrounding tubular bodies E-F:Phase contrast and fluorescence image of the chimaeric re-aggregation containing PSC.-derived renal cells (Celltracker-Green). And G, H: Confocal microscopy delineating the formation of a tubular network by human cells separate from non-green mouse cells.

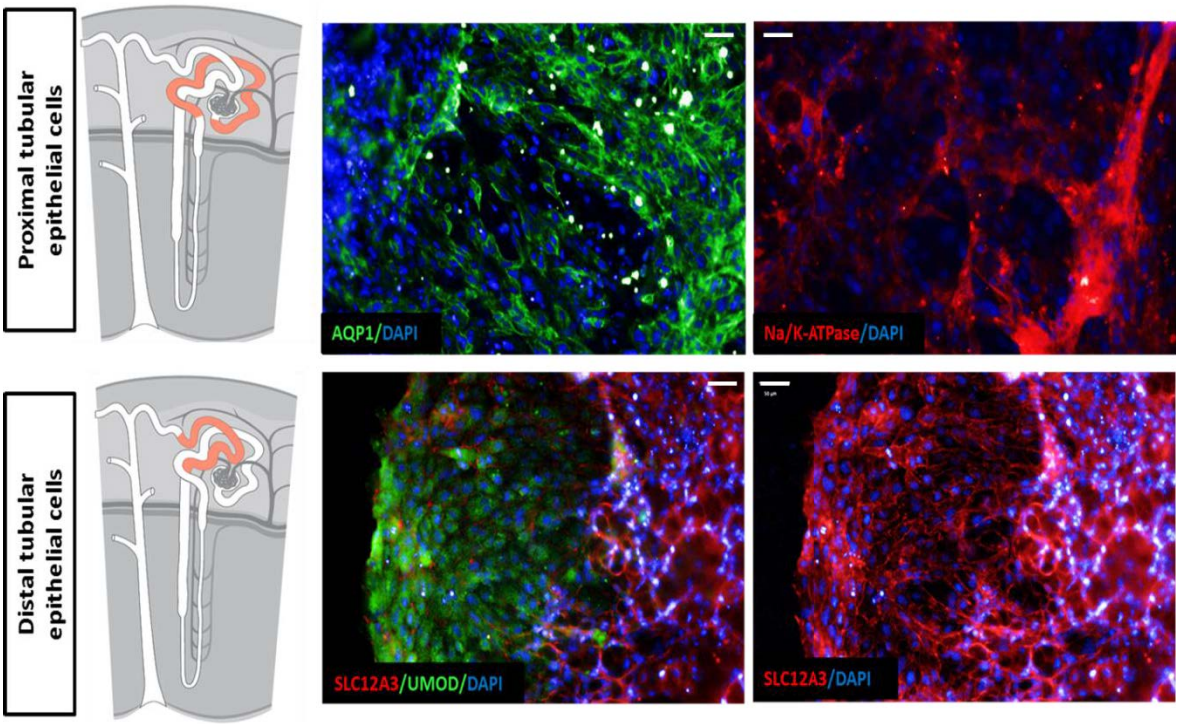

Figure 30: Tubular epithelium formation in pellet culture. Whole-mount immunofluorescence staining of Day 8 cells cultured as a pellet for 5 days in DMEM-FCS shows(A,B) proximal tubular epithelial markers: AQP1 and Na/K-ATPase and (C,D) distal tubular epithelial marker SLC12A3 and Loop of Henle marker Uromodulin expressing cells forming networks in a heterogenous mixture. Scale = 50µm.

Evidence from these experiments suggests that RV-cells can be steered with specific growth factors to obtain individual nephron constituent cell types spanning from the glomerular compartment to the entire tubular compartment until the collecting ducts that merge to form the ureter.

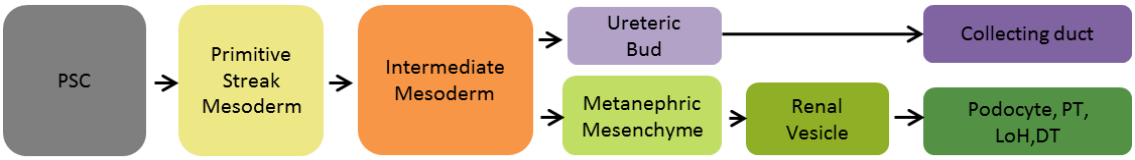

Figure 31: Progress in embryonic development *in vitro*.

4.4. Steering the differentiation of RV-like day 8 cells results in terminal cell types of the kidney:

A screen for the most suitable growth factors and extracellular matrices promoting kidney cell formation was performed to direct differentiation of day 8 cells into different terminal renal cell types. (Experimental design described in Methods section). Using APEL medium as the base, we added factors like HGF, BMP7-FGF and LiCl; additionally we used REGM for our screening. HGF is known to induce tubular elongation in the case of ureteric and tubular epithelia(Santos and Nigam, 1993), LiCl has been known to effect WNT induction leading to tubular epithelial development (Davies and Garrod, 1995). Renal epithelial growth medium has been well documented to promote selective the growth of epithelial cells due to the presence of EGF, hydrocortisone and epinephrine (Taub and Sato, 1979). While all these factors were chosen to induce differentiation we used one combination with BMP7-FGF2 to maintain nephron progenitors(Dudley et al., 1999). Among the matrices used, recombinant h-Laminin 521 provided the best cell morphology and hence was used for all further experiments (**Fig.32**).

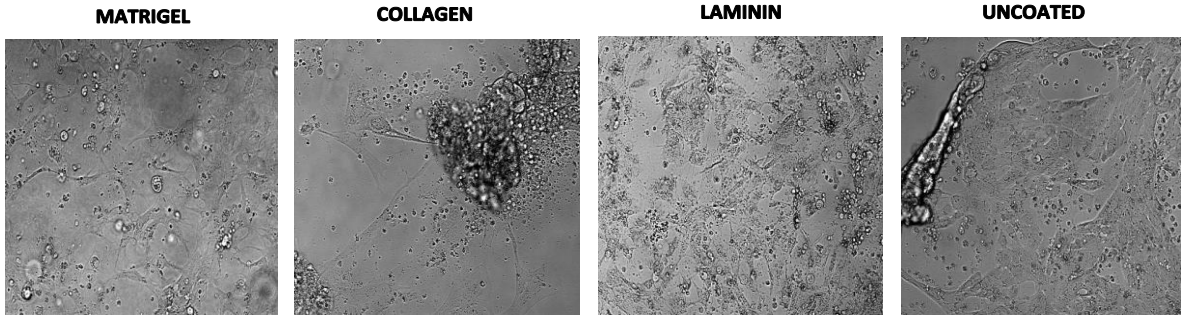

Figure 32: Morphology of human iPSC-derived renal progenitor populations on various extra-cellular matrix components.

The cells resulting from treatment of the above-mentioned factors led to representative cells of the glomerular and tubular parts of the nephron and are described in detail in the following section.

4.4.1. Deriving cells of the glomerular compartment of the nephron:

4.4.1.1. Mesangial cells.

Six days of multi-factor treatment screen of the day 8 cells resulted in cells expressing alpha smooth actin (ASMA), platelet-derived-growth factor receptor ß (PDGFRB) and DESMIN (Lindahl et al., 1998) (**Fig.33**). The best performer among the three media was BMP7-FGF2, although HGF also induced considerable mesangial cells. Contrary to our hypothesis and currently available information that BMP7 and FGF2 prevent the differentiation of the metanephric cell population, we observed a successful differentiation of day8 cells with a high efficiency of generating a mesangial population. The fact that, day 8 cells are more representative of RV rather than an induced MM could attribute to selection of such a cell fate. Interestingly, the origin of mesangial cells and pericytes is not the SIX2+ nephronal progenitor but a Foxd1 population, responsible for generating non-epithelial cell fates in the adult kidney including renal erythropoietin-producing cells, identified by their close association with non-glomerular and glomerular vasculature, respectively, and the expression of smooth muscle actin(Humphreys et al., 2010). Therefore, the occurrence of mesangial-like cells indicates the emergence of stromal cells as a result of the AB4RA-G induction verified by RNA-Seq (**Figure 34**).

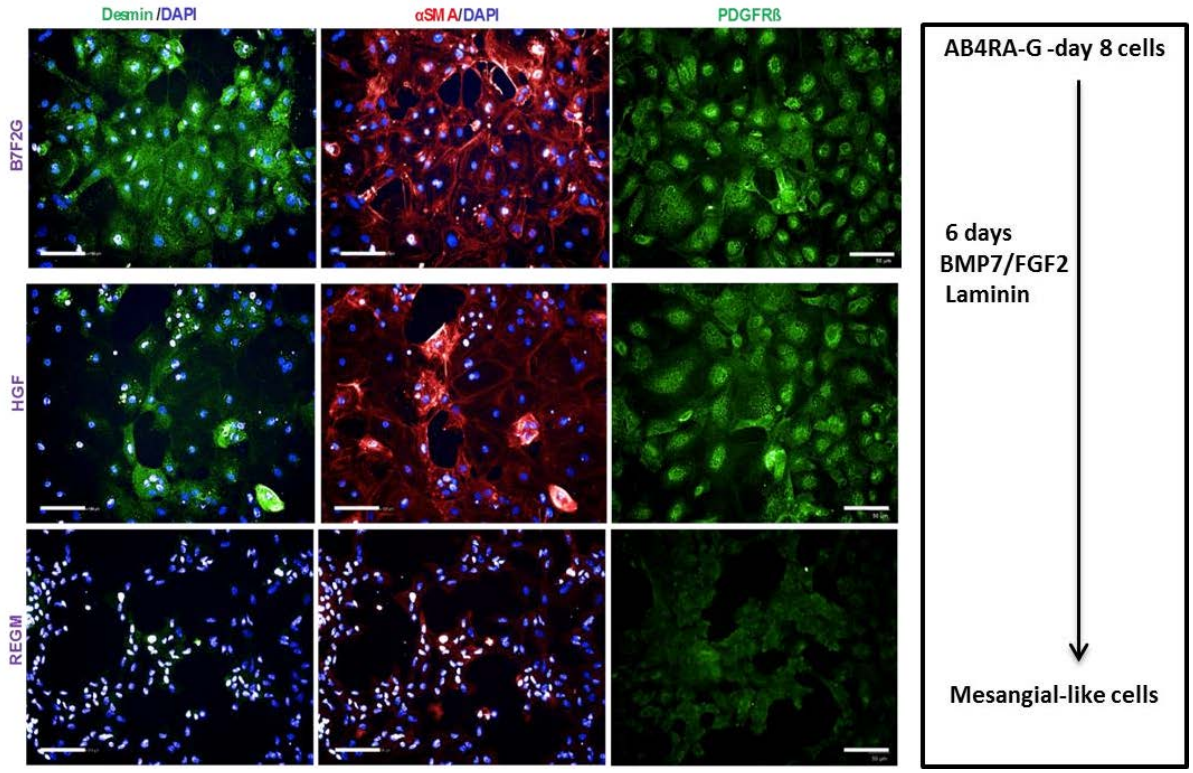

Figure 33: Screen for a mesangial cell phenotype in three different growth factor combinations. [Scale bar= 100µm]

4.4.1.2. Podocyte precursor cells

When day 8 AB4RA-G induced renal precursor cells were plated at a low density in the presence of hepatocyte growth factor (HGF), they acquired an arborized cell body with undivided nuclei indicative of a podocyte-like phenotype. Around 70% of the cells were PODOCALYXIN (PODXL1) positive, expressing SYNAPTOPODIN (SYNPO) and WT-1 (**Fig.34**) but failed to express NEPHRIN (NPHS1) in the areas of cell-cell contact.

The proximal RV marked by WT1 gives rise to the glomerular epithelium, the presence of which was already noted at day 8 in the parent cell population. The progressive occurrence of transcription factors like SULF2, MAFB and MAGI2 between day 8 and day 14 at the RNA level presents evidence of the cells being specified to the podocyte lineage (**Fig.34**). Mafb observed in the S-shaped bodies (SSB) at E13.5, at this stage of development the immature podocytes form a single layer of cells adjacent to the glomerular cleft making it an excellent early podocyte marker (Brunskill et al., 2011). These cells also begin to express high levels of VEGFA, which at the SSB stage is capable of attracting an angioblast population from the surrounding interstitium to form glomerular capillaries. An elegant series of mutants that varied Vegfa protein production in podocytes highlights the critical role of Vegfa signaling in forming the capillary bed (Eremina et al., 2003, 2007)

The reason for the immature state of podocytes could be attributed to a down-regulation in WT1 from day 8 to day14. Further analysis into the regulators of this master transcription factor revealed a decrease in downstream targets like PAX2-8 and a parallel increase in negative regulators like PRDM1 and NROB1 and WNT4 (**Figure 35**). Thus, in order to improve podocyte differentiation, an inhibitor of WNT signaling could be used.

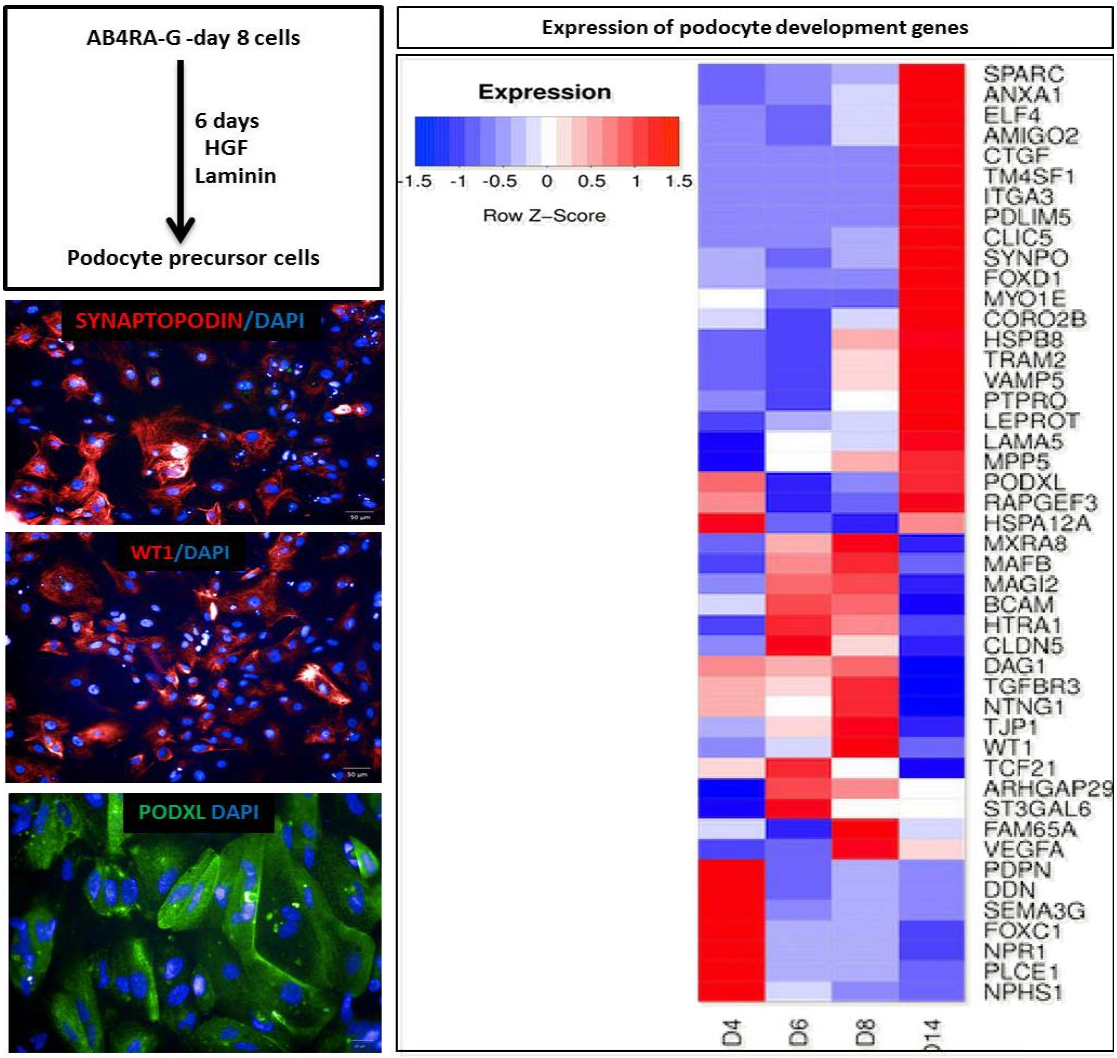

Figure 34: Terminal differentiation of renal progenitors to podocyte precursor cells. a) Scheme for podocyte differentiation. b) Immune fluorencence staining of podocyte markers –SYNPO, WT1 and PODXL c) Heatmap showing the onset of podocyte development genes during the course of AB4RA-G followed by HGF treatment.

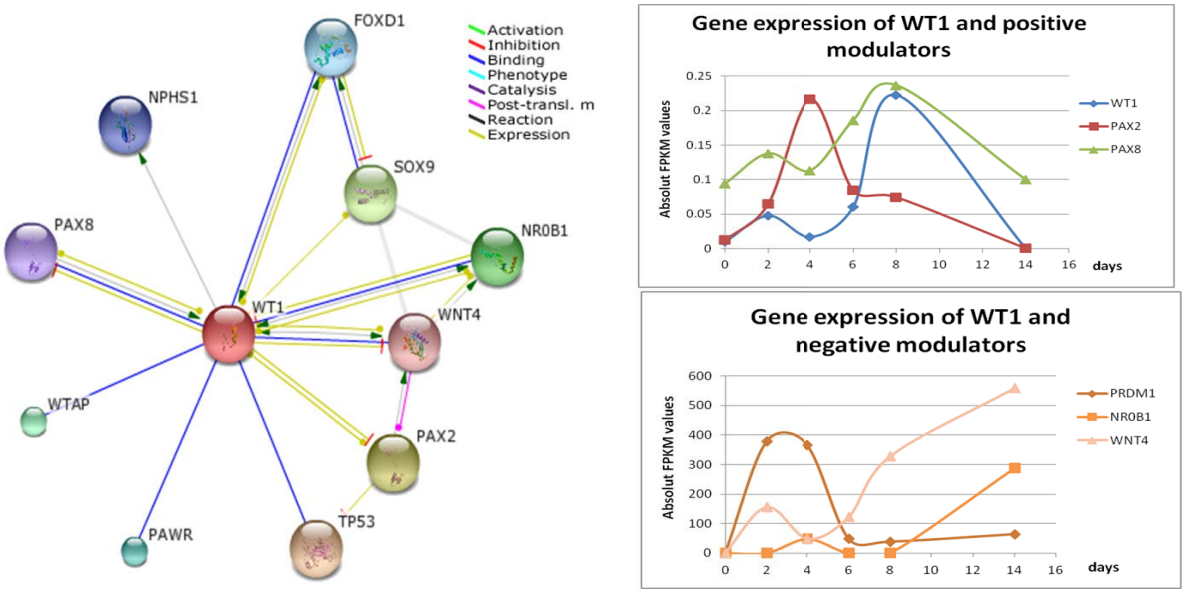

Figure 35: Regulation of WT1 during the course of differentiation. RNA- seq data revealed the expression pattern of transcriptional regulators of WT1, the interactions of which were mapped using STRING[10] DB (Credits: Ana Garcia)

4.4.2. Cells of the tubular compartment of the nephron

At day 8, cells were harvested, plated as single cells at high density on Laminin-521 and stimulated with renal epithelium growth medium (REGM) and different combinations of growth factors to trigger further differentiation. After 6 days of continued culture in REGM (day 14), the cells formed epithelial domes and tubular rings (**Fig. 36**). Closer analysis at day 14 revealed the presence of several types of tubular epithelial cells (T.E.Cs).

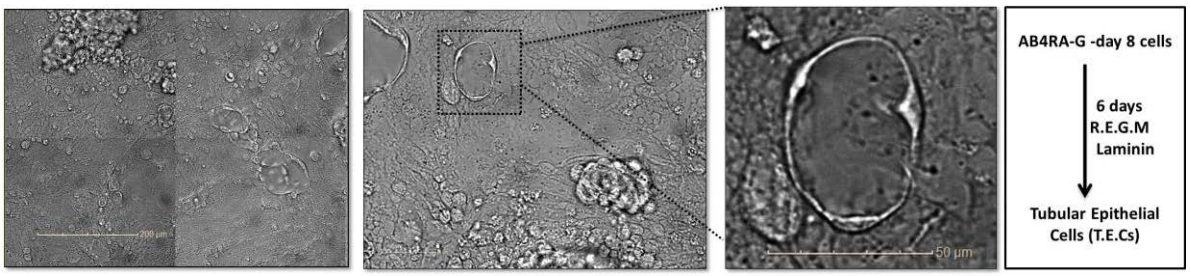

Figure 36: Terminal differentiation of renal progenitors to tubular epithelial cell types. Morphology of cells after 14-days imaged using brightfield microscopy and scheme of tubular differentiation.

4.4.2.1. Proximal tubular epithelial cells

The proximal tubule epithelial cells are characterized by brush border epithelial cells, which are highly absorptive. They possess several solute transporters and enzymes on their apical and basal surfaces that rule their functionality. Cells obtained at day 14 and their predecessors at Day 8, day 6 and 4 were checked for expression levels of proximal tubule markers obtained from literature. The onset of markers like ATPBP1and AQP1 can be observed starting at day 8 and being sustained until day 14. The higher expression of CUBN, TJP1, and LRP2 at day 8 is noteworthy (**Fig.37**). Occurrence of Sodium/Potassium ATPase (Na^+/K^+ ATPase), Aquaporin1 (AQP1) and Lotus lectin stained cells indicated a proximal-tube epithelial cell-like (PTECs) phenotype of these cells (**Fig.37**). $AQP1^+$ cells constitute 57% of the tubular epithelial cell mass at day 14.

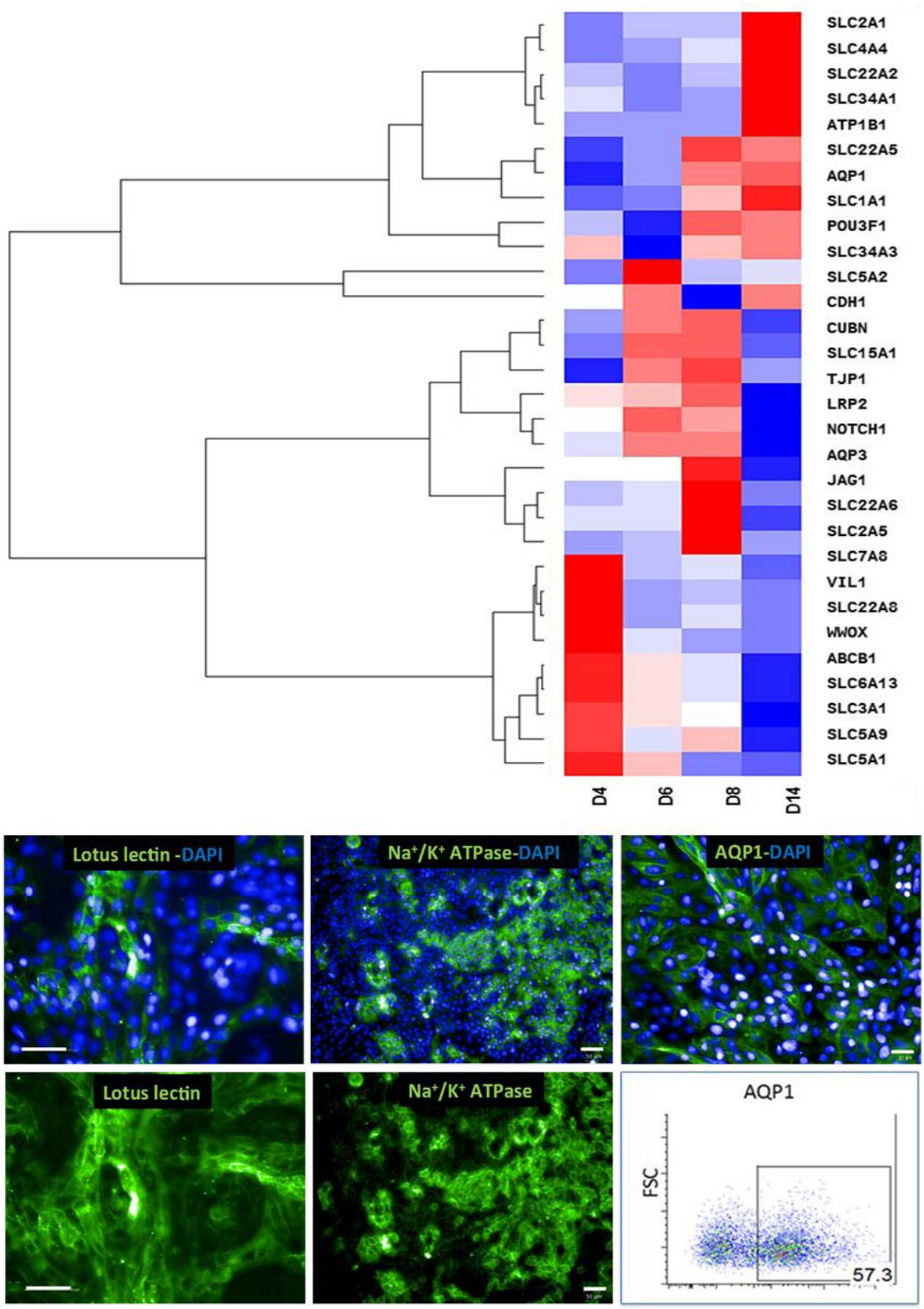

Figure 37: Proximal-tubular epithelial characteristics of Day 14 PSC-derived T.E.Cs. Heatmap of indicating the onset of proximal tubular epithelial genes during the AB4RA-G followed by REGM treatment protocol obtained from RNA-seq data. Bottom panel) Immune fluorescence staining of nephronal markers reveals proximal-tubule-like cells and efficiency of generation of AQP1^{+} cells (PTECs). (Scale bar =50μm)

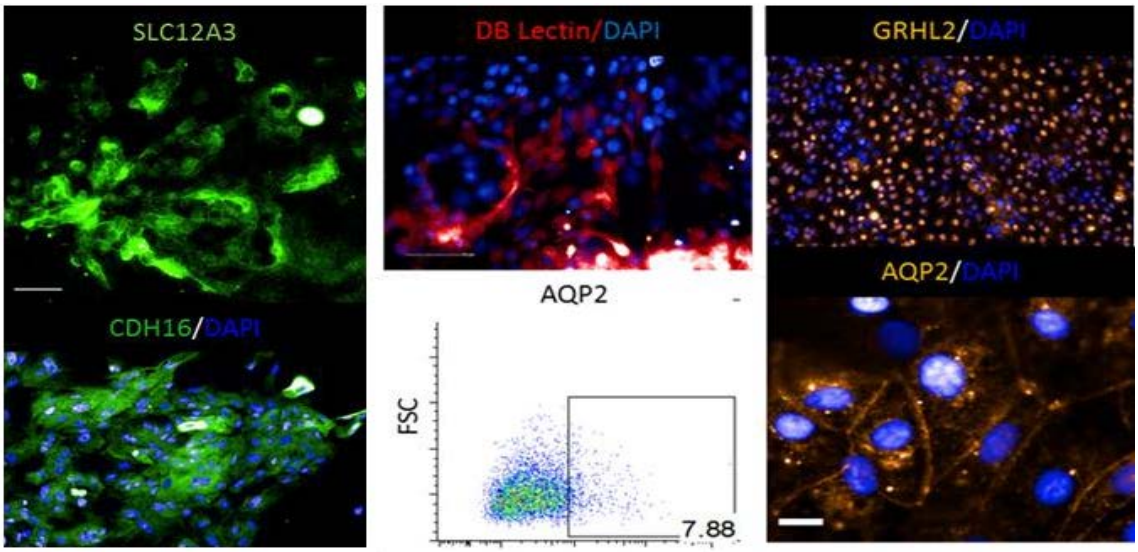

Figure 38: Distal-tubular epithelial characteristics of Day 14 PSC-derived T.E.Cs. Immune fluorencence staining of nephronal markers reveals distal-tubule-like cells and collecting duct cells; Efficiency of generation of AQP2+ cells (Principal cells).

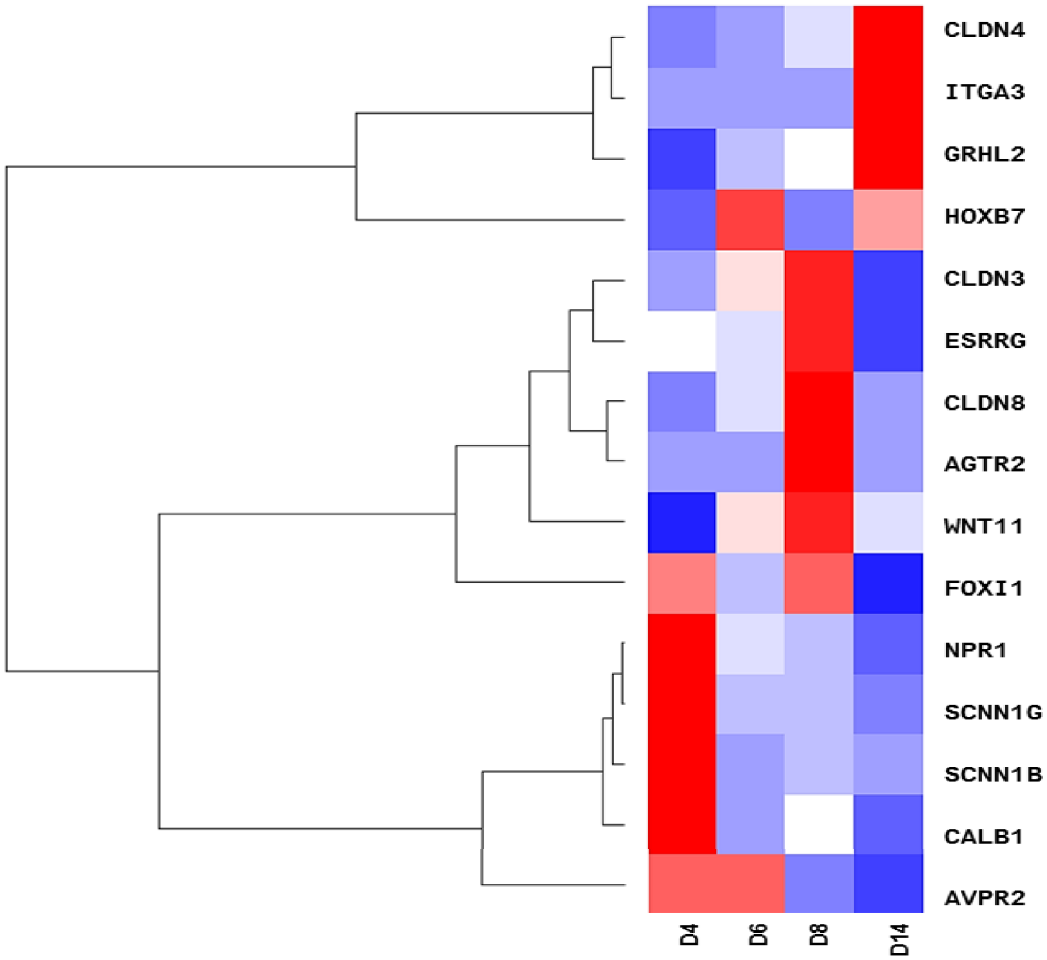

Figure 39: Differential expression of genes regulating ureteric tree formation during 14 days of differentiation. Heatmap of indicating the onset of collecting duct epithelial genes during the AB4RA-G followed by REGM treatment protocol.

4.4.2.2. Distal epithelial cells

Stemming from the distal part of the JAG1^{+} RV, the loop of Henle and distal tubule are responsible for concentrating urine. Sodium chloride co-transporter (NCCT/SLC12A3) and Kidney-specific cadherin (CDH16) were expressed in a minor population, revealing the existence of distal epithelial like cells **(Fig.38)**. The tubular rings formed in culture (**Fig. 36**), bear a close resemblance to the cross-section of distal tubules *in vivo*.

4.4.2.3. Collecting duct cells

The presence of HOXB7, WNT11 and SOX9 expressing cells lead us to expect cells of collecting duct-like identity (**Fig. 39**). Indeed, within the T.E.C were cells expressing CLDN4, CLDN8 and GRHL2. A distinctive clear zone of cobblestone-shaped aquaporin 2 (AQP2)$^{+}$ cells co-expressing grainy head-like 2 (GRHL2) and *Dolichos biflorus* (DB) lectin indicated the presence of collecting duct constituents i.e. principal-like cells (PC) (**Fig. 38**).

In summary, we were able to show the derivation of 5 nephronal cell types and organoids from AB4RA-G treated cells in 14 days, using novel induction factors **(Fig.40)**.

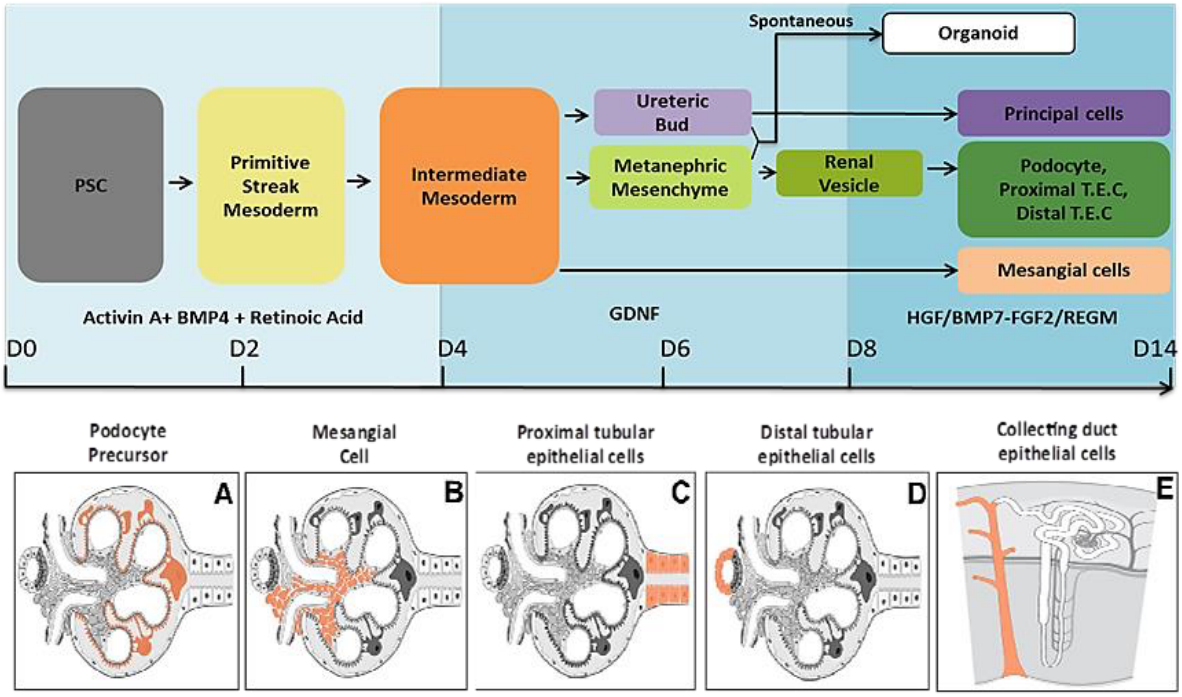

Figure 40: Protocol for differentiation of 5 nephronal cell types and organoids.

5. DISCUSSION

5.1. *In vitro* recapitulation of organogenesis:

We have developed a novel chemically defined protocol for the directed differentiation of hPSCs toward the renal lineage. Broadly, we divide the protocol into three stages to incorporate the transient enrichment of intermediate mesodermal cell populations known to precede metanephric kidney formation. A first 4-day exposure to activin A, BMP4 and retinoic acid, generating IM, UB and MM forms the basis for a second step lasting 4 days of GDNF leading to nascent nephronal progenitors of the RV and CSB stage. This protocol is highly efficient, resulting in nephrogenic cells of which 70–80% expressed the transcription factor SIX2, characteristic of the MM in three different iPSC lines. A third step steered the renal progenitors towards terminal differentiation, an evidence of their potency to generate kidney cells representative of the major nephron segments. These include glomerular podocyte precursors and mesangial cells, together with proximal and distal tubular epithelial cells, collecting duct cells and the all-encompassing nephron organoids.

We consider that optimization of stage 1, priming the cells for later signaling cues, was the most crucial step in developing an efficient differentiation protocol, because as in preliminary experiments it had the most influence over the final cellular phenotype. During embryonic development, agonists and antagonists of the activin-BMP4 pathways establish signaling gradients across the embryo, resulting in the specification of appropriate germ layer populations and derivative tissues (Agius et al., 2000; Gadue et al., 2006; Gritsman et al., 2000; Kubo et al., 2004; Ladd et al., 1998; Lowe et al., 2001; Schultheiss et al., 1997; Thisse et al., 2000). Several groups have applied stepwise protocols drawing on this understanding of embryogenesis to generate nephrons from human PSCs *in vitro* (Freedman et al., 2015; Morizane et al., 2015; Sharmin et al., 2015; Taguchi et al., 2014; Takasato et al., 2015). A variety of culture formats and media have been used, yet they require the activation of a relatively small number of growth factor signaling pathways, with all protocols exploiting canonical WNT and FGF signaling, as the initial mesodermal patterning events involve canonical Wnt signaling with or without activin A and BMP4. With the exception of Freedman et al.(Freedman et al., 2015), all protocols induce intermediate mesoderm via the addition of FGF2 or FGF9 (Little, 2016).

In contrast, our experiments show that in combination with activin A and BMP4, WNT is less effective than RA in inducing a primitive streak followed by IM establishment, as the former

favors an endodermal fate. This is consistent with a report from Tan et al., who observed that a GSK inhibition of hESC for more than 24 hours resulted in enrichment of CXCR4+ endodermal cells(Tan et al., 2013). Our data shows an increase in the much required FGF and WNT signaling in cells as an induced effect of the AB4RA combination, proving their activation without the need for exogenous addition. The involvement of activin A and BMP4 is necessary for primitive streak formation and the RA creates a morphogenetic gradient which promotes caudalization, inducing the generation of anterior and posterior IM in cell culture, which Taguchi et al. demonstrate elegantly to be the origin of UB and MM respectively (Taguchi et al., 2014).

A sum total of all these signals yielded a majority of IM, nephric duct cells and an un-induced nephric mesenchyme in association with minor populations of paraxial and lateral plate mesoderm as indicated by gene expression. Although other reports of nephronal differentiation insist upon a high yield of IM generation being crucial to obtaining kidney cells of high purity, we hypothesized that a heterogeneous mixture of mesodermal cells will contribute a signaling milieu more representative of embryonic interactions promoting better developmental progression of the renal lineage.

Subsequently, in our second stage of differentiation, we added GDNF, which is produced by MM cells and is an inducer of nephric duct cells to form UB. As expected this increases the UB formation and works to strengthen the feed-forward loop of GDNF secretion of MM cells enriching these populations within 48 hours. The developing UB activates the MM leading to the formation of CM and its subsequent epithelialization to form renal vesicle cells with signs of polarization. By day 8 of differentiation we see the occurrence of cells representative of the proximal, medial, distal nephronal segments and the ureteric tree. The derivation of UB in 4 days (Xia et al., 2013), MM in 14 days (Taguchi et al., 2014) and both MM and UB in 18 days (Takasato et al., 2014) has been reported by other groups. We see the appearance of MM and UB as early as 4 days and their activation by day 6, which by far is the fastest induction of nephrogenesis reported to date. Takasato et al. also observed the presence of RV on day 18, as compared to our protocol that takes 8 days to show polarized RV state. A reason for the late appearance of epithelialization in the Takasato (2014) protocol can be attributed to the sustenance of FGF9 and BMP7 that support $SIX2^{+}$MM in the stem state. In contrast, by maintaining the GDNF signal, we allowed the ureteric tree to develop, secreting WNT11 and WNT9B, which help in ureteric elongation and MM maintenance and activation, thus

illustrating the effectiveness of paracrine signaling and gradient formation within the cell culture system in response to growth factor treatment.

The polarized RV is the first step toward nephron formation and specification of particular functional segments. Unattended culture of day 8 cells for 2-4 days led to spontaneous emergence of complex organized structures in culture that represented proximal and distal tubular elements that had developed lumen. Moreover, the organoids showed the presence of ureteric tree and endothelial markers. The afore-mentioned studies of nephronal differentiation also report the formation of spontaneously patterning and segmenting nephrons with proximal and distal tubular segments, as well as Bowman's capsules, containing podocytes (Freedman et al., 2015; Morizane et al., 2015; Sharmin et al., 2015; Taguchi et al., 2014; Takasato et al., 2015). These organoids are obtained by harvesting PSC-derived renal cells and pelleting, placing them in suspensions or matrigel sandwiches or transplanting them under the kidney capsule in a SCID mouse whereas, organoids in our culture arose spontaneously without any intervention and up to 10 days earlier than all current reports. Despite the advantages of a quick and simple derivation, the characterization and maintenance of these structures is yet to be optimized in our study. For instance, Takasato *et al*. show 3-D orientation of glomeruli attached to tubules that are connected to collecting duct epithelia and Freedman et al. managed to keep their organoids viable for about 60 days. This suggests that the organoids at day 10 require further signals for maturation and a culture system that is permissive of oxygen diffusion to this complex structure as well as allows the cells to establish nephron architecture.

5.2. Procurement of the cellular building blocks of the kidney

The ultimate goal of this study was to derive terminal kidney cell types. For this we harvested day 8 cells and subjected them to various growth factor treatments for 6 days. We obtained 2 cell types of the glomerulus, namely mesangial cells and a nascent podocyte precursor by treatment with BMP7-FGF2 and HGF, respectively. From a different treatment using renal epithelial growth medium, we obtained tubular epithelial cells that were identified to be distinct proximal, distal and collecting duct epithelial cell populations. Kandasamy *et al.* derive proximal tubule (PT) cells within 9 days and are to-date the fastest to obtain a pure kidney cell population (Kandasamy et al., 2015). Song *et al.* derived podocytes from PSCs in 10-12 days but the protocol uses serum containing medium rendering these cells rather unfit for clinical application. Our protocol is unique in deriving at least 5 different terminal and 2 precursor cell

types in serum-free, xeno-free conditions and readily transferrable to GMP units and applicable for clinical use. Derivation of these cell types opens several topics of concern about their *in vitro* lifespan and functionality. In a number of cases, evidence supports a functional identity for component cell types within differentiation cultures, including the demonstration of appropriate uptake of albumin and response to nephrotoxins by the proximal tubular segments (Freedman et al., 2015; Morizane et al., 2015; Takasato et al., 2015). For large-scale expansions, it can be postulated that PSC-derived terminal cell types behave similarly to their *in vivo* counterparts with respect to low mitotic potential, necessitating the usage of larger quantities of PSC as starting material. These questions need to be addressed and present a good starting point for future experiments.

Progressive differentiation to a terminal state is accompanied with a decreasing mitotic capacity. Therefore, although obtaining the 5 nephronal cell types mentioned above is a considerable achievement in the field of nephrology, these cell products do not offer a promising picture of regeneration in deteriorating kidney disease. A more suitable candidate for repairing damaged nephrons would be RV progenitors. Due to their segmentational identity, they can contribute to several parts of the nephron. A lineage tracing study by Rinkevich et al. shows that adult kidneys do not possess broad progenitor population catering to the complete nephron; rather, the adult kidneys contain segment-specific progenitors that are Wnt-activated (Rinkevich et al., 2014). Moreover, Takasato *et al.* also demonstrated that PSC-derived CM cells can be exposed to a pulsatile WNT signal give rise to complex nephron organoids(Takasato et al., 2015). This leads us to believe that RV cells treated with a short pulse of WNT-agonist constitute a putative cell therapy for acute kidney injury. Recent research by Lindstörm et al., illustrates the development of the nephron through formation of a ß-catenin gradient such that the lowest concentration determines the glomerular site and highest concentration induces distal tubules(Lindström et al., 2014). Further evidence of the differential requirement of ß-catenin was illustrated by the differentiation of *in vitro* propagated CITED1^{+} progenitors in WNT agonist-containing medium resulted in tubules with marker profiles of proximal, distal and intermediate segments but no glomerular cells(Brown et al., 2015). The Nishinakamura lab was successful in circumventing the lack of glomerular development by the recombination with embryonic spinal cord culture in congregation with the medium prepared by Brown et al., illustrating the need for additional cues in the differentiation medium albeit the exact factors secreted by the spinal cord remain obscure (Tanigawa et al., 2016). Thus, a defined differentiation medium for complete nephron formation is not yet available and would provide

further cues to understanding of pathways determining specific cell types during kidney development. While our protocol induces all structures through signaling events in a complex cell mixture, the exact drivers of factors and pathways involved in cell type specification are not yet determined. Successive targeting of single factors in our differentiation medium with pathway inhibitors or shRNA may be useful in deciphering their specific contribution.

Candidates for regenerative therapies also include earlier progenitors such as MM and UB cells or IM, as they possess wider potential to contribute to nephrons. The application of IM for cell therapy can be challenging as it is a common precursor of the adrenal gland, gonads as well as the kidney, its multi-potency being a threat to ectopic tissue formation. As previously mentioned, Brown et al. developed a nephron progenitor expansion medium (N.P.E.M), which facilitated the first short-term of culture of E13.5 - 17.5 un-induced Cited1^{+} MM cells *in vitro*. Application of this medium on hPSC-derived nephron progenitors (Takasato protocol) showed their critical dependence on WNT, FGF9, SMAD inhibition and Rho-kinase inhibition, and allowed their expansion for 2 passages after which cells lost their identity (Brown et al., 2015). A more recent report shows that NOTCH inhibition and LIF are essential in maintaining nephron progenitors that retain potency to form both tubuli and glomeruli in embryonic spinal cord recombination experiments (Tanigawa et al., 2016). These studies present a first step in expansion and modulation of the fate of MM-nephron progenitors *in vitro* presenting the possibility of expansion and testing on various extracellular matrix scaffolds for generation of kidney tissues. Also crucial for all approaches of regeneration is the fact that a mature functional kidney finally requires a path to excrete urine from several glomeruli and tubules for which the presence of a collecting duct is inevitable. A protocol to expand and develop collecting duct trees form UB cells is yet to be designed.

In summary, our protocol generates a wide spectrum of building blocks for kidney regeneration from PSCs. These cells can be used to repair injured kidney segments or used to reconstitute the whole kidney or nephron. The intricate architecture of the kidney plays a key role in establishing osmotic gradients and vascular connections required for normal functioning of nephrons. Acellular porcine kidney matrices offer a solution to kidney reconstruction, by providing positional cues that allow functional specification of PSC-derived progenitors. Bio-engineering of individual nephrons to whole kidney may also be achieved by bio-printing the exact segment specific matrix with segment specific progenitors. Apart from being used in several combinations with extra-cellular matrices for tissue reconstitution, the terminal cells

can be used for drug screening and toxicity testing. Also, studying molecular mechanisms of genetic disease progression is an opportunity provided by PSCs as they can be derived from patients. Moreover, several key genes leading to fetal death on the occasion of mutations can be knocked down and studied *in vitro* during the course of development. Thus, PSC-derived kidney progenitors and cells provide a wide range of possibilities to understand and address issues in kidney biology and disease.

5.3. Assembling kidney tissues from cells: The long road from organoids to organs

A functional kidney consists of 200,000 to 2.5 million nephronal epithelial structures vascularized by blood vessels in a specific alignment with the surrounding interstitium and linked to the collecting duct to execute blood filtration, re-absorption and concentration of the urinary filtrate (Little, 2016). The closest as yet developed *in vitro* representative of such a complex organization of human cells, are the perfused repopulated acellular rodent kidneys (Song et al., 2013) and lab-generated PSC-derived organoids that contain representative portions of the kidney. Organoids are one step closer to mimicking the kidney than all individual terminal kidney cell types grouped together. While tubular segments of the nephron were common to all studies including ours, organoids with glomerular constituents in culture including non-associated podocytes and endothelial cells were reported only by the M.Little and Freedman labs (Freedman et al., 2015; Takasato et al., 2015). A key issue in encouraging the growth of organoids *in vitro* is the inclusion of vascular elements for circulatory support as well as developmental advancement.

In the metanephric kidney, epithelial (Six2+Cited1+), endothelial (Flk1+/Scl/Tal1+), and stromal (Foxd1+) cellular lineages are confined within strict lineage boundaries, and therefore, a differentiation protocol aimed at enriching Six2+Cited1+ nephron epithelial progenitors will likely not include endothelial and stromal progenitors required to generate glomerular, endothelial, and mesangial cells. Accordingly, a human iPSC–derived cell suspension enriched for nephron progenitors and depleted for endothelial progenitors gives rise to vascularized glomeruli *in vitro* (Dekel, 2016). In our studies, a FOXD1 population was detected on exposure to HGF at day 14, which can be considered as the parent population of mesangial cells. Sharmin et al. showed the presence of vascularized glomeruli with interdigitating podocytes on transplanting the organoids under the kidney capsule of mice. In these experiments, the vascularization relied on host vessels growing into the grafted material. In order to avoid host

vasculature from penetrating the graft, Sharmin *et al.* attempted to exogenously add a mixture of non-renal human cells known to readily generate vessels to their induced cell suspension. Nevertheless, the latter failed to vascularize the iPSC–derived glomerular structures (Sharmin et al., 2015). It remains to be determined whether vascularization of PSC-derived glomeruli specifically requires the derivation of the cells responsible for glomerular vascularization in development (*e.g.*, embryonic renal angioblasts residing in close proximity to nephron progenitors)(Dekel, 2016). Therefore, vascularization is essential for developmental maturation of cells and requires a separate compartment of renal progenitors that may not be favored by existing protocols. A solution to this problem lies in the modification of the protocol to enrich for vascular-stromal cells rather than an exogenous addition to the organoids.

A built-in vasculature will also allow perfusion of organoids. An important component of the renal excretory process is the exchange of electrolytes based on the specific orientation of solute transporters throughout the tubular epithelium. A major factor governing the osmotic gradient is the apico-basal distribution of water and solute transporters. While PSC-derived renal cells do express these transporters, they lack polarized expression that can only be created under the influence of flow. By vascularizing the organoid, tubular segments would receive continuous input through their lumens on one side and can transport back excess solutes into the vasculature, a step forward towards urine formation.

The *in vitro* maturation process generates renal structures mostly equivalent to those found in first trimester human fetal kidney (Takasato et al., 2015). For renal bioengineering and growing kidneys, it is noteworthy to mention that *in vivo* organogenesis of grafts of first trimester human fetal kidney led, at best, to formation of miniature kidneys producing dilute urine 2 months after transplantation, far away from what is expected from an adult kidney (Dekel et al., 2003). Therefore, essential tasks to create urine–producing functional miniature kidneys would be to extend renal maturation *in vitro* as much as possible and achieve induction and incorporation of ureteric bud–derived collecting ducts for possible urine drainage. Unlike other protocols that concentrate on MM-derivation, we induced MM and UB simultaneously, hence providing organoids with the necessary building material for drainage. Yet another critical aspect of organ function encompasses innervation and hormonal control, which are yet to be addressed *in vitro*.

Altogether, the hazy road from bench to bedside is starting to clear up, with prominent milestones being the generation of renal progenitors and organoids from PSCs that can be

tailored for individuals. Lab-grown kidneys as transplantable material are a destination that seems attainable in the next decade at the current rate of progress.

Table 15: Genes Involved in Kidney Development

Developmental Process Gene	Function	Expression in Normal Developing Kidney	Mutant Kidney Phenotype (Mouse) Role played in organogenesis	Reference
BMP4	Bone morphogenetic protein	Stromal mesenchymal cells around ureteric bud branches	Reduced and ectopic ureteral branching, ectopic ureterovesical junction, hydoureter, double collecting ducts, hypo/dysplastic kidneys (heterozygous *BMP4* null mice)	(Miyazaki et al., 2000)
BMP7	Growth factor	Mesonephric duct, UB, iMM, DT, CSB and SSB, podocytes	Increased apoptosis in metanephric mesenchyme, decreased ureter bud branching, hydroureter, severe renal hypoplasia	(Dudley et al., 1995; Luo et al., 1995)
Brnl /POU3F3	Transcription factor	RV, CSB, SSB, LoH, DT, macula densa (MD)	Disrupted differentiation of LoHs, MD, and DCT	(Nakai et al 2003)
Cadherin-6 (K-cadherin)	Transmembrane adhesion protein	RV, proximal end of CSB,SSB, developing proximal tubules and Henle's loops	Delayed fusion of some comma-shaped bodies to ureteric bud leading to loss of nephrons	(Mah et al., 2000)
Cadherin-16 (Ksp-cadherin)	Transmembrane adhesion protein	Tubulogenesis and distal portion of the nephron	homotypic cellular recognition	(Shen et al., 2005)
CD2AP	Adapter protein (interacts with nephrin)	Podocyte filtration slit diaphragm domain	Irregular foot processes, absent filtration slit diaphragms, proteinuria	(Shih et al., 1999)
Cited1	Transcription factor	uiMM	No mutant phenotype in kidney	(Boyle et al., 2008)
c-Ret	GF receptor (TK) (receptor for *GDNF*)	Mesonephric duct, UB and tips of UB	Similar to GDNF-deficient mice	(Schuchardt et al., 1994)
Decorin (Dcn)	Proteoglycan matrix component	Stromal cells	Antagonist of BMP7	(Fetting et al., 2014)
Etv4/5	Transcription Factor	UB,CD	Downstream of FGFR	(Costantini and Kopan, 2010)
Eya1	Transcription coactivator (interacts with *Six1*)	IM, MM	Intact pro- and mesonephros, but absent metanephric blastema, renal agenesis	(Li et al., 2003; Sajithlal et al., 2005; Xu et al., 1999)
FGF-8	Growth factor	PTA, RV, tubule progenitors in SSB	Increased apoptosis in S body precursors, truncated nephrons, severe renal hypoplasia	(Grieshammer et al., 2005)
Fgfr1,Fgfr2	Growth factor receptor	UB,MM	Required for RV formation	Trueb 2013
Foxc1/2	Transcription factor	IM, mesonephros, MM	Double ureters with one a hydroureter, duplex kidneys (*Foxc1* / *Foxc2* compound heterozygous mutants similar to *Foxc1* homozygous mutants)	(Kume et al., 2000)
Foxd1(BF2)	Transcription factor	Interstitial stroma cells	Decreased ureteric bud branching, large mesenchymal condensates, abnormal renal capsule, small fused pelvic kidneys	(Levinson et al., 2005)
GDNF	Growth factor	IM, mesonephros, iMM, PTA	Ureteric bud fails to form or has abnormal branching, renal hypoplasia or agenesis	(Sánchez et al., 1996)
GFRα1	GF coreceptor (forms signaling complex with *GDNF* and *c-ret*)	iMM, PTA, mesonephric duct, UB and tips of UB	Similar to GDNF-deficient mice	(Enomoto et al., 1998)

Glypican-3	Heparan sulfate proteoglycan	All MM and UB derivatives	Increased cell proliferation in cortical collecting ducts, increased apoptosis in medullary collecting ducts, renal medullary cystic dysplasia	(Grisaru et al 2001)
Grem1	Bone morphogenetic protein (BMP) antagonist	IM, mesonephric duct, MM	Ureteric bud forms but fails to invade metanephric mesenchyme, which undergoes apoptosis, renal agenesis	(Michos et al., 2004)
Grhl2	Transcription factor	ND, UB and CD	Inactivation results in defects of epithelial barrier formation and lumen expansion	Aue 2014
Hey1	Transcription factor	UB tips and PTA	Involved in transition of PTA to RV	Chen 2005
Hoxa11 , Hoxd11	Transcription factors	IM,MM	Impaired ureteric bud branching, renal hypoplasia in *Hoxa11*/ *Hoxd11*double mutants	(Patterson et al., 2001; Wellik et al., 2002)
Integrin α3 β 1	Transmembrane adhesion receptor	UB,CD, podocytes	Decreased branching of medullary collecting ducts, microcystic proximal tubules, defective glomerulogenesis	(Kreidberg et al., 1996)
Integrinα8	Transmembrane adhesion receptor	IM ,iMM, PTA	Limited ureteric bud invasion of metanephric mesenchyme, decreased ureteric branching, renal hypoplasia or agenesis	(Müller et al., 1997)
Kif26b	Intracellular motor protein	uiMM	Agenesis- uretic buds failed to invade and branch into the mesenchyme, resulting in disappearance of the kidney by embryonic day 14.5	Uchiyama 2010
Kreisler (Krml1/MafB)	Transcription factor	Podocytes, initially at capillary loop stage	Abnormal podocyte differentiation with no foot processes	Sadl et al 2002
Laminin α3ß 1	Transmembrane adhesion receptor	UB,CD, podocytes	Glomerular capillary loops dilated and fewer in number, loss of podocyte foot processes, dual GBMs (failure of fusion)	(Kreidberg et al., 1996)
Lamininα5	Basement membrane protein	Basement membranes of UB, developing tubules and glomerular basement membrane (GBM)	Abnormal glomeruli with displaced endothelial and mesangial cells, and clustered podocytes	(Miner and Li, 2000)
Laminin ß 2	Basement membrane protein	GBM beginning at capillary loop stage	Absence of podocyte foot processes, proteinuria	(Noakes et al 1995)
Lim 1 /Lhx1	Transcription factor	IM, ND, mesonephros, UB, CD, PA, SSB, podocytes	Absent pro-, meso-, and metanephros (*Lim 1* required at multiple steps of kidney development)	(Karavanov et al., 1998; Kobayashi et al., 2005a)
Lmx1b	Transcription factor	Podocytes	Abnormal foot processes, absent filtration slit diaphragms	(Chen et al 1998)
Neph1	Transmembrane protein (interacts with nephrin)	Podocyte filtration slit diaphragm	Foot process effacement, proteinuria	(Donoviel et al 2001)
Nephrin	Transmembrane protein	Podocyte filtration slit diaphragm	Foot process effacement, absent filtration slit diaphragms, proteinuria	(Putaala et al., 2001)
Npnt	Basal membrane component	Embryonic kidney	kidney agenesis or hypoplasia	Linton 2007
Notch2	Transmembrane receptor	Developing CD,CSB,SSB, podocytes	Abnormal glomeruli arrested at capillary loop stage, with disorganized podocytes and no mesangial cells	(McCright et al., 2001)

Osr1	Transcription factor	IM,MM	Specifying IM that gives rise to MM	(Mugford et al., 2008)
Pax 2	Transcription factor	IM,ND, mesonephros, UB, iMM	Intact nephric duct but mesonephric tubules and ureteric bud fail to form, renal agenesis	(Brophy et al., 2001; Dressler et al., 1990)
PDGF-B	Growth factor	Glomerular endothelial cells and podocytes	Dilated glomerular capillaries with no mesangial cells	(Leveen et al 2004)
PDGFR- ß	Growth factor receptor (receptor for *PDGF-B*)	Glomerular mesangial cells	Dilated glomerular capillaries with no mesangial cells	(Soriano, 1994)
Podocalyxin	CD34-related transmembrane protein	Podocyte apical membrane domain	Abnormal podocytes, foot process effacement, absent filtration slit diaphragms, anuria	(Doyonnas et al 2001)
Podocin /Nphs2	Membrane protein (interacts with nephrin)	Podocyte filtration slit diaphragm domain	Irregular foot processes, absent filtration slit diaphragms, proteinuria	(Roselli et al., 2004)
RARα, RARß 2	Transcription factors	RAR± ”ureteric bud, metanephric mesenchyme, stroma RAR²2 ”stroma only	Decreased ureteric bud branching (defective stroma signaling) in *RAR ± / ² 2* double mutants, renal hypoplasia	(Mendelsohn et al., 1999)
R-cadherin	Transmembrane adhesion protein	iMM, RV, CSB,SSB	Dilatation and cytoplasmic vacuolization of proximal tubules	(Shimazui et al 2000)
Sall 1	Transcription factor	Mesonephros, iMM	Ureteric bud forms but does not fully invade metanephric mesenchyme, which undergoes apoptosis, renal hypoplasia, or agenesis	(Nishinakamura et al., 2001)
Six1	Transcription factor (interacts with *Eya1*)	MM and CD	Ureteric bud forms but does not fully invade metanephric mesenchyme, which undergoes apoptosis, renal agenesis	(Ruf et al., 2004; Xu et al., 2003)
Six2	Transcription factor	MM	Agenesis and premature differentiation to nephrons	(Kobayashi et al., 2008)
Sox9	Transcription factor	Ureteric tree	Downstream of GDNF signaling; Required for Sprouty1 and Etv4/5 expression	Reginensi 2011
Sprouty1	Receptor (TK) antagonist	Mesonephric duct, UB and tips of UB	Supernumerary ureteric buds, multiple ureters, multiplex kidneys	(Basson et al 2005)
VEGF-A	Growth factor	SSB, podocytes, CD	Small glomeruli, lack capillary loops, few endothelial cells	(Eremina et al., 2003)
Wnt11	Secreted glycoprotein	UB tips	Loss of ureteric tips, reduced ureteric branching, renal hypoplasia	(Majumdar et al., 2003)
Wnt4	Secreted glycoprotein	PTA, CSB, distal SSB	Ureteric bud branching occurs, no mesenchymal-epithelial transition, renal agenesis	(Tanigawa et al., 2011)
Wnt9b	Secreted glycoprotein	Mesonephric duct, UB,CD but not branching tips	No mesenchymal-epithelial transition, renal agenesis	(Carroll and Das, 2013; Karner et al., 2011)
Wt1	Transcription factor	IM, mesonephros, MM, CSB, SSB, podocytes	Absent caudal mesonephros, ureteric bud fails to form, metanephric mesenchyme undergoes apoptosis, renal agenesis	(Donovan et al., 1999; Kreidberg et al., 1993)

6. LIST OF FIGURES

7. LIST OF TABLES

8. ABBREVIATIONS

ACE	Angiotensin-converting -enzyme
ADH	Antidiuretic hormone
AKI	Acute kidney injury
APEL	Albumin Polyvinylalcohol Essential Lipids
BIO	(2′Z, 3′E)-6-Bromoindirubin-3′-oxime
BMP	Bone morphogenetic protein
CD	Cluster of differentiation; Collecting Duct
cDNA	Complementary DeoxyriboNucleic Acid
CKD	Chronic kidney disease
CM	Conditioned medium
DNA	Deoxyribonucleic acid
DAPI	4′, 6-diamidino-2-phenylindole
DMEM	Dulbecco´s Modified Eagle´s Medium
dpc	Days post coitum
DT	Distal tubule
DTECs	Distal tubular epithelial cells
E	mouse embryonic day
EB	Embryoid body
EGF	Epidermal growth factor
ESRD	End stage renal disease
FGF	Fibroblast growth factor
FGFR	Fibroblast growth factor receptor
GDNF	Glial-derived neurotrophic factor
GUDMAP	GenitoUrinary Development Molecular Anatomy Project
hESCs	human embryonic stem cells
HFF	Human foreskin fibroblasts
hPSCs	human pluripotent stem cells
IM	Intermediate mesoderm
iMM	induced MM
iPSCs	induced pluripotent stem cells
KEGG	Kyoto Encyclopedia of Genes and Genomes
LIF	leukemia inhibiting factor
LOH	Loop of Henle
LPM	Lateral plate mesoderm
MEF	Mouse embryonic feeders
MM	Metanephric mesenchyme
ND	Nephric duct
PBS	phosphate-buffered saline
PM	Paraxial mesoderm
PS	Primitive streak
PT	Proximal tubule
PTA	Pretubular aggregate
PTECs	Proximal tubular epithelial cells
PTH	Parathyroid hormone
RA	Retinoic acid
REGM	Renal epithelial growth medium
rh	Recombinant human
RNA	Ribonucleic Acid
ROCK	Rho-associated protein kinase
RV	Renal vesicle
TEC	Tubular epithelial cells
uiMM	uninduced MM

TREATMENTS

AB4RA	ActivinA, BMP4, Retinoic acid
AB4F2	ActivinA, BMP4, FGF2
AB4B7	ActivinA, BMP4, BMP7
AB4BIO	ActivinA, BMP4, BIO
B7F2	BMP7, FGF2
G	GDNF

UNITS

°C : degrees Celsius
%: Percentage
g: grams / gravity
hr/hrs : hours
kDa: kilo Daltons
M: mol
mA: milliampere
mg: milligrams
min: minutes
ml: millilitres
mm: millimetres
mM: millimol
ng: nanograms
nm: nanometres
s: seconds
U: units
V: volt
mIU: milli international units
µg : micrograms
µl: microlitres
µM: micromol

9. REFERENCES

Agius, E., Oelgeschläger, M., Wessely, O., Kemp, C., and De Robertis, E.M. (2000). Endodermal Nodal-related signals and mesoderm induction in Xenopus. Dev. Camb. Engl. *127*, 1173–1183.

Al-Awqati, Q., and Oliver, J.A. (2002). Stem cells in the kidney. Kidney Int. *61*, 387–395.

Amaya, E., Stein, P.A., Musci, T.J., and Kirschner, M.W. (1993). FGF signalling in the early specification of mesoderm in Xenopus. Dev. Camb. Engl. *118*, 477–487.

Angelotti, M.L., Ronconi, E., Ballerini, L., Peired, A., Mazzinghi, B., Sagrinati, C., Parente, E., Gacci, M., Carini, M., Rotondi, M., et al. (2012). Characterization of renal progenitors committed toward tubular lineage and their regenerative potential in renal tubular injury. Stem Cells Dayt. Ohio *30*, 1714–1725.

Attia, L., Yelin, R., and Schultheiss, T.M. (2012). Analysis of nephric duct specification in the avian embryo. Dev. Camb. Engl. *139*, 4143–4151.

Attia, L., Schneider, J., Yelin, R., and Schultheiss, T.M. (2015). Collective cell migration of the nephric duct requires FGF signaling. Dev. Dyn. Off. Publ. Am. Assoc. Anat. *244*, 157–167.

Bachmann, S., Bostanjoglo, M., Schmitt, R., and Ellison, D.H. (1999). Sodium transport-related proteins in the mammalian distal nephron - distribution, ontogeny and functional aspects. Anat. Embryol. (Berl.) *200*, 447–468.

Barak, H., Rosenfelder, L., Schultheiss, T.M., and Reshef, R. (2005). Cell fate specification along the anterior–posterior axis of the intermediate mesoderm. Dev. Dyn. *232*, 901–914.

Barker, N., Rookmaaker, M.B., Kujala, P., Ng, A., Leushacke, M., Snippert, H., van de Wetering, M., Tan, S., Van Es, J.H., Huch, M., et al. (2012). Lgr5+ve Stem/Progenitor Cells Contribute to Nephron Formation during Kidney Development. Cell Rep. *2*, 540–552.

Boyle, S., Misfeldt, A., Chandler, K.J., Deal, K.K., Southard-Smith, E.M., Mortlock, D.P., Baldwin, H.S., and de Caestecker, M. (2008). Fate mapping using Cited1-CreERT2 mice demonstrates that the cap mesenchyme contains self-renewing progenitor cells and gives rise exclusively to nephronic epithelia. Dev. Biol. *313*, 234–245.

Brophy, P.D., Ostrom, L., Lang, K.M., and Dressler, G.R. (2001). Regulation of ureteric bud outgrowth by Pax2-dependent activation of the glial derived neurotrophic factor gene. Dev. Camb. Engl. *128*, 4747–4756.

Brown, A.C., Muthukrishnan, S.D., Guay, J.A., Adams, D.C., Schafer, D.A., Fetting, J.L., and Oxburgh, L. (2013). Role for compartmentalization in nephron progenitor differentiation. Proc. Natl. Acad. Sci. *110*, 4640–4645.

Brown, A.C., Muthukrishnan, S.D., and Oxburgh, L. (2015). A Synthetic Niche for Nephron Progenitor Cells. Dev. Cell *34*, 229–241.

Bruce, S.J., Rea, R.W., Steptoe, A.L., Busslinger, M., Bertram, J.F., and Perkins, A.C. (2007). In vitro differentiation of murine embryonic stem cells toward a renal lineage. Differentiation *75*, 337–349.

Brunskill, E.W., Aronow, B.J., Georgas, K., Rumballe, B., Valerius, M.T., Aronow, J., Kaimal, V., Jegga, A.G., Grimmond, S., McMahon, A.P., et al. (2008). Atlas of Gene Expression in the Developing Kidney at Microanatomic Resolution. Dev. Cell *15*, 781–791.

Brunskill, E.W., Georgas, K., Rumballe, B., Little, M.H., and Potter, S.S. (2011). Defining the Molecular Character of the Developing and Adult Kidney Podocyte. PLOS ONE *6*, e24640.

Bussolati, B., Bruno, S., Grange, C., Buttiglieri, S., Deregibus, M.C., Cantino, D., and Camussi, G. (2005). Isolation of renal progenitor cells from adult human kidney. Am. J. Pathol. *166*, 545–555.

Cao, Q., Zhang, X., Lu, L., Yang, L., Gao, J., Gao, Y., Ma, H., and Cao, Y. (2012). Klf4 is required for germ-layer differentiation and body axis patterning during Xenopus embryogenesis. Dev. Camb. Engl. *139*, 3950–3961.

Carroll, T.J., and Das, A. (2013). Defining the Signals that Constitute the Nephron Progenitor Niche. J. Am. Soc. Nephrol. *24*, 873–876.

Cerdá-Esteban, N., and Spagnoli, F.M. (2014). Glimpse into Hox and tale regulation of cell differentiation and reprogramming. Dev. Dyn. *243*, 76–87.

Chen, L., and Al-Awqati, Q. (2005). Segmental expression of Notch and Hairy genes in nephrogenesis. Am. J. Physiol. Renal Physiol. *288*, F939-952.

Chen, J., Bardes, E.E., Aronow, B.J., and Jegga, A.G. (2009). ToppGene Suite for gene list enrichment analysis and candidate gene prioritization. Nucleic Acids Res. *37*, W305-311.

Cheng, H.-T., Kim, M., Valerius, M.T., Surendran, K., Schuster-Gossler, K., Gossler, A., McMahon, A.P., and Kopan, R. (2007). Notch2, but not Notch1, is required for proximal fate acquisition in the mammalian nephron. Development *134*, 801–811.

Costantini, F., and Kopan, R. (2010). Patterning a complex organ: branching morphogenesis and nephron segmentation in kidney development. Dev. Cell *18*, 698–712.

D'Amour, K.A., Agulnick, A.D., Eliazer, S., Kelly, O.G., Kroon, E., and Baetge, E.E. (2005). Efficient differentiation of human embryonic stem cells to definitive endoderm. Nat. Biotechnol. *23*, 1534–1541.

Davies, J.A., and Garrod, D.R. (1995). Induction of Early Stages of Kidney Tubule Differentiation by Lithium Ions. Dev. Biol. *167*, 50–60.

Dekel, B. (2016). The Ever-Expanding Kidney Repair Shop. J. Am. Soc. Nephrol. JASN *27*, 1579–1581.

Dekel, B., Burakova, T., Arditti, F.D., Reich-Zeliger, S., Milstein, O., Aviel-Ronen, S., Rechavi, G., Friedman, N., Kaminski, N., Passwell, J.H., et al. (2003). Human and porcine early kidney precursors as a new source for transplantation. Nat Med *9*, 53–60.

Desgrange, A., and Cereghini, S. (2015). Nephron Patterning: Lessons from Xenopus, Zebrafish, and Mouse Studies. Cells *4*, 483–499.

Donovan, M.J., Natoli, T.A., Sainio, K., Amstutz, A., Jaenisch, R., Sariola, H., and Kreidberg, J.A. (1999). Initial differentiation of the metanephric mesenchyme is independent of WT1 and the ureteric bud. Dev. Genet. *24*, 252–262.

Draghici, S., Khatri, P., Tarca, A.L., Amin, K., Done, A., Voichita, C., Georgescu, C., and Romero, R. (2007). A systems biology approach for pathway level analysis. Genome Res. *17*, 1537–1545.

Drawbridge, J., Meighan, C.M., and Mitchell, E.A. (2000). GDNF and GFRalpha-1 are components of the axolotl pronephric duct guidance system. Dev. Biol. *228*, 116–124.

Dressler, G.R. (2006). The cellular basis of kidney development. Annu. Rev. Cell Dev. Biol. *22*, 509.

Dressler, G.R., Deutsch, U., Chowdhury, K., Nornes, H.O., and Gruss, P. (1990). Pax2, a new murine paired-box-containing gene and its expression in the developing excretory system. Dev. Camb. Engl. *109*, 787–795.

Dudley, A.T., Lyons, K.M., and Robertson, E.J. (1995). A requirement for bone morphogenetic protein-7 during development of the mammalian kidney and eye. Genes Dev. *9*, 2795–2807.

Dudley, A.T., Godin, R.E., and Robertson, E.J. (1999). Interaction between FGF and BMP signaling pathways regulates development of metanephric mesenchyme. Genes Dev. *13*, 1601–1613.

Duester, G. (2008). Retinoic acid synthesis and signaling during early organogenesis. Cell *134*, 921–931.

Durston, A.J., Timmermans, J.P., Hage, W.J., Hendriks, H.F., de Vries, N.J., Heideveld, M., and Nieuwkoop, P.D. (1989). Retinoic acid causes an anteroposterior transformation in the developing central nervous system. Nature *340*, 140–144.

Edwards, R.G., Purdy, J.M., Steptoe, P.C., and Walters, D.E. (1981). The growth of human preimplantation embryos in vitro. Am. J. Obstet. Gynecol. *141*, 408–416.

Enomoto, H., Araki, T., Jackman, A., Heuckeroth, R.O., Snider, W.D., Johnson, E.M., and Milbrandt, J. (1998). GFR alpha1-deficient mice have deficits in the enteric nervous system and kidneys. Neuron *21*, 317–324.

Eremina, V., Sood, M., Haigh, J., Nagy, A., Lajoie, G., Ferrara, N., Gerber, H.-P., Kikkawa, Y., Miner, J.H., and Quaggin, S.E. (2003). Glomerular-specific alterations of VEGF-A expression lead to distinct congenital and acquired renal diseases. J. Clin. Invest. *111*, 707–716.

Eremina, V., Baelde, H.J., and Quaggin, S.E. (2007). Role of the VEGF--a signaling pathway in the glomerulus: evidence for crosstalk between components of the glomerular filtration barrier. Nephron Physiol. *106*, p32-37.

Fetting, J.L., Guay, J.A., Karolak, M.J., Iozzo, R.V., Adams, D.C., Maridas, D.E., Brown, A.C., and Oxburgh, L. (2014). FOXD1 promotes nephron progenitor differentiation by repressing decorin in the embryonic kidney. Dev. Camb. Engl. *141*, 17–27.

Fleming, B.M., Yelin, R., James, R.G., and Schultheiss, T.M. (2013). A role for Vg1/Nodal signaling in specification of the intermediate mesoderm. Dev. Camb. Engl. *140*, 1819–1829.

Foley, R.N., Parfrey, P.S., and Sarnak, M.J. (1998). Clinical epidemiology of cardiovascular disease in chronic renal disease. Am. J. Kidney Dis. Off. J. Natl. Kidney Found. *32*, S112-119.

Freedman, B.S., Brooks, C.R., Lam, A.Q., Fu, H., Morizane, R., Agrawal, V., Saad, A.F., Li, M.K., Hughes, M.R., Werff, R.V., et al. (2015). Modelling kidney disease with CRISPR-mutant kidney organoids derived from human pluripotent epiblast spheroids. Nat. Commun. *6*, 8715.

Frohman, M.A., Boyle, M., and Martin, G.R. (1990). Isolation of the mouse Hox-2.9 gene; analysis of embryonic expression suggests that positional information along the anterior-posterior axis is specified by mesoderm. Development *110*, 589–607.

Gadue, P., Huber, T.L., Paddison, P.J., and Keller, G.M. (2006). Wnt and TGF-beta signaling are required for the induction of an in vitro model of primitive streak formation using embryonic stem cells. Proc. Natl. Acad. Sci. U. S. A. *103*, 16806–16811.

Georgas, K., Rumballe, B., Valerius, M.T., Chiu, H.S., Thiagarajan, R.D., Lesieur, E., Aronow, B.J., Brunskill, E.W., Combes, A.N., Tang, D., et al. (2009). Analysis of early nephron patterning reveals a role for distal RV proliferation in fusion to the ureteric tip via a cap mesenchyme-derived connecting segment. Dev. Biol. *332*, 273–286.

Gilbert, S.F. (2000). Developmental Biology (Sinauer Associates).

Grieshammer, U., Cebrián, C., Ilagan, R., Meyers, E., Herzlinger, D., and Martin, G.R. (2005). FGF8 is required for cell survival at distinct stages of nephrogenesis and for regulation of gene expression in nascent nephrons. Development *132*, 3847–3857.

Gritsman, K., Talbot, W.S., and Schier, A.F. (2000). Nodal signaling patterns the organizer. Dev. Camb. Engl. *127*, 921–932.

Guillaume, R., Bressan, M., and Herzlinger, D. (2009). Paraxial mesoderm contributes stromal cells to the developing kidney. Dev. Biol. *329*, 169–175.

Hariharan, K., Kurtz, A., and Schmidt-Ott, K.M. (2015). Assembling Kidney Tissues from Cells: The Long Road from Organoids to Organs. Cell Growth Div. 70.

Hiler, D., Chen, X., Hazen, J., Kupriyanov, S., Carroll, P.A., Qu, C., Xu, B., Johnson, D., Griffiths, L., Frase, S., et al. (2015). Quantification of Retinogenesis in 3D Cultures Reveals Epigenetic Memory and Higher Efficiency in iPSCs Derived from Rod Photoreceptors. Cell Stem Cell *17*, 101–115.

Ho, L., and Crabtree, G.R. (2010). Chromatin remodelling during development. Nature *463*, 474–484.

Humphreys, B.D. (2015). Cutting to the chase: taking the pulse of label-retaining cells in kidney. Am. J. Physiol. Renal Physiol. *308*, F29-30.

Humphreys, B.D., Lin, S.-L., Kobayashi, A., Hudson, T.E., Nowlin, B.T., Bonventre, J.V., Valerius, M.T., McMahon, A.P., and Duffield, J.S. (2010). Fate tracing reveals the pericyte and not epithelial origin of myofibroblasts in kidney fibrosis. Am. J. Pathol. *176*, 85–97.

James, R.G., and Schultheiss, T.M. (2003). Patterning of the avian intermediate mesoderm by lateral plate and axial tissues. Dev. Biol. *253*, 109–124.

James, R.G., Kamei, C.N., Wang, Q., Jiang, R., and Schultheiss, T.M. (2006). Odd-skipped related 1 is required for development of the metanephric kidney and regulates formation and differentiation of kidney precursor cells. Development *133*, 2995–3004.

Joannides, A.J., Fiore-Hériché, C., Battersby, A.A., Athauda-Arachchi, P., Bouhon, I.A., Williams, L., Westmore, K., Kemp, P.J., Compston, A., Allen, N.D., et al. (2007). A Scaleable and Defined System for Generating Neural Stem Cells from Human Embryonic Stem Cells. STEM CELLS *25*, 731–737.

Kandasamy, K., Chuah, J.K.C., Su, R., Huang, P., Eng, K.G., Xiong, S., Li, Y., Chia, C.S., Loo, L.-H., and Zink, D. (2015). Prediction of drug-induced nephrotoxicity and injury mechanisms with human induced pluripotent stem cell-derived cells and machine learning methods. Sci. Rep. *5*.

Karavanov, A.A., Karavanova, I., Perantoni, A., and Dawid, I.B. (1998). Expression pattern of the rat Lim-1 homeobox gene suggests a dual role during kidney development. Int. J. Dev. Biol. *42*, 61–66.

Karner, C.M., Das, A., Ma, Z., Self, M., Chen, C., Lum, L., Oliver, G., and Carroll, T.J. (2011). Canonical Wnt9b signaling balances progenitor cell expansion and differentiation during kidney development. Development *138*, 1247–1257.

Kim, D., and Dressler, G.R. (2005). Nephrogenic Factors Promote Differentiation of Mouse Embryonic Stem Cells into Renal Epithelia. J Am Soc Nephrol *16*, 3527–3534.

Kinder, S.J., Tsang, T.E., Quinlan, G.A., Hadjantonakis, A.K., Nagy, A., and Tam, P.P. (1999). The orderly allocation of mesodermal cells to the extraembryonic structures and the anteroposterior axis during gastrulation of the mouse embryo. Dev. Camb. Engl. *126*, 4691–4701.

Knoll, G. (2008). Trends in kidney transplantation over the past decade. Drugs *68 Suppl 1*, 3–10.

Kobayashi, A., Kwan, K.-M., Carroll, T.J., McMahon, A.P., Mendelsohn, C.L., and Behringer, R.R. (2005a). Distinct and sequential tissue-specific activities of the LIM-class homeobox gene Lim1 for tubular morphogenesis during kidney. Development *132*, 2809–2823.

Kobayashi, A., Valerius, M.T., Mugford, J.W., Carroll, T.J., Self, M., Oliver, G., and McMahon, A.P. (2008). Six2 Defines and Regulates a Multipotent Self-Renewing Nephron Progenitor Population throughout Mammalian Kidney Development. Cell Stem Cell *3*, 169–181.

Kobayashi, T., Tanaka, H., Kuwana, H., Inoshita, S., Teraoka, H., Sasaki, S., and Terada, Y. (2005b). Wnt4-transformed mouse embryonic stem cells differentiate into renal tubular cells. Biochem. Biophys. Res. Commun. *336*, 585–595.

Kopan, R., Cheng, H.-T., and Surendran, K. (2007). Molecular Insights into Segmentation along the Proximal–Distal Axis of the Nephron. J. Am. Soc. Nephrol. *18*, 2014–2020.

Kreidberg, J.A. (2010). WT1 and kidney progenitor cells. Organogenesis *6*, 61–70.

Kreidberg, J.A., Sariola, H., Loring, J.M., Maeda, M., Pelletier, J., Housman, D., and Jaenisch, R. (1993). WT-1 is required for early kidney development. Cell *74*, 679–691.

Kreidberg, J.A., Donovan, M.J., Goldstein, S.L., Rennke, H., Shepherd, K., Jones, R.C., and Jaenisch, R. (1996). Alpha 3 beta 1 integrin has a crucial role in kidney and lung organogenesis. Dev. Camb. Engl. *122*, 3537–3547.

Kriz, W., and Kaissling, B. (2013). Chapter 20 - Structural Organization of the Mammalian Kidney A2 - Alpern, Robert J. In Seldin and Giebisch's The Kidney (Fifth Edition), O.W. Moe, and M. Caplan, eds. (Academic Press), pp. 595–691.

Kubo, A., Shinozaki, K., Shannon, J.M., Kouskoff, V., Kennedy, M., Woo, S., Fehling, H.J., and Keller, G. (2004). Development of definitive endoderm from embryonic stem cells in culture. Dev. Camb. Engl. *131*, 1651–1662.

Kume, T., Deng, K., and Hogan, B.L. (2000). Murine forkhead/winged helix genes Foxc1 (Mf1) and Foxc2 (Mfh1) are required for the early organogenesis of the kidney and urinary tract. Dev. Camb. Engl. *127*, 1387–1395.

Ladd, A.N., Yatskievych, T.A., and Antin, P.B. (1998). Regulation of avian cardiac myogenesis by activin/TGFbeta and bone morphogenetic proteins. Dev. Biol. *204*, 407–419.

Laflamme, M.A., Chen, K.Y., Naumova, A.V., Muskheli, V., Fugate, J.A., Dupras, S.K., Reinecke, H., Xu, C., Hassanipour, M., Police, S., et al. (2007). Cardiomyocytes derived from human embryonic stem cells in pro-survival factors enhance function of infarcted rat hearts. Nat. Biotechnol. *25*, 1015–1024.

Lam, A.Q., Freedman, B.S., Morizane, R., Lerou, P.H., Valerius, M.T., and Bonventre, J.V. (2014). Rapid and Efficient Differentiation of Human Pluripotent Stem Cells into Intermediate Mesoderm That Forms Tubules Expressing Kidney Proximal Tubular Markers. J. Am. Soc. Nephrol. *25*, 1211–1225.

Lawson, K.A., and Pedersen, R.A. (1992). Clonal analysis of cell fate during gastrulation and early neurulation in the mouse. Ciba Found. Symp. *165*, 3-21-26.

Lawson, K.A., Meneses, J.J., and Pedersen, R.A. (1991). Clonal analysis of epiblast fate during germ layer formation in the mouse embryo. Dev. Camb. Engl. *113*, 891–911.

Levinson, R.S., Batourina, E., Choi, C., Vorontchikhina, M., Kitajewski, J., and Mendelsohn, C.L. (2005). Foxd1-dependent signals control cellularity in the renal capsule, a structure required for normal renal development. Dev. Camb. Engl. *132*, 529–539.

Li, Y., and Wingert, R.A. (2013). Regenerative medicine for the kidney: stem cell prospects & challenges. Clin. Transl. Med. *2*, 11.

Li, W., Hartwig, S., and Rosenblum, N.D. (2014). Developmental origins and functions of stromal cells in the normal and diseased mammalian kidney. Dev. Dyn. *243*, 853–863.

Li, X., Oghi, K.A., Zhang, J., Krones, A., Bush, K.T., Glass, C.K., Nigam, S.K., Aggarwal, A.K., Maas, R., Rose, D.W., et al. (2003). Eya protein phosphatase activity regulates Six1-Dach-Eya transcriptional effects in mammalian organogenesis. Nature *426*, 247–254.

Lindahl, P., Hellstrom, M., Kalen, M., Karlsson, L., Pekny, M., Pekna, M., Soriano, P., and Betsholtz, C. (1998). Paracrine PDGF-B/PDGF-Rbeta signaling controls mesangial cell development in kidney glomeruli. Development *125*, 3313–3322.

Lindgren, D., Boström, A.-K., Nilsson, K., Hansson, J., Sjölund, J., Möller, C., Jirström, K., Nilsson, E., Landberg, G., Axelson, H., et al. (2011). Isolation and characterization of progenitor-like cells from human renal proximal tubules. Am. J. Pathol. *178*, 828–837.

Lindström, N.O., Lawrence, M.L., Burn, S.F., Johansson, J.A., Bakker, E.R.M., Ridgway, R.A., Chang, C.-H., Karolak, M.J., Oxburgh, L., Headon, D.J., et al. (2014). Integrated β-catenin, BMP, PTEN, and Notch signalling patterns the nephron. eLife *3*, e04000.

Little, M.H. (2016). Growing Kidney Tissue from Stem Cells: How Far from "Party Trick" to Medical Application? Cell Stem Cell *18*, 695–698.

Lowe, L.A., Yamada, S., and Kuehn, M.R. (2001). Genetic dissection of nodal function in patterning the mouse embryo. Dev. Camb. Engl. *128*, 1831–1843.

Ludwig, T.E., Bergendahl, V., Levenstein, M.E., Yu, J., Probasco, M.D., and Thomson, J.A. (2006). Feeder-independent culture of human embryonic stem cells. Nat. Methods *3*, 637–646.

Luo, G., Hofmann, C., Bronckers, A.L., Sohocki, M., Bradley, A., and Karsenty, G. (1995). BMP-7 is an inducer of nephrogenesis, and is also required for eye development and skeletal patterning. Genes Dev. *9*, 2808–2820.

Macconi, D., Sangalli, F., Bonomelli, M., Conti, S., Condorelli, L., Gagliardini, E., Remuzzi, G., and Remuzzi, A. (2009). Podocyte repopulation contributes to regression of glomerular injury induced by ACE inhibition. Am. J. Pathol. *174*, 797–807.

Mae, S.-I., Shono, A., Shiota, F., Yasuno, T., Kajiwara, M., Gotoda-Nishimura, N., Arai, S., Sato-Otubo, A., Toyoda, T., Takahashi, K., et al. (2013). Monitoring and robust induction of nephrogenic intermediate mesoderm from human pluripotent stem cells. Nat. Commun. *4*, 1367.

Mah, S.P., Saueressig, H., Goulding, M., Kintner, C., and Dressler, G.R. (2000). Kidney Development in Cadherin-6 Mutants: Delayed Mesenchyme-to-Epithelial Conversion and Loss of Nephrons. Dev. Biol. *223*, 38–53.

Majumdar, A., Vainio, S., Kispert, A., McMahon, J., and McMahon, A.P. (2003). Wnt11 and Ret/Gdnf pathways cooperate in regulating ureteric branching during metanephric kidney development. Dev. Camb. Engl. *130*, 3175–3185.

Matlin, K.S., and Caplan, M.J. (2013). Chapter 1 - Epithelial Cell Structure and Polarity. In Seldin and Giebisch's The Kidney (Fifth Edition), (Academic Press), pp. 3–43.

Mauch, T.J., Yang, G., Wright, M., Smith, D., and Schoenwolf, G.C. (2000). Signals from trunk paraxial mesoderm induce pronephros formation in chick intermediate mesoderm. Dev. Biol. *220*, 62–75.

Mavilio, F., Simeone, A., Boncinelli, E., and Andrews, P.W. (1988). Activation of four homeobox gene clusters in human embryonal carcinoma cells induced to differentiate by retinoic acid. Differ. Res. Biol. Divers. *37*, 73–79.

Mazairac, A.H.A., de Wit, G.A., Grooteman, M.P.C., Penne, E.L., van der Weerd, N.C., den Hoedt, C.H., Lévesque, R., van den Dorpel, M.A., Nubé, M.J., Ter Wee, P.M., et al. (2012). Clinical performance targets and quality of life in hemodialysis patients. Blood Purif. *33*, 73–79.

McCright, B., Gao, X., Shen, L., Lozier, J., Lan, Y., Maguire, M., Herzlinger, D., Weinmaster, G., Jiang, R., and Gridley, T. (2001). Defects in development of the kidney, heart and eye vasculature in mice homozygous for a hypomorphic Notch2 mutation. Dev. Camb. Engl. *128*, 491–502.

McMahon, A.P. (2016). Development of the Mammalian Kidney. Curr. Top. Dev. Biol. *117*, 31–64.

Medvinsky, A., and Dzierzak, E. (1996). Definitive hematopoiesis is autonomously initiated by the AGM region. Cell *86*, 897–906.

Mendelsohn, C., Batourina, E., Fung, S., Gilbert, T., and Dodd, J. (1999). Stromal cells mediate retinoid-dependent functions essential for renal development. Dev. Camb. Engl. *126*, 1139–1148.

Michos, O., Panman, L., Vintersten, K., Beier, K., Zeller, R., and Zuniga, A. (2004). Gremlin-mediated BMP antagonism induces the epithelial-mesenchymal feedback signaling controlling metanephric kidney and limb organogenesis. Dev. Camb. Engl. *131*, 3401–3410.

Miner, J.H., and Li, C. (2000). Defective glomerulogenesis in the absence of laminin alpha5 demonstrates a developmental role for the kidney glomerular basement membrane. Dev. Biol. *217*, 278–289.

Miyazaki, Y., Oshima, K., Fogo, A., Hogan, B.L., and Ichikawa, I. (2000). Bone morphogenetic protein 4 regulates the budding site and elongation of the mouse ureter. J. Clin. Invest. *105*, 863–873.

Mohamed, J.Y., Faqeih, E., Alsiddiky, A., Alshammari, M.J., Ibrahim, N.A., and Alkuraya, F.S. (2013). Mutations in MEOX1, Encoding Mesenchyme Homeobox 1, Cause Klippel-Feil Anomaly. Am. J. Hum. Genet. *92*, 157–161.

Morizane, R., Monkawa, T., and Itoh, H. (2009). Differentiation of murine embryonic stem and induced pluripotent stem cells to renal lineage in vitro. Biochem. Biophys. Res. Commun. *390*, 1334–1339.

Morizane, R., Lam, A.Q., Freedman, B.S., Kishi, S., Valerius, M.T., and Bonventre, J.V. (2015). Nephron organoids derived from human pluripotent stem cells model kidney development and injury. Nat. Biotechnol. *33*, 1193–1200.

Mugford, J.W., Sipilä, P., McMahon, J.A., and McMahon, A.P. (2008). Osr1 expression demarcates a multi-potent population of intermediate mesoderm that undergoes progressive restriction to an Osr1-dependent nephron progenitor compartment within the mammalian kidney. Dev. Biol. *324*, 88–98.

Müller, U., Wang, D., Denda, S., Meneses, J.J., Pedersen, R.A., and Reichardt, L.F. (1997). Integrin alpha8beta1 is critically important for epithelial-mesenchymal interactions during kidney morphogenesis. Cell *88*, 603–613.

Murry, C.E., and Keller, G. (2008). Differentiation of Embryonic Stem Cells to Clinically Relevant Populations: Lessons from Embryonic Development. Cell *132*, 661–680.

Ng, E.S., Davis, R., Stanley, E.G., and Elefanty, A.G. (2008). A protocol describing the use of a recombinant protein-based, animal product-free medium (APEL) for human embryonic stem cell differentiation as spin embryoid bodies. Nat. Protoc. *3*, 768–776.

Nishikawa, M., Yanagawa, N., Kojima, N., Yuri, S., Hauser, P.V., Jo, O.D., and Yanagawa, N. (2012). Stepwise renal lineage differentiation of mouse embryonic stem cells tracing in vivo development. Biochem. Biophys. Res. Commun. *417*, 897–902.

Nishinakamura, R., Matsumoto, Y., Nakao, K., Nakamura, K., Sato, A., Copeland, N.G., Gilbert, D.J., Jenkins, N.A., Scully, S., Lacey, D.L., et al. (2001). Murine homolog of SALL1 is essential for ureteric bud invasion in kidney development. Dev. Camb. Engl. *128*, 3105–3115.

Obara-Ishihara, T., Kuhlman, J., Niswander, L., and Herzlinger, D. (1999). The surface ectoderm is essential for nephric duct formation in intermediate mesoderm. Dev. Camb. Engl. *126*, 1103–1108.

O'Brien, L.L., Guo, Q., Lee, Y., Tran, T., Benazet, J.-D., Whitney, P.H., Valouev, A., and McMahon, A.P. (2016). Differential regulation of mouse and human nephron progenitors by the Six family of transcriptional regulators. Dev. Camb. Engl. *143*, 595–608.

Osafune, K., Nishinakamura, R., Komazaki, S., and Asashima, M. (2002). In vitro induction of the pronephric duct in Xenopus explants. Dev. Growth Differ. *44*, 161–167.

Oxburgh, L., Brown, A.C., Fetting, J., and Hill, B. (2011). BMP signaling in the nephron progenitor niche. Pediatr. Nephrol. *26*, 1491–1497.

Palant, C.E., Amdur, R.L., and Chawla, L.S. (2016). The Acute Kidney Injury to Chronic Kidney Disease Transition: A Potential Opportunity to Improve Care in Acute Kidney Injury. Contrib. Nephrol. *187*, 55–72.

Parameswaran, M., and Tam, P.P. (1995). Regionalisation of cell fate and morphogenetic movement of the mesoderm during mouse gastrulation. Dev. Genet. *17*, 16–28.

Park, J.-S., Valerius, M.T., and McMahon, A.P. (2007). Wnt/beta-catenin signaling regulates nephron induction during mouse kidney development. Dev. Camb. Engl. *134*, 2533–2539.

Patterson, L.T., Pembaur, M., and Potter, S.S. (2001). Hoxa11 and Hoxd11 regulate branching morphogenesis of the ureteric bud in the developing kidney. Dev. Camb. Engl. *128*, 2153–2161.

Potter, E.L., and Thierstein, S.T. (1943). Glomerular development in the kidney as an index of fetal maturity. J. Pediatr. *22*, 695–706.

Pourquié, O., Fan, C.M., Coltey, M., Hirsinger, E., Watanabe, Y., Bréant, C., Francis-West, P., Brickell, P., Tessier-Lavigne, M., and Le Douarin, N.M. (1996). Lateral and axial signals involved in avian somite patterning: a role for BMP4. Cell *84*, 461–471.

Preger-Ben Noon, E., Barak, H., Guttmann-Raviv, N., and Reshef, R. (2009). Interplay between activin and Hox genes determines the formation of the kidney morphogenetic field. Dev. Camb. Engl. *136*, 1995–2004.

Prescott, L.F. (1966). The normal urinary excretion rates of renal tubular cells, leucocytes and red blood cells. Clin. Sci. *31*, 425–435.

Putaala, H., Soininen, R., Kilpeläinen, P., Wartiovaara, J., and Tryggvason, K. (2001). The murine nephrin gene is specifically expressed in kidney, brain and pancreas: inactivation of the gene leads to massive proteinuria and neonatal death. Hum. Mol. Genet. *10*, 1–8.

R Development Core Team (2011) R: a language and environment for statistical computing.

Raciti, D., Reggiani, L., Geffers, L., Jiang, Q., Bacchion, F., Subrizi, A.E., Clements, D., Tindal, C., Davidson, D.R., Kaissling, B., et al. (2008). Organization of the pronephric kidney revealed by large-scale gene expression mapping. Genome Biol. *9*, R84.

Ren, X., Zhang, J., Gong, X., Niu, X., Zhang, X., Chen, P., and Zhang, X. (2010). Differentiation of murine embryonic stem cells toward renal lineages by conditioned medium from ureteric bud cells in vitro. Acta Biochim. Biophys. Sin. *42*, 464–471.

Riley, P., Anson-Cartwright, L., and Cross, J.C. (1998). The Hand1 bHLH transcription factor is essential for placentation and cardiac morphogenesis. Nat. Genet. *18*, 271–275.

Rinkevich, Y., Montoro, D.T., Contreras-Trujillo, H., Harari-Steinberg, O., Newman, A.M., Tsai, J.M., Lim, X., Van-Amerongen, R., Bowman, A., Januszyk, M., et al. (2014). In vivo clonal analysis reveals lineage-restricted progenitor characteristics in mammalian kidney development, maintenance, and regeneration. Cell Rep. *7*, 1270–1283.

Rock, J., and Menkin, M.F. (1944). In Vitro Fertilization and Cleavage of Human Ovarian Eggs. Science *100*, 105–107.

Romagnani, P., Lasagni, L., and Remuzzi, G. (2013). Renal progenitors: an evolutionary conserved strategy for kidney regeneration. Nat. Rev. Nephrol. *9*, 137–146.

Roselli, S., Heidet, L., Sich, M., Henger, A., Kretzler, M., Gubler, M.-C., and Antignac, C. (2004). Early Glomerular Filtration Defect and Severe Renal Disease in Podocin-Deficient Mice. Mol. Cell. Biol. *24*, 550–560.

Rothenpieler, U.W., and Dressler, G.R. (1993). Pax-2 is required for mesenchyme-to-epithelium conversion during kidney development. Dev. Camb. Engl. *119*, 711–720.

Ruf, R.G., Xu, P.-X., Silvius, D., Otto, E.A., Beekmann, F., Muerb, U.T., Kumar, S., Neuhaus, T.J., Kemper, M.J., Raymond, R.M., et al. (2004). SIX1 mutations cause branchio-oto-renal syndrome by disruption of EYA1-SIX1-DNA complexes. Proc. Natl. Acad. Sci. U. S. A. *101*, 8090–8095.

Ruggenenti, P., Perna, A., Gherardi, G., Garini, G., Zoccali, C., Salvadori, M., Scolari, F., Schena, F.P., and Remuzzi, G. (1999). Renoprotective properties of ACE-inhibition in non-diabetic nephropathies with non-nephrotic proteinuria. Lancet Lond. Engl. *354*, 359–364.

Sainio, K., Suvanto, P., Davies, J., Wartiovaara, J., Wartiovaara, K., Saarma, M., Arumae, U., Meng, X., Lindahl, M., Pachnis, V., et al. (1997). Glial-cell-line-derived neurotrophic factor is required for bud initiation from ureteric epithelium. Development *124*, 4077–4087.

Sajithlal, G., Zou, D., Silvius, D., and Xu, P.-X. (2005). Eya 1 acts as a critical regulator for specifying the metanephric mesenchyme. Dev. Biol. *284*, 323–336.

Sánchez, M.P., Silos-Santiago, I., Frisén, J., He, B., Lira, S.A., and Barbacid, M. (1996). Renal agenesis and the absence of enteric neurons in mice lacking GDNF. Nature *382*, 70–73.

Santos, O.F., and Nigam, S.K. (1993). HGF-induced tubulogenesis and branching of epithelial cells is modulated by extracellular matrix and TGF-beta. Dev. Biol. *160*, 293–302.

Saxén, L., and Sariola, H. (1987). Early organogenesis of the kidney. Pediatr. Nephrol. Berl. Ger. *1*, 385–392.

Schmidt-Ott, K.M., Masckauchan, T.N.H., Chen, X., Hirsh, B.J., Sarkar, A., Yang, J., Paragas, N., Wallace, V.A., Dufort, D., Pavlidis, P., et al. (2007). beta-catenin/TCF/Lef controls a differentiation-associated transcriptional program in renal epithelial progenitors. Dev. Camb. Engl. *134*, 3177–3190.

Schuchardt, A., D'Agati, V., Larsson-Blomberg, L., Costantini, F., and Pachnis, V. (1994). Defects in the kidney and enteric nervous system of mice lacking the tyrosine kinase receptor Ret. Nature *367*, 380–383.

Schultheiss, T.M., Burch, J.B., and Lassar, A.B. (1997). A role for bone morphogenetic proteins in the induction of cardiac myogenesis. Genes Dev. *11*, 451–462.

Sharmin, S., Taguchi, A., Kaku, Y., Yoshimura, Y., Ohmori, T., Sakuma, T., Mukoyama, M., Yamamoto, T., Kurihara, H., and Nishinakamura, R. (2015). Human Induced Pluripotent Stem Cell-Derived Podocytes Mature into Vascularized Glomeruli upon Experimental Transplantation. J. Am. Soc. Nephrol. JASN.

Shen, S.S., Krishna, B., Chirala, R., Amato, R.J., and Truong, L.D. (2005). Kidney-specific cadherin, a specific marker for the distal portion of the nephron and related renal neoplasms. Mod. Pathol. *18*, 933–940.

Shih, N.Y., Li, J., Karpitskii, V., Nguyen, A., Dustin, M.L., Kanagawa, O., Miner, J.H., and Shaw, A.S. (1999). Congenital nephrotic syndrome in mice lacking CD2-associated protein. Science *286*, 312–315.

Smeets, B., Uhlig, S., Fuss, A., Mooren, F., Wetzels, J.F.M., Floege, J., and Moeller, M.J. (2009a). Tracing the origin of glomerular extracapillary lesions from parietal epithelial cells. J. Am. Soc. Nephrol. JASN *20*, 2604–2615.

Smeets, B., Angelotti, M.L., Rizzo, P., Dijkman, H., Lazzeri, E., Mooren, F., Ballerini, L., Parente, E., Sagrinati, C., Mazzinghi, B., et al. (2009b). Renal progenitor cells contribute to hyperplastic lesions of podocytopathies and crescentic glomerulonephritis. J. Am. Soc. Nephrol. JASN *20*, 2593–2603.

Smeets, B., Boor, P., Dijkman, H., Sharma, S.V., Jirak, P., Mooren, F., Berger, K., Bornemann, J., Gelman, I.H., Floege, J., et al. (2013). Proximal tubular cells contain a phenotypically distinct, scattered cell population involved in tubular regeneration. J. Pathol. *229*, 645–659.

Song, B., Smink, A.M., Jones, C.V., Callaghan, J.M., Firth, S.D., Bernard, C.A., Laslett, A.L., Kerr, P.G., and Ricardo, S.D. (2012). The directed differentiation of human iPS cells into kidney podocytes. PloS One *7*, e46453.

Song, J.J., Guyette, J.P., Gilpin, S.E., Gonzalez, G., Vacanti, J.P., and Ott, H.C. (2013). Regeneration and experimental orthotopic transplantation of a bioengineered kidney. Nat. Med. *19*, 646–651.

Soriano, P. (1994). Abnormal kidney development and hematological disorders in PDGF beta-receptor mutant mice. Genes Dev. *8*, 1888–1896.

Soueid-Baumgarten, S., Yelin, R., Davila, E.K., and Schultheiss, T.M. (2014). Parallel waves of inductive signaling and mesenchyme maturation regulate differentiation of the chick mesonephros. Dev. Biol. *385*, 122–135.

Sousa-Martins, P. de, Moura, A., Madureira, J., Alija, P., Oliveira, J.G., Lopez, M., Filgueiras, M., Amado, L., Sameiro-Faria, M., Miranda, V., et al. (2016). Risk factors for mortality in end-stage kidney disease patients under online-hemodiafiltration: three-year follow-up study. Biomarkers *21*, 544–550.

Steptoe, P.C., and Edwards, R.G. (1978). BIRTH AFTER THE REIMPLANTATION OF A HUMAN EMBRYO. The Lancet *312*, 366.

Sumi, T., Tsuneyoshi, N., Nakatsuji, N., and Suemori, H. (2008). Defining early lineage specification of human embryonic stem cells by the orchestrated balance of canonical Wnt/beta-catenin, Activin/Nodal and BMP signaling. Dev. Camb. Engl. *135*, 2969–2979.

Taguchi, A., Kaku, Y., Ohmori, T., Sharmin, S., Ogawa, M., Sasaki, H., and Nishinakamura, R. (2014). Redefining the in vivo origin of metanephric nephron progenitors enables generation of complex kidney structures from pluripotent stem cells. Cell Stem Cell *14*, 53–67.

Takahashi, K., and Yamanaka, S. (2006). Induction of pluripotent stem cells from mouse embryonic and adult fibroblast cultures by defined factors. Cell *126*, 663–676.

Takahashi, K., Tanabe, K., Ohnuki, M., Narita, M., Ichisaka, T., Tomoda, K., and Yamanaka, S. (2007). Induction of pluripotent stem cells from adult human fibroblasts by defined factors. Cell *131*, 861–872.

Takasato, M., and Little, M.H. (2015). The origin of the mammalian kidney: implications for recreating the kidney in vitro. Dev. Camb. Engl. *142*, 1937–1947.

Takasato, M., Er, P.X., Becroft, M., Vanslambrouck, J.M., Stanley, E.G., Elefanty, A.G., and Little, M.H. (2014). Directing human embryonic stem cell differentiation towards a renal lineage generates a self-organizing kidney. Nat. Cell Biol. *16*, 118–126.

Takasato, M., Er, P.X., Chiu, H.S., Maier, B., Baillie, G.J., Ferguson, C., Parton, R.G., Wolvetang, E.J., Roost, M.S., Chuva de Sousa Lopes, S.M., et al. (2015). Kidney organoids from human iPS cells contain multiple lineages and model human nephrogenesis. Nature *526*, 564–568.

Tam, P.P., and Beddington, R.S. (1987). The formation of mesodermal tissues in the mouse embryo during gastrulation and early organogenesis. Dev. Camb. Engl. *99*, 109–126.

Tam, P.P., and Behringer, R.R. (1997). Mouse gastrulation: the formation of a mammalian body plan. Mech. Dev. *68*, 3–25.

Tan, J.Y., Sriram, G., Rufaihah, A.J., Neoh, K.G., and Cao, T. (2013). Efficient Derivation of Lateral Plate and Paraxial Mesoderm Subtypes from Human Embryonic Stem Cells Through GSKi-Mediated Differentiation. Stem Cells Dev. *22*, 1893–1906.

Tanigawa, S., Wang, H., Yang, Y., Sharma, N., Tarasova, N., Ajima, R., Yamaguchi, T.P., Rodriguez, L.G., and Perantoni, A.O. (2011). Wnt4 induces nephronic tubules in metanephric mesenchyme by a non-canonical mechanism. Dev. Biol. *352*, 58–69.

Tanigawa, S., Taguchi, A., Sharma, N., Perantoni, A.O., and Nishinakamura, R. (2016). Selective In Vitro Propagation of Nephron Progenitors Derived from Embryos and Pluripotent Stem Cells. Cell Rep. *15*, 801–813.

Taub, M., and Sato, G.H. (1979). Growth of kidney epithelial cells in hormone-supplemented, serum-free medium. J. Supramol. Struct. *11*, 207–216.

Technau, U., and Scholz, C.B. (2003). Origin and evolution of endoderm and mesoderm. Int. J. Dev. Biol. *47*, 531–539.

Teo, A.K.K., Arnold, S.J., Trotter, M.W.B., Brown, S., Ang, L.T., Chng, Z., Robertson, E.J., Dunn, N.R., and Vallier, L. (2011). Pluripotency factors regulate definitive endoderm specification through eomesodermin. Genes Dev. *25*, 238–250.

Thisse, B., Wright, C.V., and Thisse, C. (2000). Activin- and Nodal-related factors control antero-posterior patterning of the zebrafish embryo. Nature *403*, 425–428.

Thomson, J.A., Itskovitz-Eldor, J., Shapiro, S.S., Waknitz, M.A., Swiergiel, J.J., Marshall, V.S., and Jones, J.M. (1998). Embryonic Stem Cell Lines Derived from Human Blastocysts. Science *282*, 1145–1147.

Tonegawa, A., Funayama, N., Ueno, N., and Takahashi, Y. (1997). Mesodermal subdivision along the mediolateral axis in chicken controlled by different concentrations of BMP-4. Dev. Camb. Engl. *124*, 1975–1984.

Torban, E., Dziarmaga, A., Iglesias, D., Chu, L.L., Vassilieva, T., Little, M., Eccles, M., Discenza, M., Pelletier, J., and Goodyer, P. (2006). PAX2 Activates WNT4 Expression during Mammalian Kidney Development. J. Biol. Chem. *281*, 12705–12712.

Trapnell, C., Pachter, L., and Salzberg, S.L. (2009). TopHat: discovering splice junctions with RNA-Seq. Bioinforma. Oxf. Engl. *25*, 1105–1111.

Trapnell, C., Williams, B.A., Pertea, G., Mortazavi, A., Kwan, G., van Baren, M.J., Salzberg, S.L., Wold, B.J., and Pachter, L. (2010). Transcript assembly and quantification by RNA-Seq reveals unannotated transcripts and isoform switching during cell differentiation. Nat. Biotechnol. *28*, 511–515.

Vigneau, C., Polgar, K., Striker, G., Elliott, J., Hyink, D., Weber, O., Fehling, H.-J., Keller, G., Burrow, C., and Wilson, P. (2007). Mouse embryonic stem cell-derived embryoid bodies generate progenitors that integrate long term into renal proximal tubules in vivo. J. Am. Soc. Nephrol. JASN *18*, 1709–1720.

Vogetseder, A., Picard, N., Gaspert, A., Walch, M., Kaissling, B., and Le Hir, M. (2008). Proliferation capacity of the renal proximal tubule involves the bulk of differentiated epithelial cells. Am. J. Physiol. Cell Physiol. *294*, C22-28.

Waddington, C.H. (1938). The Morphogenetic Function of a Vestigial Organ in the Chick. J. Exp. Biol. *15*, 371–376.

Wang, Q., Lan, Y., Cho, E.-S., Maltby, K.M., and Jiang, R. (2005). Odd-skipped related 1 (Odd 1) is an essential regulator of heart and urogenital development. Dev. Biol. *288*, 582–594.

Weidgang, C.E., Russell, R., Tata, P.R., Kühl, S.J., Illing, A., Müller, M., Lin, Q., Brunner, C., Boeckers, T.M., Bauer, K., et al. (2013). TBX3 Directs Cell-Fate Decision toward Mesendoderm. Stem Cell Rep. *1*, 248–265.

Wellik, D.M., Hawkes, P.J., and Capecchi, M.R. (2002). Hox11 paralogous genes are essential for metanephric kidney induction. Genes Dev. *16*, 1423–1432.

Wilm, B., James, R.G., Schultheiss, T.M., and Hogan, B.L.M. (2004). The forkhead genes, Foxc1 and Foxc2, regulate paraxial versus intermediate mesoderm cell fate. Dev. Biol. *271*, 176–189.

Wintour, E.M., Butkus, A., Earnest, L., and Pompolo, S. (1996). The erythropoietin gene is expressed strongly in the mammalian mesonephric kidney. Blood *88*, 3349–3353.

Woolf, A.S., and Pitera, J.E. (2009). Embryology. In Pediatric Nephrology, E. Avner, W. Harmon, P. Niaudet, and N. Yoshikawa, eds. (Springer Berlin Heidelberg), pp. 3–30.

Xia, Y., Nivet, E., Sancho-Martinez, I., Gallegos, T., Suzuki, K., Okamura, D., Wu, M.-Z., Dubova, I., Esteban, C.R., Montserrat, N., et al. (2013). Directed differentiation of human pluripotent cells to ureteric bud kidney progenitor-like cells. Nat. Cell Biol. *15*, 1507–1515.

Xia, Y., Sancho-Martinez, I., Nivet, E., Rodriguez Esteban, C., Campistol, J.M., and Izpisua Belmonte, J.C. (2014). The generation of kidney organoids by differentiation of human pluripotent cells to ureteric bud progenitor–like cells. Nat. Protoc. *9*, 2693–2704.

Xu, P.X., Adams, J., Peters, H., Brown, M.C., Heaney, S., and Maas, R. (1999). Eya1-deficient mice lack ears and kidneys and show abnormal apoptosis of organ primordia. Nat. Genet. *23*, 113–117.

Xu, P.-X., Zheng, W., Huang, L., Maire, P., Laclef, C., and Silvius, D. (2003). Six1 is required for the early organogenesis of mammalian kidney. Dev. Camb. Engl. *130*, 3085–3094.

Yang, L., Zhang, H., Hu, G., Wang, H., Abate-Shen, C., and Shen, M.M. (1998). An early phase of embryonic Dlx5 expression defines the rostral boundary of the neural plate. J. Neurosci. Off. J. Soc. Neurosci. *18*, 8322–8330.

Yatskievych, T.A., Ladd, A.N., and Antin, P.B. (1997). Induction of cardiac myogenesis in avian pregastrula epiblast: the role of the hypoblast and activin. Dev. Camb. Engl. *124*, 2561–2570.

Yu, J., Carroll, T.J., and McMahon, A.P. (2002). Sonic hedgehog regulates proliferation and differentiation of mesenchymal cells in the mouse metanephric kidney. Dev. Camb. Engl. *129*, 5301–5312.

Yu, P., Pan, G., Yu, J., and Thomson, J.A. (2011). FGF2 sustains NANOG and switches the outcome of BMP4-induced human embryonic stem cell differentiation. Cell Stem Cell *8*, 326–334.

Zeisberg, M., and Kalluri, R. (2008). Reversal of experimental renal fibrosis by BMP7 provides insights into novel therapeutic strategies for chronic kidney disease. Pediatr. Nephrol. *23*, 1395–1398.

ACKNOWLEDGEMENTS

Words cannot express the sincere gratitude I have for all the generous support bestowed on me by my supervisors, friends and family without whom this work could not have been accomplished. First and foremost, I would like to thank my Mother for introducing the word "stem cell" to me. I am fortunate to have parents who dreamt of my PhD with me and have spared no efforts in ensuring that there are no hurdles in my path and have always been there to catch me before I fall.

As a niche is to a stem cell, so is a lab to a PhD student. I would like to thank Dr. Petra Reinke and Dr. Andreas Kurtz for providing me the opportunity and a wonderful scientific environment to carry out new and challenging experiments. While your knowledge and advice have often shown me the way forward, you have always given plenty of room for implementing my ideas. Your trust and patience has encouraged me in my research. I am deeply grateful to Dr. Harald Stachelscheid for anchoring me in this niche and supervising me. The numerous discussions and trouble-shoots with you have definitely changed my way of thinking and made me a better researcher.

Lab work would have been a nightmare without the help and practical advice of my friends and colleagues Bella Rossbach, Su-jun Oh, and Polixeni Burazi. Special thanks to Dr. Raed Abu Dawud and Dr. Nancy Mah for all the invaluable, stimulating conversations over data analysis and experiments. I am highly indebted to you for your support and patience in dealing with me. In my daily work, I have been blessed with a friendly and cheerful group of fellow students. I am thankful to Maria Schneider, Laura Hildebrand, Iris Fischer, Imran Ullah, Enrico Fritsche and Manfred Roch for all the good vibes in the lab and the everyday lunch gathering. I have greatly benefited from the company of Naima Souidi who has been a great source of inspiration in completing the writing of this thesis. I´d like to thank Levent Akyuz, Si-Hong Luu and Sujin Park for making me feel at home in Berlin.

I am highly indebted to Linda El-Ahmed and Kedar Ketha for withstanding my sulks and complaints, celebrating my tiny victories and supporting me like my own family. Thank you for always being there. I also owe a lot to my brother and grandmother who have constantly been a source of limitless optimism during these years.

Last but not the least; I would like to express my gratitude to the B.S.R.T and Dr. Sabine Bartosch for awarding me the stipend and providing a perfect platform to add new dimensions to my scientific personality, meet experts and make some fantastic friends.

DECLARATION/ Selbständigkeitserklärung

Hiermit erkläre ich, dass ich die vorliegende Arbeit selbständig angefertigt und nur die hier aufgeführten Hilfsmittel verwendet habe. Ich versichere, dass ich die Arbeit weder in dieser noch einer anderen Form bei einer anderen Prüfungsbehörde vorgelegt habe und mich nicht anderweitig für ein Promotionsverfahren zur Erlangung des Titels Dr. rer. nat. angemeldet oder diesen Titel bereits erworben habe.

Berlin, den ……. ……

Krithika Hariharan